



THE HONG KONG  
POLYTECHNIC UNIVERSITY

香港理工大學

Pao Yue-kong Library

包玉剛圖書館

---

## Copyright Undertaking

This thesis is protected by copyright, with all rights reserved.

**By reading and using the thesis, the reader understands and agrees to the following terms:**

1. The reader will abide by the rules and legal ordinances governing copyright regarding the use of the thesis.
2. The reader will use the thesis for the purpose of research or private study only and not for distribution or further reproduction or any other purpose.
3. The reader agrees to indemnify and hold the University harmless from and against any loss, damage, cost, liability or expenses arising from copyright infringement or unauthorized usage.

### IMPORTANT

If you have reasons to believe that any materials in this thesis are deemed not suitable to be distributed in this form, or a copyright owner having difficulty with the material being included in our database, please contact [lbsys@polyu.edu.hk](mailto:lbsys@polyu.edu.hk) providing details. The Library will look into your claim and consider taking remedial action upon receipt of the written requests.

**SPATIAL INTERACTIVE  
EFFECTS ON OPTICAL DEFOCUS  
- A NEW MECHANISM IN  
MYOPIA DEVELOPMENT**

**CHIN MAN PAN**

**Ph.D**

**The Hong Kong Polytechnic University**

**2017**

**The Hong Kong Polytechnic University**

**School of Optometry**

**Spatial Interactive Effects on Optical  
Defocus - A New Mechanism in  
Myopia Development**

**Chin Man Pan**

**A thesis submitted in partial fulfilment of the  
requirements for the degree of Doctor of Philosophy**

**March 2017**

CERTIFICATE OF ORIGINALITY

I hereby declare that this thesis is my own work and that, to the best of my knowledge and belief, it reproduces no material previously published or written, nor material that has been accepted for the award of any other degree or diploma, except where due acknowledgement has been made in the text.

\_\_\_\_\_ (Signed)  
Chin Man Pan (Name of student)

# ABSTRACT

## Introduction

Myopia is mainly due to an excessively increase in axial length. The prevalence of myopia is rocketing upwards especially in east Asia regions. Although myopia can simply be treated by wearing glasses, people with high myopia are prone to various sight-threatening degenerative changes. It is important to understand the mechanism of myopia development and so, the progression of myopia could be controlled. The eye should be similar to other body organs, that possess a homeostatic control to maintain an optimal size. The process is termed emmetropization. Myopia can be regarded as an altered rate of emmetropization, and it is influenced by both genetics and environmental factors. The prevalence of myopia increases in recent decades and it is suspected because of the change of the (visual) environment. Since then, various animal experiments investigated what visual stimuli (inputs) regulate the rate of eye growth (output). Animal experiments from various species provided compelling evidence that the process of emmetropization was guided by optical defocus the eye experienced. There is strong evidence from both animal and human studies suggesting that the eye can detect the sign of defocus. In human study, the

retina was hypothesized to detect the signs of defocus, and was tested by using multifocal electroretinogram (mfERG). The human mfERG revealed that, the retinal activities reacted more vigorously to defocus in the peripheral retina than the central retina. However, it is far from clear how the retina can decode defocus. What visual cues does the retina use to decode optical defocus? The visual images are composed of spatial frequencies and the eye possesses various visual channels to decode them. Some animal studies suggested that emmetropization was specially tuned to particular spatial frequencies. It is possible the local detection of defocus at retinal level is also spatially tuned. If the detection of defocus is spatially tuned, spatial frequency can be a regulator for the rate of eye growth in response to optical defocus. In terms of controlling myopia, the spatial composition of the environment surrounding us may be myopiagenic. In this study, we aimed to investigate the changes of human retinal activity to spatial frequencies. Then, the influence of spatial frequency on human retina in responding to optical defocus was investigated. Furthermore, the effects of spatial-defocus interaction on chick myopia development were studied.

## **Objectives**

- 1) To investigate how the outer and inner retina responding to spatial frequency by using global flash mfERG;
- 2) To investigate how the regional activity changes in retina when high and low spatial frequencies are defocused;
- 3) To investigate the effect of different spatial patterns (high and low spatial frequency) on myopia development in chicks;
- 4) To investigate the effect of spatial composition with various ratios of spatial frequencies on myopia progression in chicks.

## **Methods**

Experiment 1 and 2 were human studies. The human retinal activities were recorded using high contrast Global flash (MOFO) mfERG paradigm. Each cycle of stimulation is consisted of a focal flash (M), followed by a full-screen dark frame (O), a full-screen global flash (F), and another full-screen dark frame (O). This paradigm enhances the activity from the inner retinal neurons, and to separate the outer and inner retinal responses. Two important components, the direct (DC) and induced (IC), reflect the retinal activities from outer and inner retina respectively.

In Experiment 1, twenty-four young adults were recruited. Black and white

gratings of four spatial frequencies, 0.24, 1.2, 2.4 and 4.8 cycle per degree (cpd) were presented in front of the mfERG stimulation. The amplitudes and implicit times of the DC and IC were pooled into six concentric rings for analysis. Repeated measures analysis of variance (ANOVA) was applied to study the effect of spatial frequency on mfERG responses.

In Experiment 2, twenty-three young adults were recruited for mfERG measurement. The setup was similar as in Experiment 1. The retinal electrical responses for low (0.24cpd) and high (4.8cpd) spatial frequency under fully corrected conditions, and of short-term negative defocus (-2D) and short term positive defocus (+2D) conditions were measured. Repeated ANOVA was applied to study the effect of spatial frequency with optical defocus on mfERG response for different retinal regions.

Experiment 3 and 4 were animal studies. The visual environment was manipulated to observe the eye growth response in chick. The refractive error in term of spherical equivalent was measured by using Hartinger refractometer. The ocular dimensions including anterior chamber depth, lens thickness, vitreous chamber depth and axial length were obtained by using ultrasound A-scan.

In Experiment 3, One eye of normal chicks (10-11 days old) was fitted with

a lens-cone device (40mm in length) monocularly and the fellow eye was as the control. At one side of the cone that close to the eye, lenses with powers of +25D, +20D, +15D and +10D were placed. At the other end of the cone, either high spatial frequency visual patterns (0.4mm x 0.4mm black and white checks, 0.9 cpd) or low spatial frequency visual patterns (1.2mm x 1.2mm black and white checks, 0.3 cpd) were used as visual stimuli. The measurements were carried out before wearing the device, on day 4 and day 7 after lens-cone device wearing. The overall effects of spatial frequency and defocus on interocular difference in ocular dimensions and refractive error were tested with two-way ANOVA.

In Experiment 4, one eye of normal chicks (10-11 days old) was fitted with a lens-cone device monocularly and the fellow eyes were as the control. The setting and time course was similar to Experiment 3. At the proximal end of the device, a constant hyperopic defocus of -15D would be induced. At the distal end, visual patterns were made by varying the composition of high (H) spatial frequency and low (L) spatial frequency with different ratios by area. (3H1L, 1H1L, 1H3L). A 75:25 ratio by area of high to low spatial checks was denoted as 3H1L, a 50:50 ratio of high to low spatial checks was denoted as 1H1L, and a 25:75 ratio of high to low spatial checks was

denoted as 1H3L. The overall effects of SF were tested with one-way ANOVA. Trend analysis by one-way ANOVA was carried out to investigate how varying the spatial composition ratio effect on the interocular ocular growth and refractive error change.

## **Results**

In Experiment 1, there was low amplitude DC at low spatial frequency, which increased with increasing spatial frequency, and which decreased with increasing eccentricity. The IC was high in amplitude at all spatial frequencies and reduced in amplitude with increasing eccentricity.

In Experiment 2, a significant sign-dependent response to defocus in the DC response was observed. They located mainly in the peripheral retinal regions. The sign dependent response at low spatial frequency was more obvious than that at high spatial frequency, and was located more peripherally. The IC response showed no clear trends for either defocus condition.

In Experiment 3, both spatial stimulus and defocus had significant main effects on interocular vitreous chamber depth and on refractive error on day 4 and day 7. Eye growth was significantly faster and more myopic for chicks wearing the device with low spatial visual stimuli than those with

high spatial stimuli.

In Experiment 4, there was a trend that increase in low spatial composition ratio resulted in more myopic on day 4. The effect became more obvious on day 7 and became significant. Corresponding eyeball elongation was observed as the ratio of low spatial composition increased.

## **Conclusions**

This study showed that there was a spatial-defocus interaction, from human retinal activity to myopia progression in chick eye. The mfERG measurement showed that in human retina, the outer and inner retina have different characteristics in processing spatial details. In addition, the peripheral retina could differentiate positive and negative defocus more effectively for low spatial frequencies than the central retina. The human retina was hypothesized to have a decoding system for optical defocus, which was tuned to low spatial frequency, and was located in the retinal near periphery. In chick studies, the results echoed with the human results. The myopia progression induced by hyperopic defocus was shown to depend on spatial stimulus. The rate of compensation to induced hyperopic defocus was higher with low spatial frequency stimulus. In addition, under the same magnitude of hyperopic defocus, trends of increased myopia and ocular

elongation were observed when the spatial composition was gradually increased from higher to lower spatial frequency. Various combinations of spatial details influence eye growth even at the same levels of hyperopic defocus. It was speculated that interactive mechanisms between spatial and optical defocus on myopia development may be useful in future to apply for controlling myopia progression.

## **PUBLICATIONS**

### **Publications arising from the thesis**

1. Chin, M. P., Chu, P. H., Cheong, A. M. and Chan, H. H. (2015a) 'Human electroretinal responses to grating patterns and defocus changes by global flash multifocal electroretinogram', PLoS One, 10(4), pp. e0123480.
2. Chin, M. P., Cheong, A. M. and Chan, H. H. Spatial Interactive Effects on Myopia Development in Chick (Manuscript prepared for submission).

### **Conference Presentations**

1. Chin, M.P., Chu, P.H.W., Cheong, M.Y., and Chan, H.H.L. (2012). Electretinal response to spatial frequencies in human eye. American Academy of Optometry Annual Meeting 2012. Phoenix, USA. Poster Presentation.
2. Chin, M.P., Chu, P.H.W., Cheong, M.Y., and Chan, H.H.L. (2013). Effects of Spatial Frequency With Optical Defocus on Human Electroretinal Responses. The 9<sup>th</sup> International Symposium of Ophthalmology. Guangzhou, China. Poster Presentation.
3. Chin, M.P., Li, Z.C., Cheong, A.M.Y., and Chan, H.H.L. (2015). Compensatory eye growth responded to the imposed defocus is influenced by spatial content in chick. The Association for Research in Vision and Ophthalmology annual meeting. Denver, USA. Poster Presentation.

### **Other Publications and Presentations**

1. Chin, M. P., Siong, K. H., Chan, K. H., Do, C. W., Chan, H. H. and Cheong, A. M. (2015b) 'Prevalence of visual impairment and refractive errors among different ethnic groups in schoolchildren in Turpan, China', Ophthalmic and Physiological Optics, 35(3), pp. 263-70.
2. Chu, P.H.W., Li, H.Y., Chin, M.P., So, K.F., and Chan, H.H.L. (2015). 'Effect of Lycium Barbarum (Wolfberry) Polysaccharides on preserving retinal function after partial optic nerve transection.' PLoS ONE, 8(12), pp. e81339.
3. Wong, H.Y., Chin, M.P., Lee, C.W., Yung, M.Y. and Chan, H.H.L. (2014). Detection of early macular functional changes using slow double-stimulation mfERG paradigm. American Academy of Optometry Annual Meeting 2014. Denver, USA.

## ACKNOWLEDGEMENTS

I would like to take this opportunity to express my most sincere thanks to people who contributed or provide valuable advices to the completion of work.

I am deeply indebted to my chief supervisor, Dr. Henry Chan who's outstanding knowledge and insightful ideas in electrophysiology and myopia. He has been giving me plenty of professional guidance and support on both my research and outlook on life. I was privileged to under the supervision with him, and he has also guided me through the whole writing process with great patience and provided helpful advices necessary to complete my thesis.

I am also grateful to my co-supervisor, Dr. Allen Cheong, for devoting much time for helping me to review my manuscripts and your suggestions are very much appreciated. I need to thank Dr. Kee Chea-Su, for devoting much time for providing suggestions and teaching me skills on handling refractometer.

I would also like to thank the optometry research student group, where I have made good friends with good memories during these years of research student life. We always cheer each other up.

Finally, I have to thank my family especially my wife Cynthia Tsoi, who provides me with unconditional emotional support and continuous caring.



5.2.	Methods.....	51
5.2.1.	Experiment Setup.....	51
5.2.2.	Presentation of grating stimuli.....	52
5.2.3.	Global flash mfERG stimulation.....	54
5.2.4.	Subject recruitment.....	56
5.2.5.	Recordings.....	57
5.2.6.	Data analysis.....	58
5.3.	Results.....	59
5.4.	Discussion.....	66
	5.4.1. Potential influence of edge effects as well as retinal lateral interactions on retinal activity.....	69
5.5.	Conclusion.....	70
Chapter 6. Experiment 2. Human electroretinal responses to defocus under different spatial stimulus.....		
		71
6.1.	Introduction.....	72
6.2.	Methods.....	73
6.2.1.	Experiment Setup.....	73
6.2.2.	Subject recruitment.....	74
6.2.3.	Evaluating the cycloplegic effect and residual accommodation.....	75
6.2.4.	Data analysis.....	76
6.3.	Results.....	76
6.4.	Discussion.....	84
6.4.1.	Regional sensitivity to defocus.....	84
6.4.2.	Spatial frequencies and defocus.....	86
6.4.3.	Does retinal image at different spatial frequency and retinal defocus affect myopia?.....	90
6.4.4.	The consideration of aliasing effect in the experimental design.....	91
6.4.5.	The pros and cons of using non-scaled stimulus patterns in human study.....	91
6.5.	Conclusion.....	92
Chapter 7. Experiment 3. Spatial dependency of myopia development in chick.....		
		93
7.1.	Introduction.....	95
7.2.	Methods.....	97
7.2.1.	Animals.....	97
7.2.2.	Lens-cone system.....	97

7.2.3.	Visual target .....	101
7.2.4.	Measurement .....	102
7.2.5.	Experimental Groups and Treatment Protocol .....	104
7.3.	Data analysis .....	105
7.4.	Results .....	105
7.4.1.	Refractive Error.....	108
7.4.2.	Axial length.....	111
7.4.3.	Vitreous chamber depth.....	113
7.4.4.	Eyeball elongation and refractive errors ....	116
7.5.	Discussion .....	118
7.5.1.	Emmetropization with and without hyperopic defocus .....	118
7.5.2.	Response to magnitude of defocus.....	123
7.6.	Conclusion .....	125
Chapter 8. Experiment 4. Compensation to constant hyperopic defocus is locally spatial sensitive .....		
		126
8.1.	Introduction .....	128
8.2.	Methods.....	130
8.2.1.	Animals .....	130
8.2.2.	Lens-cone system.....	131
8.2.3.	Visual target.....	132
8.2.4.	Measurement .....	135
8.2.5.	Experimental Groups and Treatment Protocol.	136
8.3.	Data analysis .....	136
8.4.	Results .....	137
8.4.1.	Refractive Error.....	139
8.4.2.	Vitreous chamber depth and axial length...	140
8.4.3.	Anterior chamber depth and lens thickness	143
8.5.	Discussion .....	145
8.5.1.	Could accommodation compensate differently to the imposed defocus under different spatial frequency? .....	146
8.5.2.	Possible mechanism for spatial tuning in decoding defocus .....	147
8.6.	Conclusion .....	148
Chapter 9. General Discussion and Future Directions .....		
		149
9.1.	Spatial vision and spatial frequency.....	149
9.2.	Spatial vision and optical defocus.....	151

9.3. Retinal site for detecting defocus.....	153
9.4. From retinal activity to eye growth.....	154
9.5. Emmetropization end-point.....	155
9.6. Future Directions.....	160
9.6.1. Interactive retinal tuning to spatial frequency and defocus .....	160
9.6.2. Clinical implication of spatial frequency in myopia control .....	161
9.7. Limitations .....	163
9.7.1. Square-wave spatial frequencies were used in the experiments .....	163
9.7.2. Adopting the relatively low spatial frequency in the experiments .....	164
9.7.3. Effect of magnification factor .....	165
APPENDICES .....	168
APPENDIX A .....	168
APPENDIX B .....	169
REFERENCES.....	170

## ABBREVIATIONS

ACD	Anterior chamber depth
ANOVA	Analysis of variance
AXL	Axial length
cpd	Cycle per degree
CRT	Cathode ray tube
D	Dioptre
DC	Direct component
DTL	Dawson-Trick-Litzkow
ERG	Electroretinogram
FD	Form deprivation
FDM	Form-deprivation myopia
GABA	Gamma-aminobutyric acid
IC	Induced component
LCD	Liquid-crystal display
LIH	Lens induced hyperopia
LIM	Lens induced myopia
LT	Lens thickness
mfERG	Multifocal electroretinogram
MOFO	Global flash Multifocal electroretinogram
N1	First negative trough response in conventional mfERG
N2	Second negative trough response in conventional
NMDA	N-methyl-D-aspartic acid
P1	First positive peak response in conventional mfERG
PERG	Pattern electroretinogram
R	Pearson's correlation coefficient
RE	Refractive error
SD	Standard deviation
SE	Spherical-equivalent
SEM	Standard error of the mean
SF	Spatial frequency
SPSS	Statistical Package for the Social Sciences
TTX	Tetrodotoxin
VCD	Vitreous chamber depth
VERIS	Visual Evoked Response Imaging System

# LIST OF FIGURES

## Chapter 1

**Figure 1.1. Schematic diagram demonstrates light rays entering the eye (A)** In emmetropia, the light ray enters the eye and focus on the fovea in human eye. **(B)** In axial myopia, the light ray enters the eye and focuses in front of the fovea.

## Chapter 3

**Figure 3.1.** A typical 103 scaled (left) and non-scaled (right) hexagon pattern for mfERG recording.

**Figure 3.2. Topographical presentation of the retinal response. (A)** Three-dimensional plot. **(B)** Trace array. **(C)** Ring-averaged response from central (Ring 1) to mid-peripheral (Ring 6) regions.

**Figure 3.3. The first order response.** A schematic diagram illustrates how the first-order response is obtained. The white and black hexagons represent the bright (flash) and dark (no flash) presentations respectively. The hexagon that in grey colour represents the frame not under consideration in the computation of the response. The first-order kernel is obtained by averaging the responses from all dark presentations, and subtracting the averaged responses from all bright presentations within the m-sequence. (Figure is adapted and modified from Sutter (2000)).

**Figure 3.4. The waveform appearance of a typical first-order kernel response.** It consists of an initial negative trough (N1), a second positive peak (P1), and a negative trough (N2).

**Figure 3.5. The second order response.** A schematic diagram illustrates the second-order response is obtained. The white and black hexagons represent the bright (flash) and dark (no flash) presentations respectively. The hexagon that in grey colour represents the frame not under consideration for the computation of the response. The second-order kernel is achieved by adding all the responses with different stimuli between

preceding and current frames (i.e. either bright-to-dark or dark-to-bright), and subtracted from all the responses with the same stimulus between two consecutive frames (i.e. Bright-to-bright or dark-to-dark) (Figure is adopted and modified from Sutter (2000)).

**Figure 3.6. Schematic diagram for global flash paradigm of mfERG.** Upper: The sequence of global flash paradigm: local multifocal flashes frame(M), dark frame (O), global flash frame(F), dark frame (O). Lower: Waveform of global flash mfERG showing the amplitude and implicit time of DC, and the amplitude and implicit time of IC.

## Chapter 5

**Figure 5.1. Figure 5.1. Schematic diagram of mfERG setup.** The SF gratings were presented on a 22-inch LCD display. The global flash mfERG stimulation was driven by VERIS Science 6.0.6d19. The mfERG signal was amplified a gain of X 100,000 with a bandpass of 10-300 Hz.

**Figure 5.2. Figure 5.2. Stimuli with different spatial frequencies presented to subjects for mfERG recording.** Spatial frequencies of 0.24, 1.2, 2.4 and 4.8 cpd were used. Only ring 1 to 3 were shown in the figure.

**Figure 5.3. Schematic diagram for grouping the mfERG responses and the waveform of MOFO mfERG.** Left: Both DC and IC responses were pooled into concentric rings with eccentricity from ring 1 (1.75°) to ring 6 (19.20°) Right: Schematic diagram for DC amplitude and implicit time, IC amplitude and implicit time of MOFO mfERG.

**Figure 5.4. The global flash mfERG response to spatial frequency. (A)** The typical global flash mfERG waveform measured from one subject with 4 SF gratings for six different retinal regions. **(B)** Normalized amplitudes of DC and IC response to SF of all subjects.

**Figure 5.5.** Absolute amplitudes of DC (mean  $\pm$  SEM) with SF of 0.24cpd to 4.8cpd from ring 1 to 6. The DC responses were generally increased with SF in all regions. Those marked with an asterisk “\*” are statistically different from the 0.24cpd.

**Figure 5.6.** Absolute amplitudes of IC (mean  $\pm$  SEM) with SF of 0.24cpd to 4.8cpd of ring 1 to 6. In ring 1 and 2, the IC responses were similar. While from ring 3 to 6, the IC responses behaved differently from the central retina. Those marked with an asterisk “\*” are statistically different from the 0.24cpd while those with an asterisk “#” are statistically different between 4.8cpd and 2.4cpd.

## Chapter 6

**Figure 6.1. The typical global flash mfERG waveform from one subject for high and low spatial frequency under different defocus.** Upper panel: (A), (B) and (C) are responses from 0.24cpd under defocus of -2D, plano and +2D respectively. Lower panel: (D), (E) and (F) are response from 4.8cpd under defocus of -2D, plano and +2D respectively.

**Figure 6.2. Percentage change of DC and IC with imposing defocus under 0.24cpd or 4.8cpd.** (A) Percentage change of DC amplitudes (mean  $\pm$  SEM) with imposing defocus under 0.24cpd or 4.8cpd across the region. (B) Percentage change of IC amplitudes (mean  $\pm$  SEM) with imposing defocus under 0.24cpd or 4.8cpd across the region. Left panel is 0.24cpd and right panel is 4.8cd. Those marked with an asterisk “\*” are statistically different between +2D and -2D defocus.

## Chapter 7

**Figure 7.1. Lens-cone device and animal preparation.** (A) Schematic diagram of a lens-cone device. A lens was placed at proximal end of the device. A visual target with different spatial patterns was positioned at the distal side of the device. (B) and (C) Attachment of the lens-cone device on the chick’s right eye. The eye was

tried to position at the centre of the lens and the device was stabled by Velcro. **(D)**. 10 to 11 days old chicks were used as they adapted to the lens-cone device quicker and returned to normal feeding behavior in a day.

**Figure 7.2. Schematic diagrams of high contrast black and white checkers as visual stimulus. (A)** Uniform small checkers as high spatial content. The size of the check was 0.4mmX0.4mm (0.9 cpd at 4 cm). **(B)** Uniform checkers as low spatial content. The size of the check was 1.2mmX1.2mm (0.3 cpd at 4 cm).

**Figure 7.3. Ultrasound waveforms generated from a chick eye.** The major peaks corresponding to the cornea, anterior lens surface, posterior lens surface and posterior segment are visible (from left to right). Post-acquisition analysis was carried out on the waveform ‘peak assignments’ to identify the components including anterior chamber depth (ACD), lens thickness (LT), vitreous chamber depth (VCD) and axial length (AXL).

**Figure 7.4. The interocular difference in refractive error from before treatment (A), after 4 days (B) and 7 days (C) of monocular treatment using lens-cone device.** X-axis represents the magnitude of defocus applied to the right eye. Y-axis represents the interocular refractive error (treatment minus control). Blue bar and red bar represent the low and high SF content respectively. Error bars represent standard error of mean. Asterisks denote statistical significance with  $p < 0.05$ .

**Figure 7.5. The interocular differences in axial lengths from before treatment (A), after 4 days (B) and 7 days (C) of monocular treatment using a lens-cone device.** X-axis represents the amount of defocus applied. Y-axis represents the interocular axial length (treatment minus control). Blue and red bars represent the low and high SF content respectively. Error bars represent standard error of the mean. Asterisks denote

statistical significance with  $p < 0.05$ .

**Figure 7.6. The interocular differences in vitreous chamber depth from before treatment (A), after 4 days (B) and 7 days (C) of monocular treatment using lens-cone device.** X-axis represents the magnitude of defocus applied on the right eye. Y-axis represents the interocular vitreous chamber depth (treatment minus control). Blue and red bars represent the low and high SF content respectively. Error bars represent standard error of the mean. Asterisks denote statistical significance with  $p < 0.05$ .

**Figure 7.7.** Interocular VCD difference versus interocular RE difference on (A) day 4 and (B) day 7.

**Figure 7.8.** The Maltese crosses (A and B) and visual patterns used in the current experiment (C and D) and their respective spatial energy spectrums are shown in (E) and (F). It is noted that, in both Maltese crosses, the contributions from lower range of SFs are rather similar and there is an increase of high SFs for the striped Maltese cross (B). For the patterns in (C) and (D), the contributions from high and low SF are very different. (Figure 7.8A and B were adopted from Diether and Wildsoet (2005) study.)

## Chapter 8

**Figure 8.1. Schematic diagram of a lens-cone device.** The lens was placed at proximal end of the device. Visual target with different spatial patterns was positioned at the distal side of the device. Refer to Section 8.2.3 for the description of spatial composition of visual stimuli (H;3H1L; 1H1L;1H3L;L).

**Figure 8.2. The patterns of visual stimuli used in the experiment.** (A) and (E) Uniform checkers of high and low SF which were used in Experiment 3. (B), (C) and (D) were the patterns composed of checker mixtures of high and low SF. (B) 3H1L: One area unit of large checkers with 3 area units of small checkers. (C) 1H1L: One area unit of large checkers with one area unit of small checkers. (D) 1H3L: One area unit

of small checkers with 3 area units of large checkers.

**Figure 8.3.** The interocular differences in refractive error from before treatment (blue line), after 4 days (red line) and 7 days (green line) with monocular treatment with lens-cone device. X-axis represents the spatial frequency compositions. Y-axis represents the interocular difference in refractive error (treatment minus control). Error bars represent the standard error of the mean. Asterisks denote statistical significance with  $p < 0.05$ .

**Figure 8.4.** The interocular differences in vitreous chamber depth (A) and axial length (B) from before treatment (blue line), after 4 days (red line) and after 7 days (green line) with monocular treatment with lens-cone device. The X-axis represents the spatial frequency compositions of the stimuli. The Y-axis represents the interocular difference of (A) VCD and (B) AXL (treatment minus control). Error bars represent the standard error of the mean. Asterisks denote statistical significance with  $p < 0.05$ .

**Figure 8.5.** The interocular difference in anterior chamber depth (A) and lens thickness (B) from before treatment (blue line), after 4 days (red line) and after 7 days (green line) with monocular treatment with lens-cone device. The X-axis represents the spatial frequency compositions of the stimuli. The Y-axis represents the interocular difference of (A) AXL and (B) LT (treatment minus control). Error bars represent the standard error of the mean.

## Chapter 9

**Figure 9.1. Visual processing in the retina.** (A) Schematic diagram for channeling spatial information in retina. Visual stimulus is composed of a range of spatial frequencies. The retina is hypothesized to possess various channels acting as filters for different spatial frequencies. (B) Contrast sensitivity function (CSF, solid line) is formed by combining numerous individual

channels (dashed lines) (Billock, 2000; Billock and Harding, 1996; Sekuler *et al.*, 1984).

**Figure 9.2. Images and respective spatial spectra.** The full picture and its spatial spectrum are shown in **(A)**. The image in **(A)** is broken down into nine individual images and their spatial spectra were shown in **(B)**. Note that the profile of the images is similar, obeying  $1/f'$  function while the slopes are varied.

**Figure 9.3. Visual environment characterizing different profiles of spatial composition and defocus.** **(A)** Spatial composition, green: more high spatial frequency; red: more low spatial frequency. **(B)** Defocus, green: myopic defocus; red: hyperopic defocus. Saturation of the colors represents relative strength.

## Appendix

**Appendix A.** Global flash mfERG response for spatial frequency in high myopic subjects. DC amplitude and IC amplitude of 12 age-matched subjects with spherical equivalent of  $-6.54 \pm 1.63D$ , are shown. The general trends of DC and IC amplitudes against spatial frequency for the high myope group were similar to those from the low myope group (Refer to **Figure 5.6**).

## LIST OF TABLES

### Chapter 5

**Table 5.1.** The DC and IC implicit for different spatial frequency and retinal region.

### Chapter 6

**Table 6.1.** Summary of amplitude (mean  $\pm$  SEM) of DC and IC from ring 1 to 6 under different defocus conditions with 0.24cpd or 4.8cpd.

**Table 6.2.** The DC and IC implicit time for high and low SF under defocus and plano conditions for different retinal regions.

### Chapter 7

**Table 7.1.** Treatment condition for each group of chicks.

**Table 7.2.** Interocular differences in response to monocular lens cone device wear on day 4. Statistical significances between H and L spatial group for each defocus group. Asterisk denotes  $p < 0.05$ . Abbreviations: N = Number of animals in group.

**Table 7.3.** Interocular differences in response to monocular lens-cone device wear on day 7. Statistical significances between H and L spatial group for each defocus group. Asterisk denotes  $p < 0.05$ . Abbreviations: N = Number of animals in group.

**Table 7.4.** Pearson's correlation and its significance between refractive error and ocular biometric parameters (ACD, LT, VCD and AXL).

### Chapter 8

**Table 8.1.** Treatment condition for each group of chicks. H=100 % high SF; 3H1L=75% high SF: 25% low SF; 1H1L=50% high SF:50% low SF; 1H3L= 25% high SF:75% low SF; L= 100% low SF.

**Table 8.2.** Interocular differences in response to monocular lens-cone device wear. Abbreviations: N = Number of animals in group.

### Appendix

**Appendix B.** The interocular difference of vitreous chamber depth in response to different lens powers and different

spatial frequency patterns. With induction of -25D defocus, chick eyes with low SF stimulus elongated faster than with high SF stimulus, similar to the trend shown in other defocus conditions.

**Part I.**  
**INTRODUCTION AND LITERATURE**  
**REVIEW**

## Chapter 1. Introduction

Myopia (commonly known as short-sightedness/near-sightedness) is mainly due to an excessive increase in axial length (AXL) (Adams, 1987; Lin *et al.*, 1996; Meng *et al.*, 2011; Meyer *et al.*, 1999) . When the AXL is longer than the focal length of the eye, the optical power of the eye (at fovea) cannot match with the excessively long AXL and the focal point will focus in front of the retina (**Figure 1.1.**). The prevalence of myopia varies across regions and ethnicities (Chin *et al.*, 2015b; Lam *et al.*, 2004; Logan *et al.*, 2011; Pan *et al.*, 2015a; Pan *et al.*, 2015b; Pan *et al.*, 2012). Prevalence of myopia is higher in East Asian countries than other countries (Meng *et al.*, 2011; Pan *et al.*, 2012; Park and Congdon, 2004), with the myopia prevalence in some urban areas reaching as high as 80-90% (Lam *et al.*, 2004; Lin *et al.*, 2004). Myopia is a global vision threatening problem (Holden *et al.*, 2016), especially in the Chinese population.

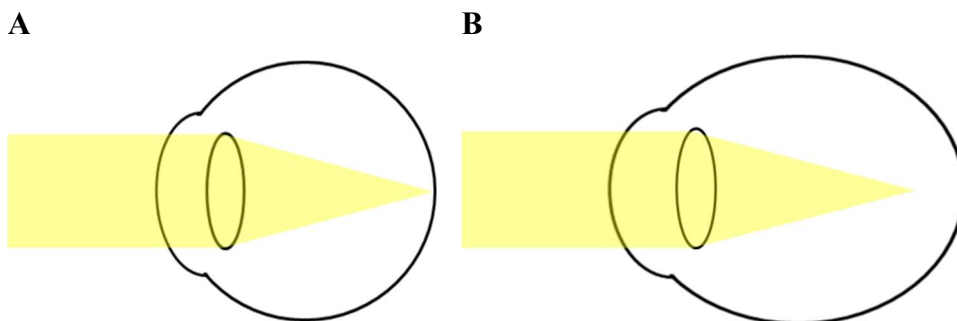


**Figure 1.1. Schematic diagram demonstrates light rays entering the eye (A) In emmetropia, the light ray enters the eye and focus on the fovea in human eye. (B) In axial myopia, the light ray enters the eye and focuses**

in front of the fovea.

The development of myopia is known to be influenced by both genetic and environmental factors. (Siegwart and Norton, 2011; Wojciechowski, 2011).

Twin studies and myopic familial pattern studies have shown the genetic influence on myopia (Baird *et al.*, 2010; Dirani *et al.*, 2006; Hammond *et al.*, 2001; Wojciechowski *et al.*, 2005). In a recent study concerning the refractive development for monozygotic twins, the more myopic twin was found to be associated with having a higher occupational status, performing more close work, and living in a more urban area than their twin (Ramessur *et al.*, 2015). The rapid increase in myopia prevalence in recent decades highlights the significance of environmental factors.

Consistently, myopia prevalence in urban areas was reported to be higher than in rural regions (Czepita *et al.*, 2008; He *et al.*, 2009; Ip *et al.*, 2008a; Lu *et al.*, 2009; Shih *et al.*, 2010; You *et al.*, 2014). Ip and co-workers (2008) reported that myopia prevalence was lower in outer sub-urban regions than that in inner city region. In addition, environmental risk factors such as near work (Angle and Wissmann, 1980; Hepsen *et al.*, 2001; Mohan *et al.*, 1988), less outdoor activities (He *et al.*, 2015; Rose *et al.*, 2008; Sherwin *et al.*, 2012b), and high education level (Jonas *et al.*, 2016; Mutti *et al.*, 2002) are associated with higher magnitude of myopia. It is clearly that

environmental/external factors influence both myopia progression as well as prevalence.

Myopia progression is mainly the result of axial elongation of eyeball and the structural changes during myopia progression causes retinal thinning.

Clinically, high myopia is correlated with various degenerative retinal changes such as lattice degeneration, retina hole or tear, posterior staphyloma, lacquer crack, and choroidal neovascularization (Neelam *et al.*, 2012; Ohno-Matsui *et al.*, 2015; Wong *et al.*, 2014). The World Health Organization regards myopia as one of the threatening eye conditions causing blindness (Pascolini and Mariotti, 2012). It is important to understand the mechanism of myopia development to prevent or slow the progression of myopia.

## Chapter 2. Emmetropization

For decades, considerable efforts have been dedicated to understanding eye growth and the mechanism of myopia development (myopia can be regarded as an altered rate of eye growth) and various ways to prevent and control myopia. The focal length of the eye is short at birth, so that the retina is usually located in front of the focal plane, resulting in hyperopia (Baldwin, 1990; Ehrlich *et al.*, 1997; Kuo *et al.*, 2003; Tarczy-Hornoch, 2012). It is suggested that when hyperopia is detected by the retina, the eye growth rate is increased by modulating different biochemical and biomechanical properties of the scleral shell (McBrien *et al.*, 2000; Rada *et al.*, 2006; Siegwart and Norton, 1999; Siegwart and Norton, 2005). Then, the AXL increases and the retina moves closer to the focal plane of the eye, reducing the magnitude of hyperopia. Eventually, when the AXL matches with the focal plane, an emmetropic eye results so that a distant object is focused on the retina without accommodation, and the whole process is termed emmetropization. It is suggested that ocular parameters such as anterior chamber depth, crystalline lens thickness, axial length, as well as refractive error are initially controlled by genetics (Siegwart and Norton, 2011). The eye should be similar to other body organs, that possess a

homeostatic control to maintain an optimal size (Wallman and Winawer, 2004). The growth of the eyeball during the infant and juvenile periods, in theory, is the same as for other body parts. They are presumably programmed by genetic factors, which follows a time course that increases in relationship to age (Siegwart and Norton, 2011). However, it appears that the rate of refractive error change is related to initial refractive error in infants (Mutti *et al.*, 2005; Saunders *et al.*, 1995). For example, infant eyes that are more hyperopic at 3 months of age grow more rapidly than average; in contrast, eyes that are less hyperopic at 3 months old grow much slower (Mutti *et al.*, 2005). These adjustments suggest that emmetropization is guided by visual signals.

Although there is reported spontaneous myopia of some wild animals (Jiang *et al.*, 2009), it is observed that normal postnatal refractive development is mild hyperopia or close to emmetropia in various species (Belkin *et al.*, 1977; Graham and Judge, 1999; Norton and McBrien, 1992; Wallman *et al.*, 1981; Zhou *et al.*, 2006). The process of emmetropization was investigated using wide range of animal species, including fish (Shen *et al.*, 2005), pigeon (Fitzke *et al.*, 1985), chick (Irving *et al.*, 1992; Wallman *et al.*, 1978), tree shrew (Sherman *et al.*, 1977), guinea pig (Howlett and McFadden, 2006;

Howlett and McFadden, 2009), marmoset (Troilo and Judge, 1993; Troilo *et al.*, 2000; Whatham and Judge, 2001), mouse (Barathi *et al.*, 2008; Schaeffel *et al.*, 2004; Tejedor and de la Villa, 2003), cat (Belkin *et al.*, 1977), American kestrel, (Andison *et al.*, 1992) and monkey (Guyton *et al.*, 1989; Raviola and Wiesel, 1978; Smith *et al.*, 1999; Smith and Hung, 1999; Smith *et al.*, 2002; Smith *et al.*, 2007; Wiesel and Raviola, 1977). While emmetropization exists in wide range of species, human myopia is caused by excessive increase in AXL, which, to infer, can be regarded as uncontrolled/ disturbance of emmetropization by some environmental/external factors.

## **2.1. Environmental factors affecting eye growth**

The eye is regarded as a part of the brain, and is believed to be plastic during infancy and early childhood. It possesses the ability to respond to changes in the sensory input (Mrsic-Flogel *et al.*, 2007). It is believed that, by manipulating environmental factors, the rate of eye growth can be altered. Over 150 years ago, there were studies suggesting near work induced myopia. Cohn (1867) noticed children developed myopia after they had started attending school (cited in Sato,1980) (Sato, 1980). Cohn suggested attending school causing the use of the eyes for close work

produced myopia. Tscherning (1882) found that persons with occupations involving less near work had lower prevalence of myopia (Farmers and fishermen 2.4% versus advanced students 32.4%) (Norn and Jensen, 2004; Tscherning, 1882). People with higher education levels and higher socioeconomic classes presumably spend more time in studying, thus performing more near work. Since then, epidemiological studies have indicated schooling, reading, study, and other kinds of near work are associated with myopia development, despite that association studies do not imply causality. (Czepita *et al.*, 2008; Goss and Rainey, 1999; He *et al.*, 2015; Ip *et al.*, 2008b; Jonas *et al.*, 2016; Lin *et al.*, 2014; Lu *et al.*, 2009; Mutti *et al.*, 2002).

## **2.2. Excessive accommodation mechanism**

As the association of near work and myopia is highlighted in many studies, accommodation of the eye becomes the suspect in myopia development. The hypothesis of excessive accommodation and accommodation lag was the explanation for the pathogenesis of human myopia for many years (Donders and Moore, 1864; Mutti *et al.*, 2006; Tarczy-Hornoch, 2012; Young, 1977). The hypothesis is that as near work triggers accommodation, in turn there is a feedback mechanism for the eye to elongate. Simply

speaking, more accommodation triggers faster eye growth. Initially, this hypothesis was supported by some clinical studies using progressive or bifocal lenses to reduce accommodation demands and therefore to slow down myopia progression (Leung and Brown, 1999). However, subsequent large scale randomized studies showed poor success in controlling myopia using bifocal and progressive lenses. In contrast, application of atropine, a muscarinic cholinergic agent which can paralyze accommodation, was shown to be effective in slowing myopia in some human and animal studies (Bedrossian, 1979; Brodstein *et al.*, 1984; Young, 1965). But, other cycloplegic agents, such as tropicamide (Saw *et al.*, 2002), failed to halt myopia progression. It is suggested that the posterior retina rather than the intraocular muscle is the possible site of action for atropine in retarding myopia progression (Cottrill and McBrien, 1996; Luft *et al.*, 2003; McBrien *et al.*, 1993) as chick myopia was inhibited by atropine, but this drug has no effect on accommodation. Furthermore, evidence against the accommodation hypothesis from animal studies showed that when the accommodation signal was blocked either by section of the ciliary nerves (Schmid and Wildsoet, 1996; Shih *et al.*, 1994) or pharmaceutically (Schwahn and Schaeffel, 1994; Wildsoet and Wallman, 1995), myopic

development still persisted. These indicate accommodation is not essential for emmetropization.

## **2.3. Visual feedback and eye growth**

### **2.3.1. Form deprivation myopia**

The growth of the eyeball is clearly a response to visual stimulus. In some previous human studies, conditions that degraded the quality of the visual image, such as congenital cataract (von Noorden and Lewis, 1987; Zhang and Li, 1996), ptosis (Gusek-Schneider and Martus, 2001), or corneal opacification (Gee and Tabbara, 1988), resulted in myopia progression, which highlights the importance of visual information in controlling eye growth. Similar phenomena were also widely explored in animal studies. In 1970s, Hubel and Wiesel sutured the eyelid of a monkey eye and noticed that its size was significantly larger than the fellow eye (Wiesel and Raviola, 1977). Depriving vision, such as suturing the lid (Marsh-Tootle and Norton, 1989; Sherman *et al.*, 1977; Yinon *et al.*, 1982), inducing cornea opacity (Wiesel and Raviola, 1979), or wearing diffuser goggles (Howlett and McFadden, 2006; Smith and Hung, 2000), cause excessive eyeball elongation in various species of animals. Depriving vision of the animals results in axial elongation and has become a commonly used animal model

for investigating myopia. It is termed form-deprivation myopia (FDM).

### **2.3.2. Image properties in form deprivation myopia**

When the eye experiences form deprivation (FD) as described above, the retinal image quality is greatly degraded. It further reduces the retinal illuminance and the retinal image contrast. These cause a greater loss of high spatial details compared with low spatial information. Thus, luminance, spatial frequencies, and contrast of the retinal image are believed to be the primary factors in modulating eye growth in the FDM animal model.

Bartman and Schaeffel (1994) suggested the magnitude of FDM is related to the quality of visual stimulus (Bartmann and Schaeffel, 1994). This idea, however, is challenged by later experiments that demonstrated that the eye can emmetropize under the stimulus of scrambled images (Hess *et al.*, 2006; Schaeffel, 2006).

#### **2.3.2.1. Contrast**

The role of contrast in FDM was investigated in various animal models. In an early study, Bartmann and Schaeffel (1994) suggested the amount of FDM was correlated with reduction of retinal image contrast (Bartmann and Schaeffel, 1994). Most studies demonstrated when contrast is reduced to certain level, FDM results (Schmid *et al.*, 2006; Schmid and Wildsoet, 1997; Tran *et al.*, 2008). Schmid and Wildsoet (1997) showed that presenting contrast stimulus as low as 9% for 20 mins per day could already retard

FDM (Schmid and Wildsoet, 1997). More systematic investigation on how varying contrast influences on emmetropization was later performed by Schmid and co-workers (Schmid *et al.*, 2006). Their results showed that the visual signal to emmetropization would function if certain level of image contrast was reached (higher than sensitivity threshold).

### **2.3.2.2. Spatial frequency**

A visual image consists of a range of spatial frequencies for the eye to decode. In humans, the spatial resolution peaks at the central fovea and decreases with retinal eccentricity (Hunziker, 2007). The relationship of normal eye growth and spatial frequency content has been investigated (Bartmann and Schaeffel, 1994; Diether and Wildsoet, 2005; Hess *et al.*, 2006; Schaeffel, 2006; Schmid and Wildsoet, 1997; Wallman *et al.*, 1987). In chick, Bartmann and Schaeffel (1994) showed, without the influence from accommodation and colour, increased frosting of the occluders resulted in increased myopia development. This implied that eye growth is a graded response and is modulated by the image quality (Bartmann and Schaeffel, 1994). The frosted occluders can be regarded as a low pass filter. The more frosted the occluders, the lower the spatial frequency stimulus is presented to the eye. Other species like guinea pigs (Bowrey *et al.*, 2015)

and monkeys (Smith and Hung, 2000) also demonstrate that eye growth is sensitive to the cutoff spatial frequency. The concept of spatial frequency as a modulation signal in FDM was later investigated by Schmid and Wildsoet (1997). They found that by exposing the chicks with mid spatial frequency of 0.86 cycle per degree (cpd) for a duration of 20 mins per day was more effective than either high (4.3 cpd) or low SF (0.086 cpd) to prevent FDM. They suggested emmetropization was sensitive to spatial frequency changes (Schmid and Wildsoet, 1997). The spatial frequency used in Schmid and Wildsoet (1997) was within the chick's acuity sensitivity. Interestingly, Bowrey and colleagues (2015) demonstrated myopia could be induced even the loss of high spatial frequency was beyond the eye sensitivity in guinea pig. The spatial frequency that affecting inhibition of FDM may not be the same as those involved in eliciting FDM.

### **2.3.2.3. Luminance**

As mentioned in Chapter 1, people living in urban area have a higher prevalence of myopia. Some studies associated higher myopia rate with reducing time spending on outdoor activities. As a result, there is a reduction in exposure to higher light intensity, which is suggested as a protective factor to myopia development (Dirani *et al.*, 2009; Jones *et al.*,

2007; Rose *et al.*, 2008; Wu *et al.*, 2013). The difference in light intensity between indoors (100 to 1,000 lux) and outdoors (120,000 to 200,000 lux) are huge. While exposure to sunlight has been suggested to have an anti-myopia effect, relevant animal studies were by Ashby and colleagues (Ashby *et al.*, 2009; Ashby and Schaeffel, 2010) that experimental myopia in chicks induced by diffusers can be arrested by higher luminance levels. In addition, high ambient light has been shown to have a protective effect against FDM in rhesus monkey (Smith *et al.*, 2012). However, when increased light levels were combined with negative lens wear (See 2.3.3), the eyes eventually compensated fully for the power induced (Ashby and Schaeffel, 2010). Thus, that the sign response and endpoint for lens compensation is not affected by bright lights.

#### **2.3.2.4. Chromatic aberrations and chromaticity**

Studies have suggested that the eye is capable of using cues from longitudinal chromatic aberration to guide the growth of eyeball (Rucker and Wallman, 2009). Chromatic aberrations were thought to be a factor for guiding eye growth as multiple focal planes presented at the same time can be compared to derive directional information. For example, the accommodative response to chromaticity has been well documented (Kruger

*et al.*, 1993; Rucker and Kruger, 2004; Seidemann and Schaeffel, 2002) demonstrating that longer wavelengths (red) light are focused more posteriorly in the retina than shorter wavelengths (blue) light. To study the effects of chromaticity on ocular growth and refractive development, Foulds and colleagues (2013) found that keeping chicks under red light resulted in myopia progression. In contrast, keeping chicks under blue light resulted in hyperopia (Foulds *et al.*, 2013). Although similar results were reported in guinea pigs (Long *et al.*, 2009), contradictory results recently obtained from work on monkeys showed that long-wavelength lighting may be beneficial in reducing myopia progression (Smith *et al.*, 2015). Thus, chromaticity may not be a fundamental factor in the emmetropization process (Wildsoet *et al.*, 1993). Although emmetropization has been seen in wide range of species, the visual channels possessed for detecting the wavelength spectrum vary between species (Jacobs, 2009). For instance, most terrestrial non-primate mammals are dichromatic, and birds are tetrachromacy (Hart, 2001) while humans and most primates are trichromatic (Boothe, 2001). Thus, chromaticity may not be a crucial factor to guide eye growth.

### **2.3.3. Optical defocus induced refractive errors**

Other than FDM, another animal model for investigating myopia is

spectacle lens induced compensation (Irving *et al.*, 1991; Schaeffel *et al.*, 1988). The eye grows according to the sign and magnitude of the ophthalmic lens applied. When a plus lens is placed in front of the eye, presuming the eye is under exposure to myopic defocus. The AXL increases (predominantly from vitreous chamber depth elongation) at a slower rate than normal and becomes hyperopic which is lens induced hyperopia (LIH). Contrastingly, when the eye is experiencing hyperopic defocus from a minus lens, the AXL elongation speeds up and the eye becomes myopic, thus lens induced myopia (LIM). Some researchers have argued when a minus lens is placed in front of the eye, it triggers accommodation and the eye emmetropizes using an accommodation cue. This hypothesis was challenged by cutting off the accommodation input (Schaeffel *et al.*, 1990; Schmid and Wildsoet, 1996), and the chick eye could still possess compensatory response to the direction of defocus given. These studies provide solid evidence that the eye can differentiate the sign of defocus without accommodation. A similar induced eyeball growth response can also be observed with a cylindrical lens (Irving *et al.*, 1991).

It remains unknown how the retina detects optical defocus (Schaeffel and Wildsoet, 2013). Several biochemical messengers have been identified at the

retinal level that are possibly involved in defocus detection, such as glucagon (Buck *et al.*, 2004; Feldkaemper *et al.*, 2004; Feldkaemper and Schaeffel, 2002), ZENK expression (Ashby *et al.*, 2010; Bitzer and Schaeffel, 2002; Fischer *et al.*, 1999), retinoic acid, (McFadden *et al.*, 2004; Mertz and Wallman, 2000; Troilo *et al.*, 2006) and dopamine (Guo *et al.*, 1995). These messengers show changes in concentration in response to different signs of defocus. In addition, retinal cellular activity was also found to be modulated by signs of defocus in animals (Zhong *et al.*, 2004), along with different electroretinal responses to different signs of defocus in humans (Ho *et al.*, 2012b), providing evidence that the eye can differentiate signs of defocus at the retinal level.

#### **2.3.4. FDM and LIM**

FDM is induced by wearing a diffuser causing the image quality to be highly degraded. It is proposed that the blurred image triggers eye growth towards myopia and sharp image triggers the eye to become hyperopic (Norton and Siegart, 1995). FDM is an open loop condition as there is no definite endpoint, whereas LIM is a closed loop condition in that eye growth reduces the hyperopic defocus imposed by a negative lens. The eye growth stops when the axial length matches the focal length (Morgan *et al.*, 2013). It has been debated in detail whether FDM and LIM are the same process (Morgan *et al.*, 2013). In human myopia development, FDM may be less representative in clinical situation, as most children have myopic progression without depriving their vision. Therefore, studies involving lens induced myopia related to the eye growth are focus of this review.

#### **2.3.5. Hyperopic defocus and myopic defocus**

One hypothesis to explain why near work would induce myopia is chronic hyperopic defocus. Chronic hyperopic blur, which is the results of accommodation lag at near working distance (Charman, 1999; Goss and Rainey, 1999; Goss and Wickham, 1995), may be a factor for myopia development. Although there is an argument that accommodation lag may be the result rather than the cause of myopia (Mutti *et al.*, 2006). Moreover,

some studies pointed out that the amount of time spent performing near work may not be linearly correlated to the development of myopia (Jones *et al.*, 2006). Outdoor activities had been reported to suppress the myopia development (Dirani *et al.*, 2009; Jones *et al.*, 2007; Lu *et al.*, 2009; Rose *et al.*, 2008). Yet, apart from defocus, factors for myopia development are changing from near work to outdoor activities. For example, the outdoor luminance level is much higher than indoors as discussed above (refer to 2.3.2.3.). Another hypothesis is that myopic defocus in outdoor environment counteracts the effect of hyperopic defocus of near work in myopia development. This hypothesis is supported by different animal studies. Although the sign of defocus dictated the direction of the eye growth, the rate of hyperopic and myopic defocus compensation was not equal (Kee *et al.*, 2001; Winawer and Wallman, 2002). Zhu and co-workers (2003) demonstrated that brief periods of myopic defocus can counteract the effects of daylong hyperopic defocus to avoid myopia development in chicks (Winawer and Wallman, 2002; Zhu *et al.*, 2003). In addition, the compensation to myopic and hyperopic defocus was shown to be different with the same spatial stimulus (Diether and Wildsoet, 2005). When chick eyes were exposed to defocusing ( $\pm 7D$ ) stimuli of a striped Maltese cross

target (high spatial frequencies) and solid Maltese cross (low spatial frequencies), compensation for myopic defocus was found to be more effective for the striped Maltese cross (Diether and Wildsoet, 2005). It is possible that different mechanisms are for decoding hyperopic defocus and myopic defocus. In addition, studies have shown that the set point in emmetropization was graded by the total ratio of hyperopic to myopic defocus which the eye experienced (McFadden *et al.*, 2014; Tse *et al.*, 2007; Tse and To, 2011). If myopic defocus is indeed as an inhibitor for myopia progression, it would be beneficial if myopia is under-corrected or only partially corrected. In human studies, however, the opposite consequence was found, as under-correction speeds up the rate of myopia progression in myopic children (Adler and Millodot, 2006; Chung *et al.*, 2002). The mechanism in decoding myopic and hyperopic defocus may be far more complicated than the concept of myopic defocus “neutralizing” hyperopic defocus.

#### **2.3.5.1. Contrast adaptation**

Empirical experience and observation from previous studies showed that vision was improved when defocus persists over extended periods of time (George and Rosenfield, 2004; Mon-Williams *et al.*, 1998; Pesudovs and

Brennan, 1993). It has been suggested that there is a process either within the eye or higher centre, for adjusting/deblurring defocused retinal images (Heinrich and Bach, 2001; Heinrich and Bach, 2002). The mechanism that enhances or reduces contrast sensitivity, based on the input contrast from the visual scene, is referred to as contrast adaptation (Diether *et al.*, 2001; Heinrich and Bach, 2001; Ohlendorf and Schaeffel, 2009). If the contrast is high, the sensitivity is reduced and if it is low, the sensitivity is enhanced (Diether *et al.*, 2001; Heinrich and Bach, 2001; Ohlendorf and Schaeffel, 2009). Recently, studies suggested that myopes had greater adaptation during near work than emmetropes (McGonigle *et al.*, 2016; Yeo *et al.*, 2012). In addition, an asymmetrical response in defocus induced contrast adaptation highlighted the possibility of contrast adaptation as an error signal for emmetropization. (Diether *et al.*, 2001; Ohlendorf and Schaeffel, 2009).

The adaptation process to spatial frequencies was documented to be selective using psychophysical experiment as early as 1969 (Blakemore and Campbell, 1969a). Later, Webster and Miyahara (1997) found that exposing the eye to natural images for a period of time would result in reducing sensitivity at low spatial frequencies, biasing contrast sensitivity towards

higher frequencies (Webster and Miyahara, 1997). However, psychophysical techniques cannot easily separate the contrast-adaptation mechanisms in cortical and retina level. Since emmetropization is a locally regulated process (refer to 2.5), the retinal contribution to the contrast adaptation process may indicate its role in eye growth. Heinrich and Bach (2002) applied pattern electroretinogram (PERG) to show evidence for the retinal contribution to contrast adaptation. The retina responded differently to low SF(0.5cpd) and high spatial frequency (5cpd) adaptation (Heinrich and Bach, 2002). It was found that adaptation to high spatial frequency significantly decreased the amplitude and latency of PERG, while no changes in amplitude nor in latency were observed at low SF. Although increasing evidence suggests that the contrast adaptation in the retina is both spatially and defocus selective, it cannot prove the role/ link for contrast adaptation (Ohlendorf and Schaeffel, 2009) in information processing for eye growth control. It may be just an epiphenomenon of the visual system.

#### **2.3.5.2. Detecting defocus**

On-going studies are investigating how the eye can detect signs of defocus from visual images. It has been argued that the magnitude of blur (Norton and Siegwart, 1995) is a key for LIM. Thus, eye growth accelerates with an

increased amount of blur caused by negative lenses while eye growth rate decreases with positive lenses. Image blur is suggested to be an important feedback signal for emmetropization (Wallman and Winawer, 2004). Other studies argue against this idea and suggest that the eye can detect the sign of defocus. Firstly, the eye has been shown to compensate for signs of defocus when the magnitude of blur was maintained. For judging “blur”, the phase alignment of image and relative energy distribution across the spatial frequencies was employed (Webster *et al.*, 2002). Yet, Hess and colleagues (2006) found that eye growth was conserved even when the visual images were scrambled, without phase alignment. Secondly, when completing defocus exist, the eye emmetropizes to the summation of “total defocus” (McFadden *et al.*, 2014; Tse *et al.*, 2007; Tse and To, 2011). What cue does the retina use to extract defocus? As discussed in 2.3.5.1., it was shown the eye emmetropized more effectively for myopic defocus with inclusion of higher spatial frequencies (Diether and Wildsoet, 2005). This creates more questions on emmetropization as for myopia development/progression, and how the eye “emmetropizes” to compensate for hyperopic defocus. Base on their result, Diether and Wildsoet hypothesized the compensation to hyperopic defocus was independent of high and low spatial patterns. To

complicate the situations, the low-pass filtered Maltese cross would induce myopia, irrespective of the sign of imposed defocus. Does the low-pass filtered pattern mimic FDM? Or is it due to removal of a particular range of spatial frequencies and the retina becoming insensitive to detect signs of defocus? In human studies, there is electrophysiological evidence that the retina responds to hyperopic and myopic defocus differently (Ho *et al.*, 2012b). Yet, it is still unclear how the retina decodes defocus.

#### **2.4. Central and peripheral retina in regulating eye growth**

In humans, the fovea is an important region as if the highest spatial resolution is located. The fovea is sensitive to blur and optical defocus, so it is logical to assume it possess a dominating role in the emmetropization process. There are studies suggesting high spatial frequencies (presuming detected by higher spatial sensitive cells) are effective for inhibiting FDM (Schmid and Wildsoet, 1997) or engaging in decoding defocus (Diether and Wildsoet, 2005). On the other hand, emmetropization can also be observed in animals which have lower visual acuities (Petry *et al.*, 1984; Schmid and Wildsoet, 1998), and not many animals possess an ultra-high resolution foveal centre. That means that high acuity retinal region may not essential

for the emmetropization process. By using a diffuser lens with a central aperture (clear zone), Smith and co-workers (2005) have shown that peripheral form deprivation can influence the central refractive development in monkeys (Smith *et al.*, 2005). Furthermore, Smith and colleagues (2007) ablated the fovea with laser and found that emmetropization and FDM were not interrupted (Smith *et al.*, 2007). In addition, Smith and colleagues (2009) showed that compensatory eye growth to defocused lenses is still effective when the fovea was ablated. They provided evidence that high acuity or visual signal from the fovea region may not be essential during emmetropization. In addition, local defocus on the peripheral retina resulted in the enlargement of the eyeball in that particular region (Diether and Schaeffel, 1997; Miles and Wallman, 1990), adding evidence to the role of the peripheral retina engaging in emmetropization.

## **2.5. Local and self-regulated eye growth**

The retina is the first site for receiving and encoding the visual stimulus in the visual pathway. It has been debated whether the eye growth is a locally controlled process or needs involvement of a higher visual centre (Schaeffel and Wildsoet, 2013). The classical experiment was conducted by Wallman and colleagues (1987) who demonstrated that partial form deprivation

triggered compensated eye growth to the deprived retinal region only (Wallman *et al.*, 1987). Following the other studies demonstrated the eye can regulate its growth without input from the brain (Choh *et al.*, 2006; Wildsoet and McFadden, 2010). When the eye is isolated by optic nerve sectioning (Troilo *et al.*, 1987; Wildsoet and Collins, 2000; Wildsoet and McFadden, 2010) or the signal from the brain to eye is blocked by Tetrodotoxin (TTX) (McBrien *et al.*, 1995; Norton *et al.*, 1994; Wildsoet and Wallman, 1995), FDM or LIM still persisted. In addition, visual manipulations at a localized region resulted in the eye modulating the growth response locally (Diether and Schaeffel, 1997). When a hemi-field spectacle lens was placed on a chick eye, the eye grew locally in the half of the eye that was under defocus. Bi-directional change, depending on the sign of the lenses, was also observed (Diether and Schaeffel, 1997).

It is important to note that the localized eye growth in response to visual stimulus is not related to fovea or foveolar centralis, echoing that the high spatial sensitive region may not be important in the process of emmetropization. It would need to be shown whether the eye can respond to defocus locally, as FDM and LIM are known to have different mechanisms. Wildsoet and Wallman (1995) determined that when the retina was isolated

from the brain by TTX, the compensation response to either hyperopic or myopic defocus partially reduced (Wildsoet and Wallman, 1995). In addition, optic nerve section also slightly reduced compensation to hyperopic defocus, suggesting there is a certain amount of involvement of the central nervous system in response to emmetropization (Wildsoet and Wallman, 1995). Schaeffel and associates had proposed that the response of eye growth in chicks to diffusers and lenses reveals different mechanisms (Schaeffel *et al.*, 1995). Based on their study, FDM and LIH are controlled locally within the retina, while LIM is somehow centrally controlled. The above studies used a chick model, but a study using guinea pig showed an intact optic nerve was required for compensated eye growth (McFadden and Wildsoet, 2009). From this study, emmetropization in mammals and birds may involve different mechanisms.

The retina is responsible for both spatially and temporally processing of an image. It is reasonable to assume that the image processing in the retina is involved in eye growth regulation. In animal studies, when certain types of retinal cells were inhibited by injecting N-methyl-D-aspartic acid (NMDA) (Fischer *et al.*, 1997), or certain type of retinal neurons were ablated (Fischer *et al.*, 2008), the eye grew excessively. While there is evidence

showing the importance of the retina in controlling the eye growth, what cue does retina, especially in human eye, use for decoding defocus? If the sign and magnitude of defocus can be decoded locally by the retina, the retinal neural activity would be responsive to defocus. The electroretinogram (ERG) is a possible tool to investigate the activity or function at the retinal level in human eye under various defocus conditions.

## **Chapter 3. Multifocal electroretinogram**

### **3.1. Basics of electroretinogram**

The electroretinogram is a measurement tool for recording retinal electrical signals in response to flash of light received by the retina, and the pupil is dilated. For a clinical recording of the retinal response, an active electrode is placed on the cornea and a reference electrode is placed at the ipsilateral outer canthus of the tested eye. In addition, a ground electrode is placed on the forehead or earlobe. Classically, the electrical signal from the whole eye is recorded by full-field (Ganzfeld) flash electroretinogram and responses from different retinal cells/layers can be obtained by modulating the stimulation paradigm.

### **3.2. Multifocal electroretinogram (mfERG)**

Although full field ERG is a common clinical tool for investigating retinal function, it cannot provide topographical information regarding the retinal response and cannot detect localized functional defects. A modification of the ERG, focal ERG, has been developed to examine particular retinal loci by varying the size and location of the stimulating beam (Seiple *et al.*, 1986). However, it requires multiple measurements for multiple retinal loci to give topographical responses. Thus, focal ERG is mostly for the

measurement of the macular response (Birch and Fish, 1988; Miyake *et al.*, 1989; Seiple *et al.*, 1986). Multifocal electroretinogram (mfERG) which was developed by Sutter and Tran (1992), records the topographical responses of the retina within a relative short period of time (Sutter and Tran, 1992). The mfERG can detect localized functional changes in the retina.

### 3.2.1. Basic concept

The stimulus pattern of mfERG is usually consists of 61 or 103 scaled or non-scaled concentric hexagons (**Figure 3.1.**), which are usually displayed on a CRT or LCD stimulator (Hood *et al.*, 2012). The extent of the retinal area investigated depends on the size of the stimulation pattern and the working distance between the subject and the stimulator.

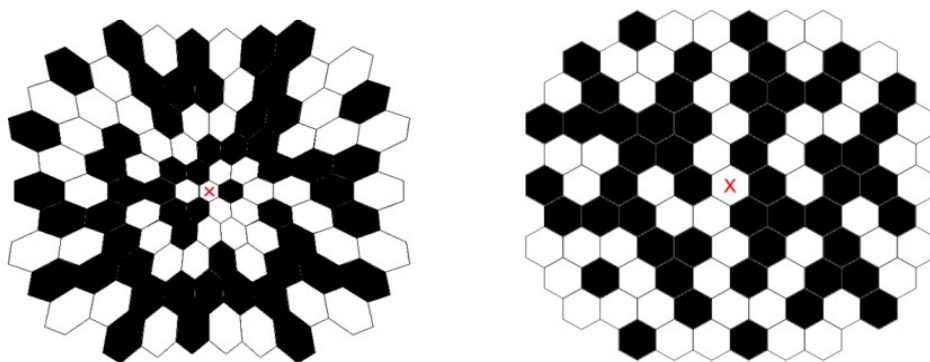


**Figure 3.1.** A typical 103 scaled (left) and non-scaled (right) hexagon pattern for mfERG recording.

The mfERG examines the retinal response from multiple regions simultaneously. For each hexagon, it flickers temporally based on a pseudo-random binary m-sequence of flickering. Each hexagon has its own binary m-sequence and is independent of others. By applying cross-correlation, the individual topographical retinal response from each hexagonal stimulus can be obtained. **Figure.3.2.** shows the result of topographical responses from an individual trace, grouped in a ring or three-dimensional plot.

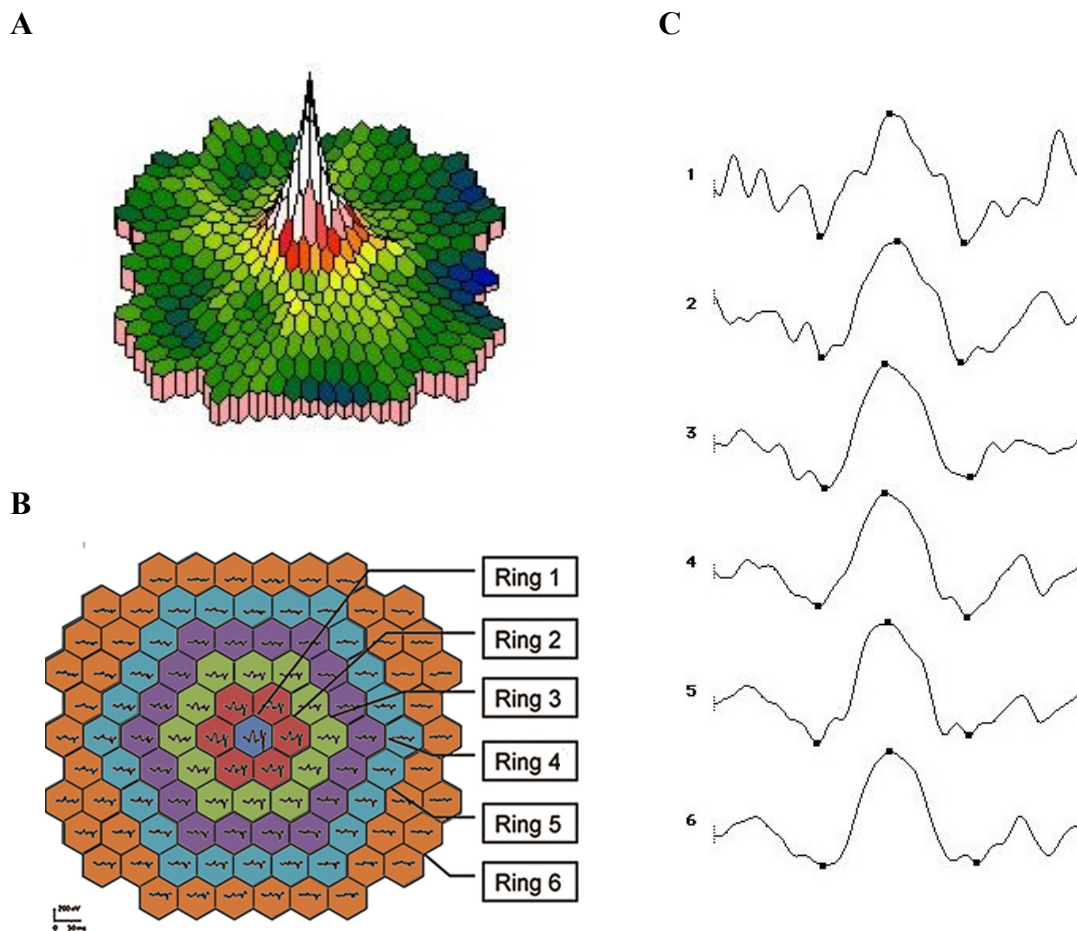


**Figure 3.2. Topographical presentation of the retinal response. (A)** Three-dimensional plot. **(B)** Trace array. **(C)** Ring-averaged response from central (Ring 1) to mid-peripheral (Ring 6) regions.

### 3.2.2. First-order and second-order kernel responses

The mfERG response is a mathematic computation of the response through cross-correlation, and it is therefore not a direct biological response from retinal cells. By cross-correlation method, the response can be derived as first-order, second-order, third-order kernel responses and so on. The first-order response is derived by an averaged retinal response to a light stimulus (Hood *et al.*, 2002) (**Figure 3.3**).

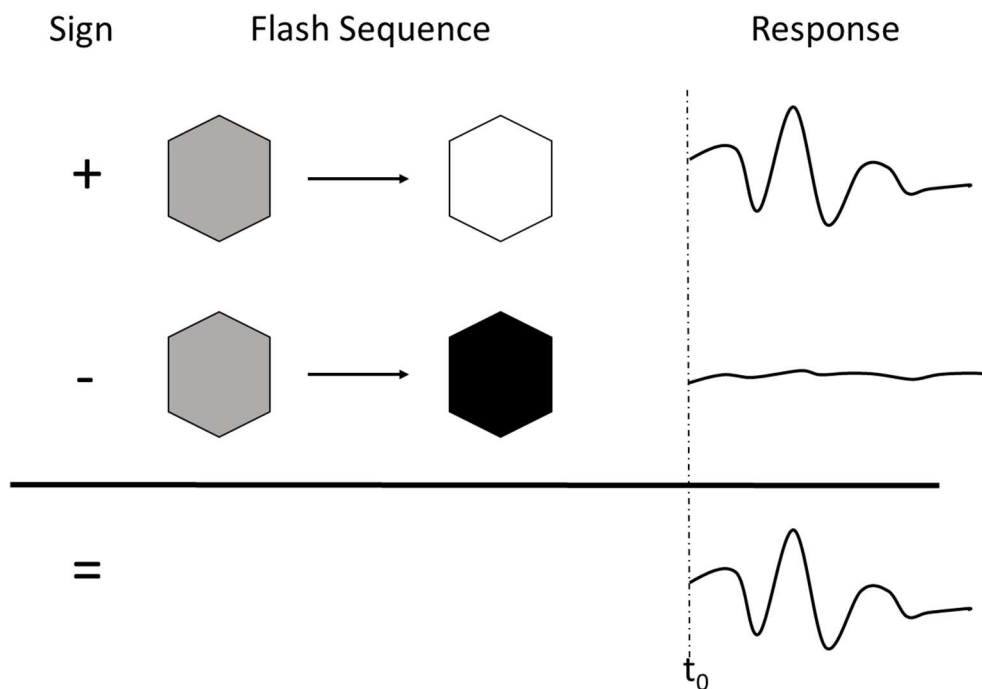


**Figure 3.3. The first order response.** A schematic diagram illustrates how the first-order response is obtained. The white and black hexagons represent the bright (flash) and dark (no flash) presentations respectively. The hexagon that in grey colour represents the frame not under consideration in the computation of the response. The first-order kernel is obtained by averaging the responses from all dark presentations, and subtracting the averaged responses from all bright presentations within the m-sequence.

(Figure is adapted and modified from Sutter (2000)).

The waveform appearance of a typical first-order kernel response is shown in **Figure 3.4**. It consists of an initial negative trough (N1), a second positive peak (P1), and a negative trough (N2). The cellular contribution to each component of mfERG responses is derived by removing the responses from retinal cells layer by layer using a pharmaceutical dissection method in animal studies. The first-order kernel response was found to be contributed to mainly from the outer retinal activity and only partly from the inner retina (Hood, 2000; Hood *et al.*, 2002; Ng *et al.*, 2008a; Ng *et al.*, 2008b).

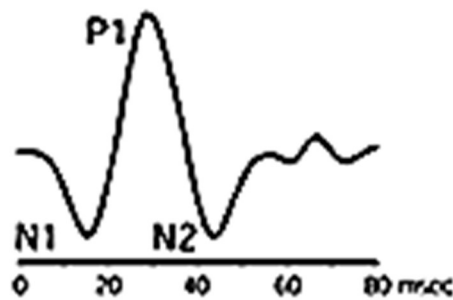


**Figure 3.4. The waveform appearance of a typical first-order kernel response.** It consists of an initial negative trough (N1), a second positive peak (P1), and a negative trough (N2).

In detail, the N1 response originates from both cone photoreceptors and OFF-bipolar cells in monkey (Hood, 2000; Hood *et al.*, 2002). The P1 response originates from ON-bipolar cells (Hood, 2000; Hood *et al.*, 2002;

Ng *et al.*, 2008a; Ng *et al.*, 2008b). The N2 response consists of components from both ON- and OFF-bipolar cells and NMDA sensitive retinal components such as amacrine cells in pig eye (Ng *et al.*, 2008a; Ng *et al.*, 2008b). While the first-order kernel response is dominated by outer retinal cells, the second-order kernel response involves much more contribution from inner retinal cells and small contributions from outer retinal cells (Hood, 2000; Hood *et al.*, 2002; Ng *et al.*, 2008a; Ng *et al.*, 2008b) The second-order kernel response is derived by subtracting the response with change of stimuli between two consecutive frames (**Figure 3.5**). So, it is an interactive response between the preceding frame and the current frame. It thus reflects an adaptive response to consecutive stimulations (Sutter, 2000; Sutter, 2001).

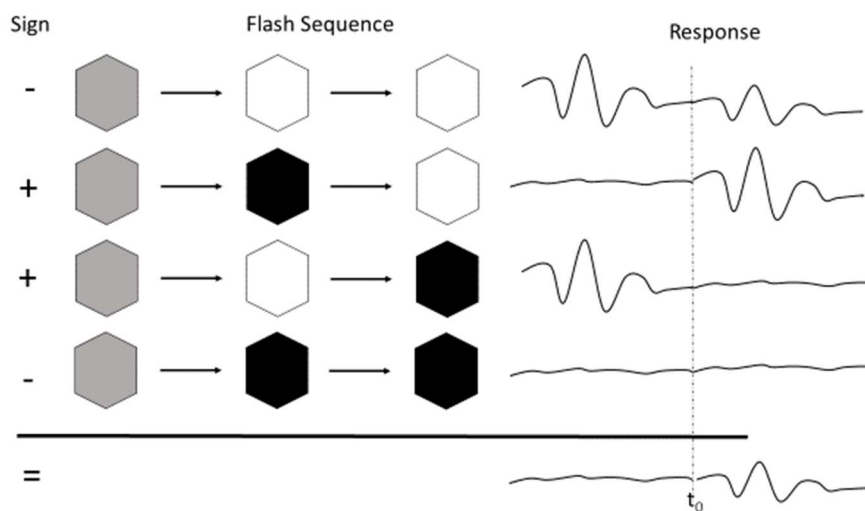


**Figure 3.5. The second order response.** A schematic diagram illustrates

the second-order response is obtained. The white and black hexagons represent the bright (flash) and dark (no flash) presentations respectively. The hexagon that in grey colour represents the frame not under consideration for the computation of the response. The second-order kernel is achieved by adding all the responses with different stimuli between preceding and current frames (i.e. either bright-to-dark or dark-to-bright), and subtracted from all the responses with the same stimulus between two consecutive frames (i.e. Bright-to-bright or dark-to-dark) (Figure is adopted and modified from Sutter (2000)).

The second order response is also a mathematical extraction instead of a real response directly generated from cells in the retina and cannot be completely eliminated by injecting blockers (Hood *et al.*, 2003). A fall in the first slice of the second-order response suggests an abnormality in adaptive processing rather than a missing component or cellular response (Hood, 2000; Yoshii *et al.*, 2001). It is noted that there are some discrepancies in the waveform of the second-order kernel response between humans and animals (Hood, 2000; Hood *et al.*, 2002; Ng *et al.*, 2008a; Ng *et al.*, 2008b). The first slice of the second-order kernel mfERG was shown to be contributed mainly from the inner retina with minor contribution from the outer retina in a porcine eye study (Ng *et al.*, 2008a). In addition, a previous study also reported that there were variations in the waveforms with retinal location for the second-order mfERG responses in human (Wu and Sutter, 1995). Since the second-order response is shown to have a relatively low signal-to-noise

ratio, it is seldom to apply this parameter in studying the inner retinal activities.

### **3.3. Enhancing inner retina response: Global flash (MOFO)**

#### **mfERG**

The first-order response of conventional mfERG is predominantly from the outer retina (Hare and Ton, 2002; Hood *et al.*, 2002; Hood *et al.*, 2003; Hood *et al.*, 1997). Various studies suggested that the characteristics of the inner retina is associated retinal adaptive activity (Fortune *et al.*, 2002; Shimada *et al.*, 2005; Shimada *et al.*, 2001; Sutter *et al.*; Sutter *et al.*, 1999).

Shimada and co-workers developed the global flash paradigm to isolate mfERG components from the inner retina (Shimada *et al.*, 2005). This paradigm consists of periodic global (full screen) flashes interleaved with multifocal pseudorandom m-sequence stimulations, and this modification of stimulation is believed to emphasize the adaptive activity from the inner retina (**Figure 3.6.**). There are two distinct features for the global flash stimulation paradigm, the direct component (DC) and the induced component (IC). The DC, which mainly reflects the activity from the outer retina, is the average response to the focal stimulation (Shimada *et al.*, 2005). On the other hand, IC represents the effect of the preceding focal

flash on the response to the global flash. The IC response reflects predominantly inner retinal function (Shimada *et al.*, 2005).

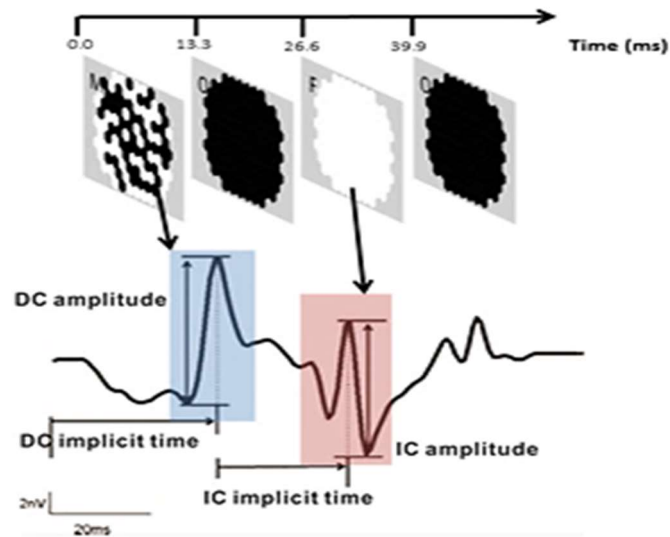


**Figure 3.6. Schematic diagram for global flash paradigm of mfERG.** Upper: The sequence of global flash paradigm: local multifocal flashes frame(M), dark frame (O), global flash frame(F), dark frame (O). Lower: Waveform of global flash mfERG showing the amplitude and implicit time of DC, and the amplitude and implicit time of IC.

### **3.4. Investigating myopia using mfERG technique**

#### **3.4.1. Conventional mfERG**

Several studies have investigated the conventional mfERG responses in the myopic eye. Most studies reported that the amplitudes of N1, P1, N2 were reduced in myopic eyes even with correction lenses (Chan and Mohidin, 2003; Kawabata and Adachi-Usami, 1997). However, Luu and colleagues (2006) compared adult and children mfERG response and showed only adult mfERG was correlated with severity of myopia (Luu *et al.*, 2006).

Although they suggested the reduction of mfERG in myopia may be due to optical, electrical and retinal factors (Luu *et al.*, 2006). The mechanisms behind are still unclear.

##### **3.4.1.1. Optical factor**

Myopic eyes usually have longer AXL with prolate shaped eyeball, and as a result, the retinal illuminance is generally reduced. It is suggested that reduction in mfERG may be due to the decreased illumination and reduced image size with a correction lens. This suggestion is argued by Kawabata and Adachi-Usami (1997) that high myopes were shown to have much lower saturated mfERG amplitude than expected, suggesting the reduction in amplitude is more related to functional change (Kawabata and Adachi-

Usami, 1997).

#### **3.4.1.2. Electrical factor**

Electrical factor is related to an increase of resistance caused by the increased distance between the retina and the electrode (Perlman *et al.*, 1984). Yet this suggestion was challenged by Chen and colleagues (1996) as it is disobeyed Ohm's law (Chen *et al.*, 1992). If the resistance increased, by Ohm's law ( $V=IR$ ), the mfERG amplitudes should also be increased rather than decreased.

#### **3.4.1.3. Retinal factor**

Reduced retinal cell density is suggested to be related with increased myopia (Beresford *et al.*, 1998; Chui *et al.*, 2005). Reduction in mfERG amplitude may be due to reduction in retinal cell density. Morphological changes in the photoreceptor outer segment (Crewther, 2000) have been also considered as one of the retinal factors. Although morphological changes in the photoreceptor in myopic eyes have been reported in chick models, it is unknown whether a similar alteration occurs in humans.

#### **3.4.2. Global flash (MOFO) mfERG**

Chen and colleagues (2006) first applied MOFO mfERG to investigate myopia in human (Chen *et al.*, 2006b), particular quantifying the inner

retinal (IC) contributions on magnitude of myopia. They adjusted the AXL difference (optical factor) as covariance, and there was no difference in MOFO mfERG response (both DC and IC amplitudes) between myopes and emmetropes. The adjustment for AXL was challenged because the eye shapes for myope and emmetrope were different. In general, prolate shaped eye was found in myope and spherical shaped eye was found in emmetrope (Deller *et al.*, 1947; Millodot, 1981; Seidemann and Schaeffel, 2002). The influence of retinal illumination due to AXL may not be consistent over the retinal regions. On the other hand, Ho and co-workers (2011) found that the IC amplitudes were significantly reduced at low and middle contrast conditions in myopes, suggesting there are some inner retina impairments in the myopic eye (Ho *et al.*, 2011). In a subsequent study, Ho and colleagues (2012) found that children with myopia progression had reduced IC amplitudes at the central and some paracentral regions, implying that the inner retinal function was more affected than the outer retina during myopia progression (Ho *et al.*, 2012a).

Apart from using global flash mfERG to investigate the functional changes due to myopia development, the global flash mfERG was also applied to investigate how the retina detects optical defocus, Ho and co-workers was

the first to find that the retinal activity is responding to sign of optical defocus differently (Ho *et al.*, 2012b). The DC amplitude decreased under negative defocus conditions in paracentral region; while the IC amplitude increased under positive defocus conditions (Ho *et al.*, 2012b).

Evidence from past studies have demonstrated the retina locally can pick up visual signal and regulate the growth itself (refer to 2.5). While Ho and colleagues (2005) were first to use mfERG to show retinal activity is responding differently to sign of defocus. It is far from clear how the retina can decode defocus. What visual cue does the retina use to decode optical defocus?

## Chapter 4. Purpose of investigation

There is strong evidence from both animal and human studies supporting the ability the eye to detect the signs of defocus. Animal studies have shown the eye grows to compensate lens induced defocus. In human studies, it was observed that there was a short term choroidal thickness change when the eye was exposed to defocus (Read *et al.*, 2010). In addition, retinal cell activity has been shown to be sign-dependent under optical defocus (Ho *et al.*, 2012b). Further follow up questions would be “How does the retina detect defocus and recognize the signs” and “How does this relate to eye growth”. The eye evolved from only light detection to decoding and extracting visual information from the environment. The visual stimulus is composed of various attributes, including spatial, temporal, contrast, and chromatic characteristics. Previous studies have shown that all these attributes may be involved in emmetropization. Animal studies have suggested that emmetropization is tuned to specific spatial frequencies (SF) (Diether and Wildsoet, 2005; Schmid and Wildsoet, 1997). They observed high SF (relative to the sensitivity spectrum of the animal) inhibited myopia. In human study, sign-dependent change was found to be more vigorous in the paracentral region, in which the retinal region has relatively low spatial

resolution compared with the foveal region (Ho *et al.*, 2012b). The gap of knowledge here is how the local detection of defocus at retinal level is spatially tuned. Do any SFs promote or inhibit myopia development? It was shown that when a positive lens was superimposed with various level of image-degrading diffuser, which could be regarded as low-pass filter. For the weaker diffuser, the chick eye could still develop compensatory hyperopic response. When the levels of diffuser have become stronger, the compensatory hyperopic response was reduced (Park *et al.*, 2003). This may imply when certain spatial details within the visual stimulus are absent, the eye cannot detect the optical defocus. In addition, it remains to be determined which part of the retina is more sensitive to spatial details of a visual stimulus? If defocus detection is spatially tuned in the eye, does this relate to emmetropization? The objectives of the current study are:

1. To investigate the outer and inner retina respond to spatial frequency by using global flash mfERG;
2. To investigate the regional changes in retinal activity by using the MOFO mfERG when high and low spatial frequency stimuli are out of focus;
3. To investigate the effect of different spatial patterns (high and low

spatial frequency) on myopia progression in chicks;

4. To investigate the effect of spatial composition with various ratios of spatial frequencies on myopia progression in chicks.

The outcome of is predicted that the spatial processing begins at retinal level. In human, the outer and inner retina may possess different characteristics in processing spatial frequency. Furthermore, the sign-dependent retinal activity to defocus maybe influenced by spatial frequency. If the retinal responses are dependent on defocus and spatial frequency, there maybe an interactive effect on eye growth. Thus, the spatial content within the visual stimuli may affect the compensation eye growth to defocus.

This study will help to deepen our understanding of how retinal signaling responds to spatial frequency with optical defocus. It will enrich our knowledge of how the retina picks up cues in decoding defocus. The mechanism of myopia development in terms of spatial preference will also be investigated.

**Part II.**  
**EXPERIMENTS**

**Chapter 5. Experiment 1. Electroretinal response  
to spatial frequencies in human eye**

(Modified from the manuscript published in: *PLoS One*, 10(4),  
pp. e0123480)

## **Abstract**

The electrical response of the retina was examined as a function of the retinal region, using stimuli of various spatial frequencies. Black and white gratings (printed on plastic transparent sheets) of four spatial frequencies (SF), including 0.24, 1.2, 2.4 and 4.8 cycle per degree (cpd) were presented in front of the mfERG stimulation. The amplitudes and implicit times of the direct (DC) and induced (IC) components of mfERG responses were pooled into six concentric rings for analysis. There was low amplitude DC at low SF, which increased with increasing SF, and which decreased with increasing eccentricity. The IC was high in amplitude at all SF and reduced in amplitude with increasing eccentricity. The findings suggested that the outer and inner retina had different characteristics in processing spatial details.

## **5.1. Introduction**

With the exceedingly fast growing prevalence of myopia (short-sightedness) worldwide, myopia has become an important global public health problem (Grosvenor, 2003; Pan *et al.*, 2012; Saw *et al.*, 2005). In the past few decades, many studies have improved our understanding of myopia development, in particular the factors affecting eye growth and refractive

errors. The retina, as the first site of the visual pathway to receive visual signals, has been shown to be local controller of eye growth (Diether and Schaeffel, 1997; Smith *et al.*, 2010; Wallman *et al.*, 1987), which is tightly influenced by visual experience. Partial/full deprivation of vision results in unconstrained elongation of the eyeball, which corresponds to myopia development, in animals (chicks (Hodos and Kuenzel, 1984; Wallman *et al.*, 1978), fish (Shen *et al.*, 2005), guinea pig (Howlett and McFadden, 2006), mice (Schaeffel *et al.*, 2004), marmoset (Troilo and Judge, 1993), rhesus macaque (Smith *et al.*, 1999), tree shrew (Norton *et al.*, 1994; Shaikh *et al.*, 1999)) and human (von Noorden and Lewis, 1987; Zhang and Li, 1996), reflecting the importance of visual stimuli in regulating eye growth (Refer to 2.3.). However, what types of visual stimulus are required for regulating emmetropization? Visual stimuli projected onto the retina comprise a wide range of SFs, which plausibly tune the emmetropization process (Diether and Wildsoet, 2005; Hess *et al.*, 2006; Schmid and Wildsoet, 1997; Tran *et al.*, 2008; Zhi *et al.*, 2013): Schmid and Wildsoet (1997) found that exposure to SFs within the range of 0.086 and 4.3cpd could inhibit form-deprived myopia in chicks (Schmid and Wildsoet, 1997). Although SF dependency of emmetropization was reported to be tuned to middle spatial

frequencies in animals (Diether and Wildsoet, 2005; Hess *et al.*, 2006; Schmid and Wildsoet, 1997; Tran *et al.*, 2008), it is unclear whether similar SF dependence occurs in humans. Compelling evidence has demonstrated the significant role of the retina in eye growth regulation (Wallman and Winawer, 2004). Further study can help elucidate how self-regulation works in the retina.

The multifocal electroretinogram (mfERG) measures electrical activity of multiple retinal loci in response to light stimuli (Sutter and Tran, 1992) and would allow investigate on how of the retina responses to visual stimulus in various retinal regions. Ho and co-workers measured the global flash (MOFO) mfERG in humans and reported different physiological characteristics were obtained under hyperopic and myopic defocus conditions (Ho *et al.*, 2012b). In addition, the peripheral retina showed a more vigorous change than the central retina in response to optical defocus. In this study, this methodology was applied to examine the changes in retinal activities responding to specific SF. It was speculated that in different parts of the human retina may respond differently to visual stimuli with various SF.

## 5.2. Methods

### 5.2.1. Experiment Setup

The schematic diagram of mfERG setup for Experiment 1 and 2 is shown in **Figure 5.1**. The spatial frequency (SFs) gratings (refer to “Presentation of grating stimuli” session) were presented on a 22-inch colour liquid crystal display monitor (Model: VX2260wm, ViewSonic, Hong Kong, China) during the mfERG stimulation. The mfERG stimulation (Refer to “Global flash mfERG stimulation” session) was performed using the Visual Evoked Response Imaging System software (VERIS Science 6.0.6d19; Electro-Diagnostic Imaging Inc., San Mateo, CA, USA). The stimulus array consisted of 103 non-scaled hexagons and the stimulus pattern subtended  $33.7^\circ$  vertically and  $38.4^\circ$  horizontally at a viewing distance of 40 cm. Non-scaled hexagons were used in this study to maintain the same SFs at different eccentricities.

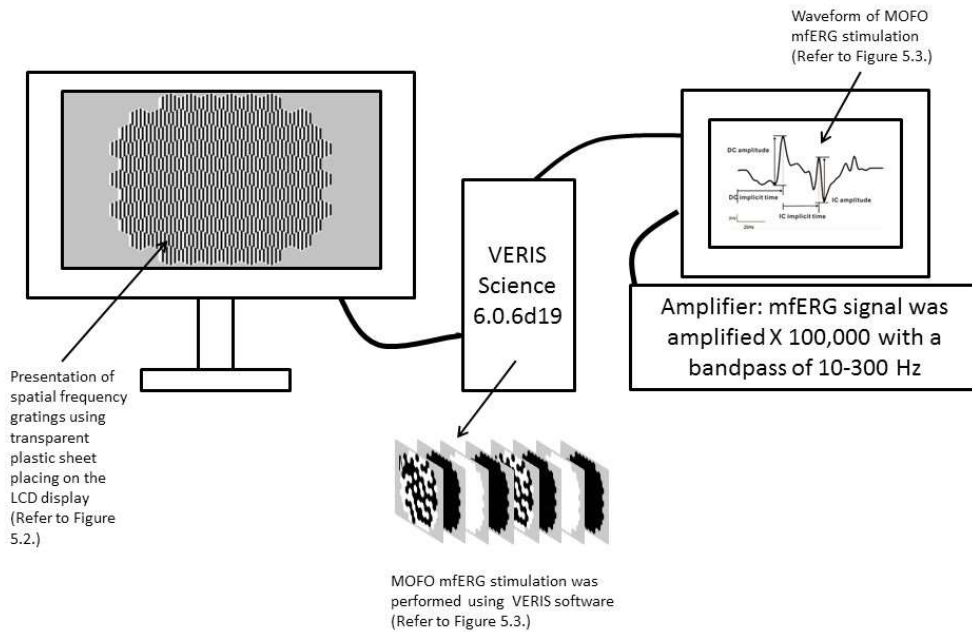


**Figure 5.1. Schematic diagram of mfERG setup.** The SF gratings were presented on a 22-inch LCD display. The global flash mfERG stimulation was driven by VERIS Science 6.0.6d19. The mfERG signal was amplified a gain of X 100,000 with a bandpass of 10-300 Hz.

### 5.2.2. Presentation of grating stimuli

The gratings were drawn precisely using Adobe Illustrator CS4. The outline of 103 hexagons was incorporated into the software. Then the gratings were printed on transparent film as alternating black and transparent stripes within each hexagon. The widths of the gratings were 14.4, 2.88, 1.44 and 0.72 mm, corresponding to SF of 0.24, 1.2, 2.4 and 4.8 cpd at 40 cm (Figure 5.2.). The spatial frequencies selected in this experiment were below the Nyquist limit of photoreceptors and ganglions in human eye (Anderson *et al.*, 1991), and 4.8cpd could still be “resolved” at peripheral

20°. The luminance variations for different sizes of gratings in each hexagon during the mfERG flash were minimized by presenting equal areas of black stripes in all gratings. The luminance of individual hexagon overlaying the gratings was measured using a spectro-radiometer (Model: SR3, Topcon, Japan). It was attempted to measure the luminance of the whole individual hexagon by orientating the size field of the spectro-radiometer just within the individual hexagon. The luminance was found to be approximately the same whenever gratings were used.

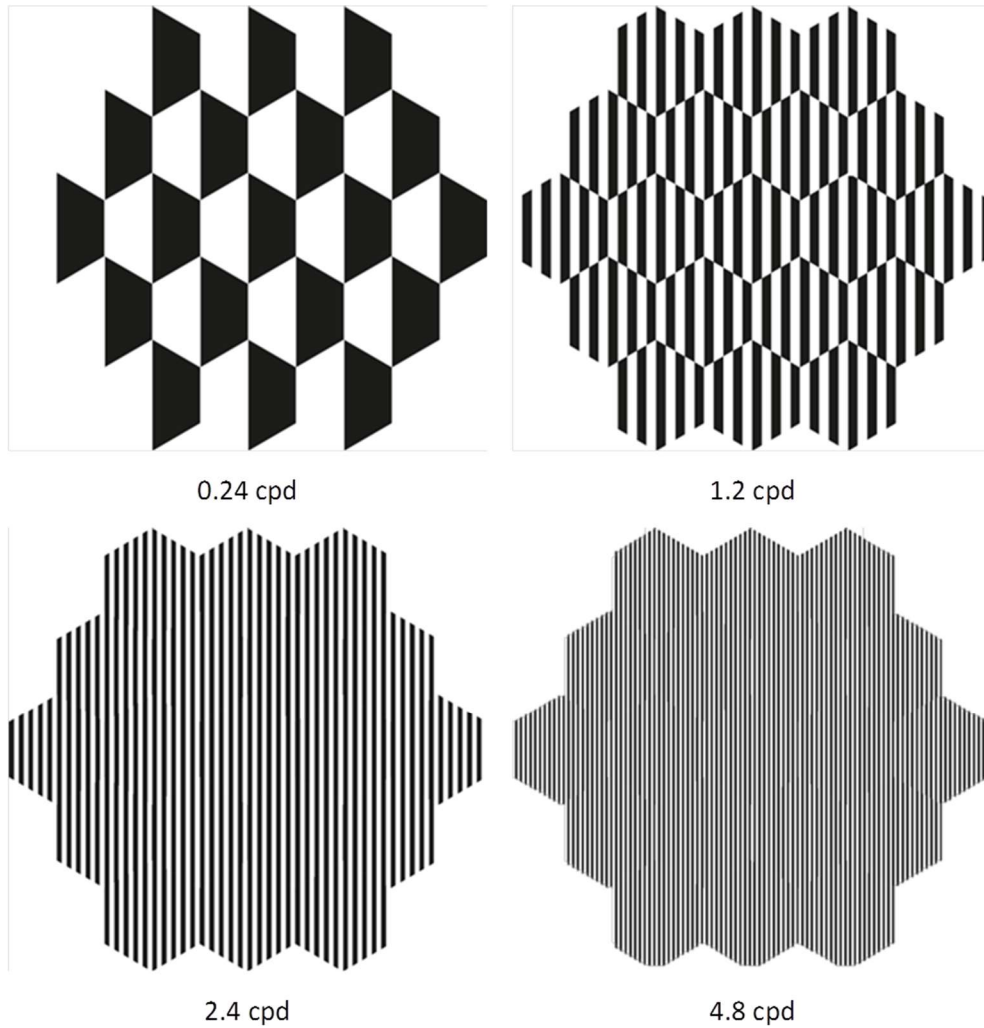


**Figure 5.2. Stimuli with different spatial frequencies presented to subjects for mfERG recording.** Spatial frequencies of 0.24, 1.2, 2.4 and 4.8 cpd were used. Only ring 1 to 3 were shown in the figure.

### 5.2.3. Global flash mfERG stimulation

High contrast (96 % contrast; bright phase, 180 cd/m<sup>2</sup>; dark phase, 4 cd/m<sup>2</sup>)

MOFO mfERG was selected to measure retinal activity. In each cycle of

MOFO mfERG stimulation consisted of a pseudo-random focal flash (M),

followed by a full-screen dark frame (O), a full-screen global flash (F), and

another full-screen dark frame (O) (**Figure 5.3.**). This can enhance the

activity of the inner retinal neurons, in order to obtain separate outer and inner retinal responses (Chen *et al.*, 2006b; Chu *et al.*, 2006; Ho *et al.*, 2011; Ho *et al.*, 2012b; Shimada *et al.*, 2005; Shimada *et al.*, 2001). In this study, as grating patterns were presented on the display during the measurement of each MOFO cycle, gratings were seen during the bright frames, i.e. M frame and F frame, while it became dark in the dark frames. Half the area of each hexagon was covered by the dark strips of the gratings, so the luminance was reduced to half during M frame and F frame. All the grating patterns had the same number of black and white strips within each mfERG hexagonal stimulus and hence the measured luminance of different grating patterns was the same. The luminance ratio of global flash to focal flash was maintained at 1:1 in this study to obtain both optimal DC and IC responses (Lung and Chan, 2010). A direct component (DC) and an induced component (IC) obtained from the MOFO mfERG help to assess the outer and inner retinal activities. In addition, regional variations of the responses could be observed in the same measurement.

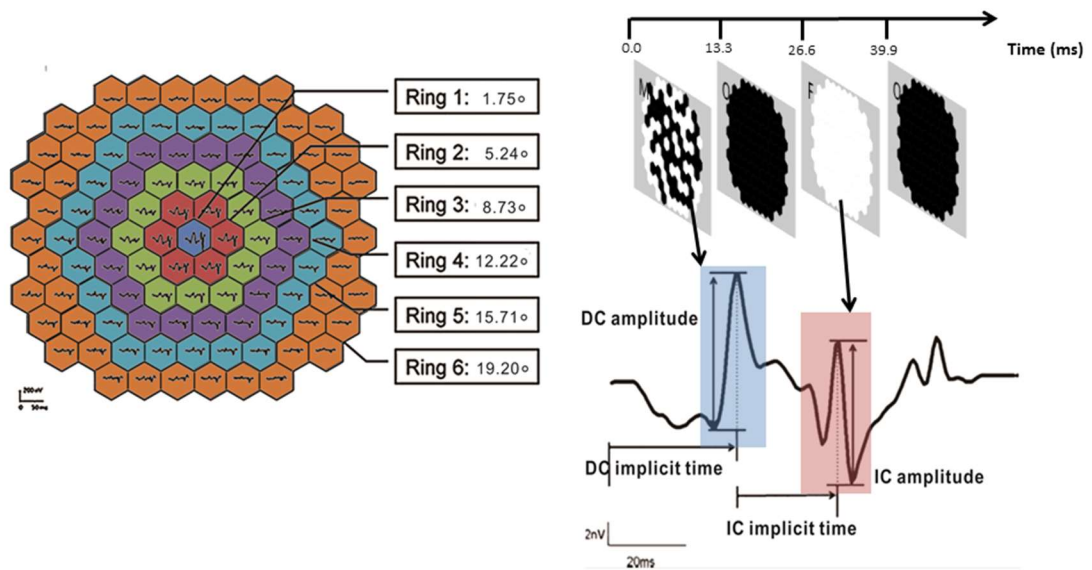


**Figure 5.3. Schematic diagram for grouping the mfERG responses and the waveform of MOFO mfERG.** Left: Both DC and IC responses were pooled into concentric rings with eccentricity from ring 1 (1.75°) to ring 6 (19.20°) Right: Schematic diagram for DC amplitude and implicit time, IC amplitude and implicit time of MOFO mfERG.

#### 5.2.4. Subject recruitment

Twenty-three young adults aged from 21 to 27 years (mean =  $22.5 \pm 1.6$  years) participated in the study. The inclusion criteria for refractive errors was from +1.50D to -4.00D and astigmatism was not more than -1.25D.

Detailed eye examination was conducted before the experiment. Intraocular pressure and depth of anterior chamber angles were assessed to ensure suitability for dilated fundus examination and mfERG measurement.

Subjects with colour vision deficiency, eye diseases, abnormal ocular media, history of general diseases with potential ocular manifestation, or a history

of photosensitive epilepsy were excluded from participation. The tested eye was randomly chosen. Tested eyes had best corrected logMAR visual acuity of 0.00 (Snellen acuity of 6/6) or better. The procedures of this study were reviewed and approved by the Human Ethics Committee of The Hong Kong Polytechnic University (HSEARS No. 20110905002) and adhered to the tenets of the Declaration of Helsinki. After detailed explanation of the study, written informed consent was obtained from each subject. Subject information was anonymized and de-identified prior to analysis.

### **5.2.5. Recordings**

The mfERG responses were recorded using a Dawson–Trick–Litzkow (DTL) thread electrode as active, which was positioned on the inferior cornea along the lower lid margin. Gold-cup reference and ground surface electrodes were placed at the outer canthus of the tested eye and at the forehead respectively. The pupil of the tested eye was dilated (>7mm) using 0.5% Tropicamide (Alcon, Australia). The tested eye of the subjects was fully corrected for the 40cm viewing distance using 35mm diameter corrective lenses. The retinal image size among the subjects was kept essentially constant by placing the corrective lenses at the anterior focal plane of the tested eye. The mfERG signal was amplified X 100,000 with a

bandpass of 10-300 Hz (Model: 15A54, Physiodata Amplifier system, Grass Technologies, Astro-Med, Inc., West Warwick, RI, USA). With the  $2^{12}$  binary m-sequence used, the recording time for each condition was about 7 min and 17 sec. The recording was divided into 32 slightly overlapping segments, and subjects were permitted to rest between segments. Subjects were instructed to fixate the red-cross target in the middle of the central hexagon of the stimulus display. The electrical signals were monitored by the examiner using the real-time display provided by the VERIS system and any segments contaminated with blinks or other artifacts were discarded and re-recorded.

### **5.2.6 Data analysis**

The direct (DC) and induced (IC) components of mfERG first-order kernel responses were extracted and pooled into six concentric rings for analysis (**Figure 5.3., left panel**). For the central hexagon (Ring 1), the radius angle subtended  $1.75^\circ$  and the most peripheral hexagons (Ring 6), the radius angle subtended  $19.20^\circ$ . The amplitude of the DC was defined as the difference from the first negative trough to the first positive peak while the IC amplitude was defined as the difference from the second positive peak to the second negative trough (Chu *et al.*, 2008; Chu *et al.*, 2006; Ho *et al.*, 2012b;

Shimada *et al.*, 2005). The implicit time of the DC was defined as the time taken to reach the first positive peak and the implicit time of the IC was measured from the presentation of the global flash to the second positive peak (**Figure 5.3, right panel**).

Predictive Analytics SoftWare (PASW19.0, SPSS Inc., Chicago, IL, USA) was used for data analysis. Repeated measures analysis of variance (ANOVA) was applied to study the effect of SF on mfERG responses. Post hoc tests with Bonferroni adjustment were applied to correct the level of significance due to multiple comparisons of different retinal regions. The level of significance was set at 0.05.

### **5.3. Results**

The refractive errors (spherical-equivalent) of the recruited subjects ranged from +1.13 to -3.25D (mean =  $-1.02 \pm 1.13$ D) and astigmatism ranged from 0.00D to -1.25D (mean =  $-0.44 \pm 0.44$ D). The typical waveforms of the global flash mfERG for the four grating patterns are shown in **Figure 5.4A**.

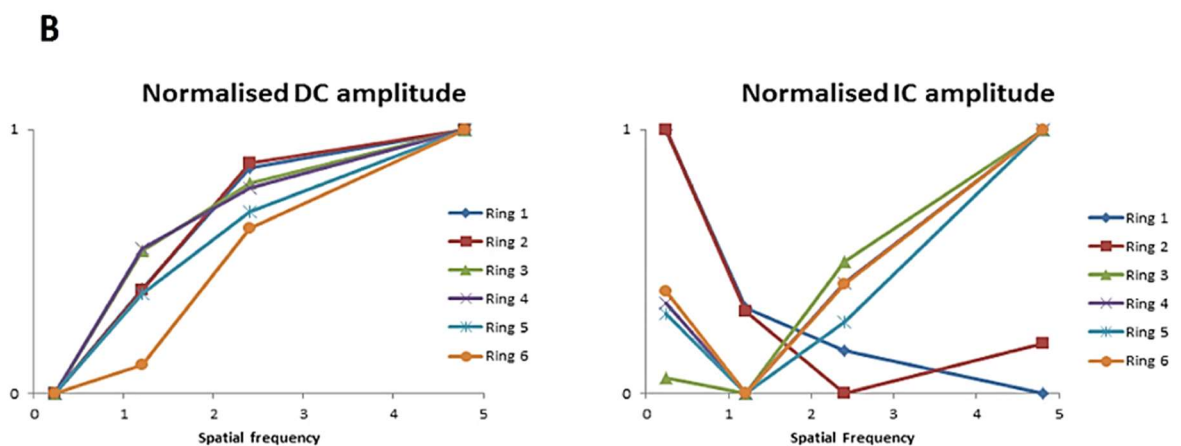
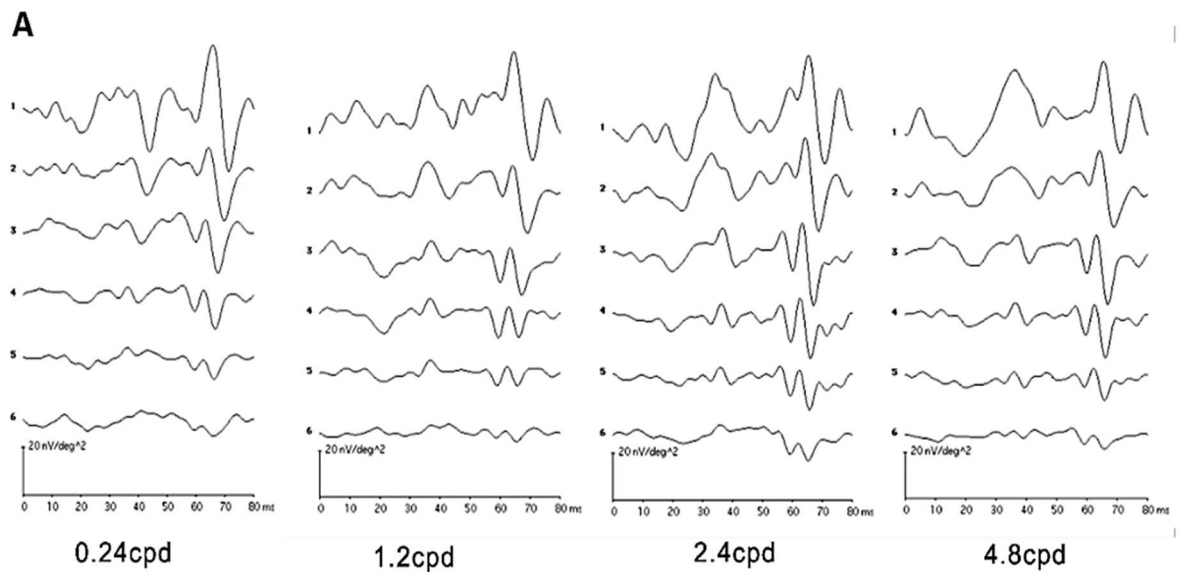


**Figure 5.4. The global flash mfERG response to spatial frequency. (A)** The typical global flash mfERG waveform measured from one subject with 4 SF gratings for six different retinal regions. **(B)** Normalized amplitudes of DC and IC response to SF of all subjects.

The first and second peaks of the waveforms are the DC and IC respectively.

There was low amplitude DC with a low SF grating (0.24cpd). The DC amplitude increased with increasing number of gratings, and decreased with increasing eccentricity at all eccentricities.

The IC was high in amplitude for all grating SF and reduced in amplitude

with increasing eccentricity. The IC waveform altered from a biphasic peak-trough formation in the central retina to a much-reduced triphasic form with reduced amplitude in the periphery. The changes of retinal response to SF were illustrated by the summary of normalizing DC and IC amplitude (**Figure 5.4B**). For DC, the responses to SF in central and peripheral regions were similar. While for IC, the central retinal response to spatial frequency differed from the peripheral retinal response.

**Figure 5.5** showed the relationship between DC amplitude and stimulus SF.

The DC amplitudes were significantly different with both SF of gratings (2-way repeated measures ANOVA: ( $F = 14.36, p < 0.001$ )) and eccentricity ( $F = 351.67, p < 0.001$ ). For the central and paracentral retina (rings 1 and 2),

DC amplitude increased significantly as SF increased (Repeated measures ANOVA: ring 1: ( $F = 10.70, p < 0.001$ ); ring 2: ( $F = 13.66, p < 0.001$ )). In

addition, the responses to 2.4 and 4.8 cpd stimuli were comparable. In the

peripheral retina (rings 5 and 6), the relationship between DC amplitude and

stimulus SF was essentially linear. Rings 3 and 4 appeared to have a

characteristic which is 'transitional' between the central and peripheral

responses. In contrast, the IC amplitudes showed two different

characteristics with increasing SF (**Figure. 5.6**). For the central retina (ring

1), IC amplitude was high with thick grating and decreased with increasing number of gratings. (Repeated measures ANOVA: ( $F = 16.65$ ,  $p < 0.001$ )). A similar trend was observed in the paracentral (ring 2) region. For rings 3-6, amplitudes were low at low SF, and increased as SF increased. There was a significant main effect of eccentricity (2-way repeated measures ANOVA: ( $F = 105.15$ ,  $p < 0.001$ )) in these data, while SF alone was not a statistically significant factor ( $F = 1.75$ ,  $p = 0.18$ ). However, there was a significant interaction between SF and eccentricity ( $F = 13.11$ ,  $p < 0.001$ ), indicating significantly different response amplitude profiles at different eccentricities.

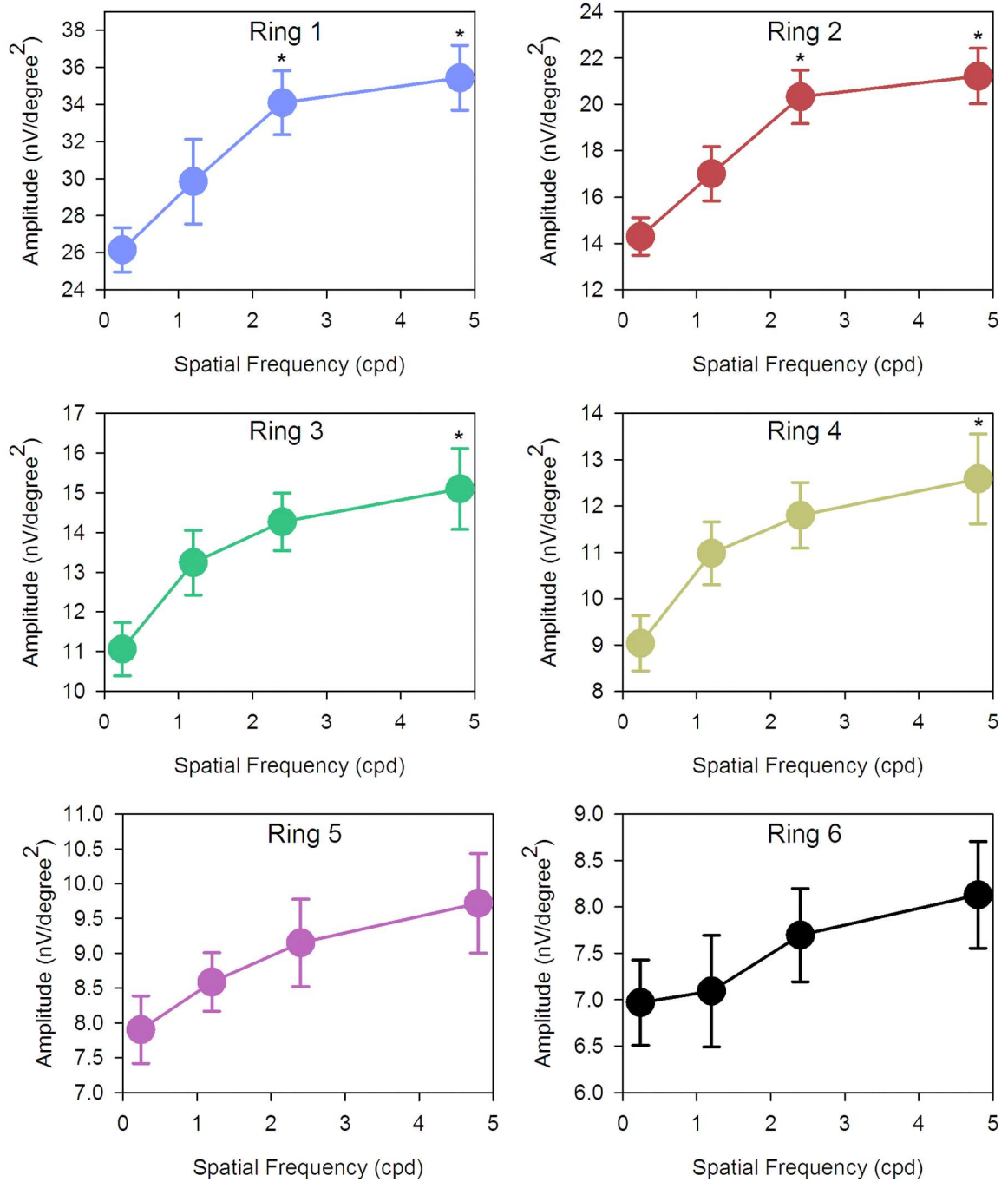


**Figure 5.5.** Absolute amplitudes of DC (mean  $\pm$  SEM) with SF of 0.24cpd to 4.8cpd from ring 1 to 6. The DC responses were generally increased with SF in all regions. Those marked with an asterisk “\*” are statistically different from the 0.24cpd.

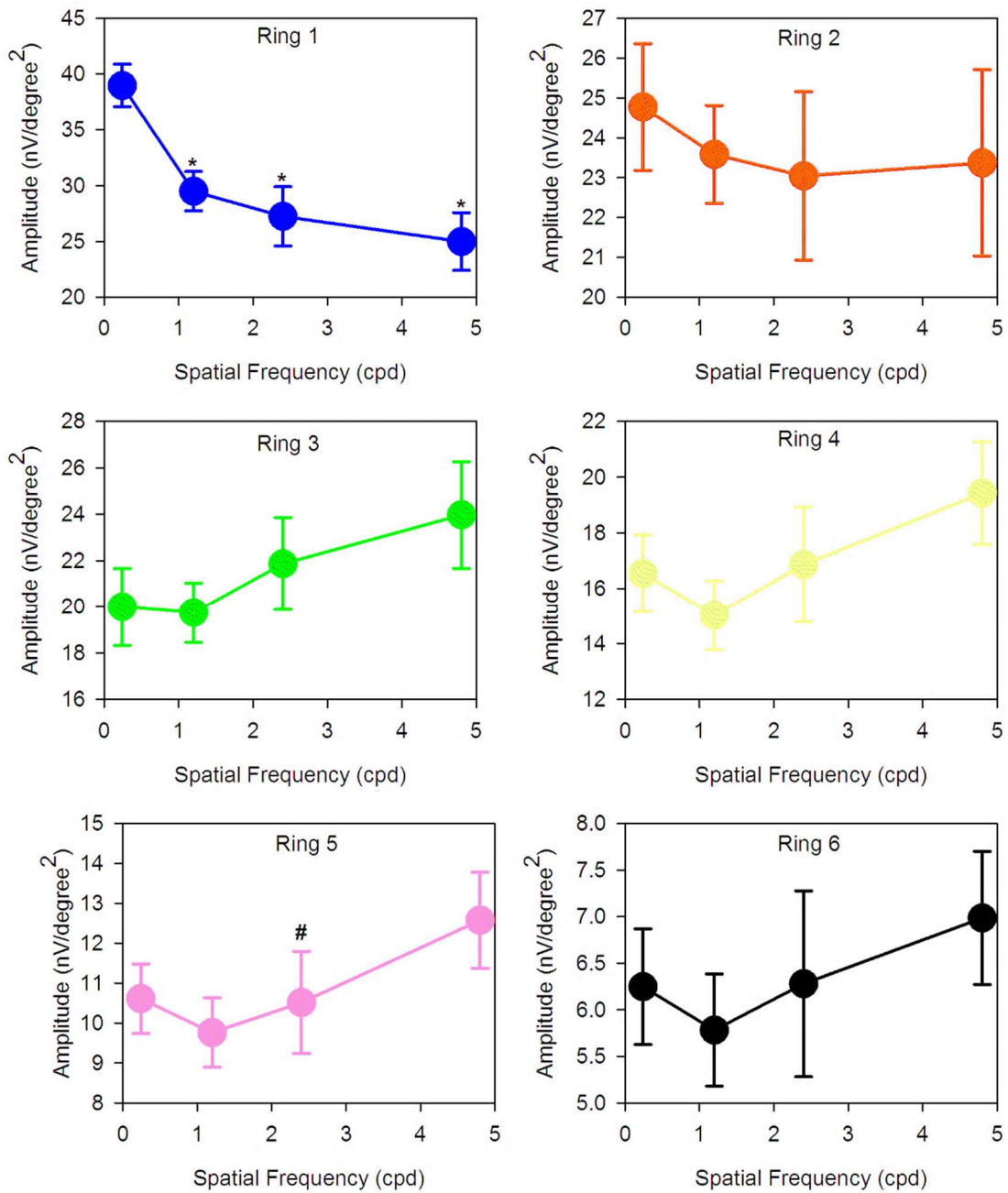


**Figure 5.6.** Absolute amplitudes of IC (mean  $\pm$  SEM) with SF of 0.24cpd to 4.8cpd of ring 1 to 6. In ring 1 and 2, the IC responses were similar. While from ring 3 to 6, the IC responses behaved differently from the central retina. Those marked with an asterisk “\*” are statistically different from the 0.24cpd while those with an asterisk “#” are statistically different between 4.8cpd and 2.4cpd.

<b>DC implicit time (ms, Mean±SEM)</b>				
<b>SF (cpd)</b>	<b>0.24</b>	<b>1.24</b>	<b>2.4</b>	<b>4.8</b>
<b>Ring 1</b>	37.17 ±0.42	36.75 ±0.35	36.8 ±0.40	37.3 ±0.27
<b>Ring 2</b>	36.63 ±0.32	37.05 ±0.37	37.1 ±0.34	37.3 ±0.20
<b>Ring 3</b>	36.4 ±0.19	37.09 ±0.28	37.2 ±0.20	37.2 ±0.25
<b>Ring 4</b>	36.16 ±0.18	36.7 ±0.23	36.2 ±0.30	36.6 ±0.19
<b>Ring 5</b>	36.3 ±0.19	36.79 ±0.19	36.4 ±0.20	36.6 ±0.24
<b>Ring 6</b>	36.7 ±0.26	37.15 ±0.21	36.8 ±0.23	36.8 ±0.23

<b>IC implicit time (ms, Mean±SEM)</b>				
<b>SF (cpd)</b>	<b>0.24</b>	<b>1.24</b>	<b>2.4</b>	<b>4.8</b>
<b>Ring 1</b>	38.2 ±0.26	38.65 ±0.24	38.9 ±0.23	38.8 ±0.30
<b>Ring 2</b>	37.41 ±0.20	37.72 ±0.21	37.6 ±0.24	37.5 ±0.22
<b>Ring 3</b>	36.35 ±0.18	36.9 ±0.19	36.8 ±0.23	36.6 ±0.18
<b>Ring 4</b>	35.92 ±0.17	36.37 ±0.20	36 ±0.18	36.1 ±0.19
<b>Ring 5</b>	36.01 ±0.17	36.37 ±0.24	36.1 ±0.25	36 ±0.23
<b>Ring 6</b>	35.92 ±0.16	36.41 ±0.32	36.7 ±0.44	35.8 ±0.22

**Table 5.1.** The DC and IC implicit for different spatial frequency and retinal region.

The DC and IC implicit time was summarized in Table 5.1. DC implicit time reduced with increasing eccentricity, and repeated measures two-way ANOVA showed a significant main effect of eccentricity ( $F = 4.01$ ,  $p=0.017$ ), but post-hoc analysis revealed few consistent effects between measurement points.

IC implicit time reduced with increasing eccentricity, and increased with increasing SF. Two-way repeated measures ANOVA showed significant

main effects for eccentricity ( $F = 119.56$ ,  $p < 0.001$ ) and SF ( $F = 6.14$ ,  $p = 0.001$ ). For all SF, post hoc analysis revealed the implicit time was significantly increased from ring 1 to ring 4 (all  $p < 0.001$ ). For ring 3, the implicit time for 1.2cpd was significantly longer than that for 0.24cpd ( $p < 0.001$ ). For ring 4, the implicit times for 1.2cpd were significantly longer than those for 0.24cpd (adjusted  $p < 0.008$ ) and 2.4cpd ( $p < 0.001$ ).

#### **5.4. Discussion**

The findings demonstrated that response to the components of MOFO mfERG differed from low to high spatial frequency. In addition, the response amplitude of DC and IC were not linear with the width of the gratings. The DC amplitude increased rapidly from 0.24cpd to 2.4cpd and then slowed from 2.4cpd to 4.8cpd across the retinal eccentricity (**Figure 5.5**). However, the trend of IC amplitude was different. The IC amplitude was the highest at 0.24cpd and decreased with increasing SF at central (i.e. ring 1 and 2) (**Figure 5.6**). However, at the mid peripheral retina (from ring 3 to 6), the trends were opposite and the IC amplitude increased with SF. In the MOFO mfERG, the DC response is the average response to a focal flash generated by m-sequences of the multifocal stimulus (Chu *et al.*, 2008; Chu *et al.*, 2006; Shimada *et al.*, 2005). It mainly represents the activity from the

outer retina composed of contributions from photoreceptors, and ON- and OFF-bipolar cells (Chu *et al.*, 2007; Chu *et al.*, 2008; Chu *et al.*, 2006; Shimada *et al.*, 2005; Shimada *et al.*, 2001). The global flash after the focal flash in the m-sequence stimulation produces the IC response, which represents the retinal adaptive response, and reflects activity from the inner retina, including amacrine cells and retinal ganglion cells (Chu *et al.*, 2007; Chu *et al.*, 2008; Shimada *et al.*, 2005; Sutter *et al.*, 1999). In this study, the luminance of the focal flash and the global flash was approximately constant while varying the SF and the luminance ratio of global flash to focal flash was not changed. As the mean luminance of the stimuli at the different spatial frequencies was similar, the changes in DC and IC with SFs were not due to the difference of luminance of different SFs. The grating acuity was closely correlated to the receptive field size of retinal ganglion cell which was increased with eccentricity. However, the trends of DC and IC amplitude response to SF were not totally followed the variation of the retinal ganglion cell field size. Hence, the changes of mfERG responses may only be explained partly by the receptive field size. The different trends of DC and IC with increasing SF indicate that the outer and inner retina may decode and process SF in different ways. The mfERG response pattern for

the central area (rings 1 and 2) differed greatly from those of the peripheral regions. It is possible that the variations of the waveform with eccentricity may reflect different adaptive mechanisms across the retina. This regional change in responsiveness may be caused by variation in the rod/cone mix with eccentricity, change in the ways in which receptors and receptive fields are connected (Chu *et al.*, 2006; Chu *et al.*, 2011).

Previous studies have used various ERG techniques to investigate the SF effect on retinal response (Arden, 1987; Berninger and Schuurmans, 1985; Falsini *et al.*, 1991; Yamada *et al.*, 2006). Yamada and colleagues (2006) applied focal macular ERG and found that the oscillatory potentials, which reflect the inner retina activity, decreased with increasing SF (Yamada *et al.*, 2006), and the current study's findings are consistent with theirs. It has long been suggested that the retina has different channels which are selectively sensitive (tuned) to particular ranges of SF (Campbell and Robson, 1968; Enroth-Cugell and Robson, 1966; Sachs *et al.*, 1971; Shapley and Lennie, 1985). The mfERG findings support the idea that both the outer (Thibos and Werblin, 1978; Werblin, 1974; Werblin and Dowling, 1969) and inner (Cook and McReynolds, 1998; Flores-Herr *et al.*, 2001; Sinclair *et al.*, 2004) retina possessing spatial sensitivity to SF. In addition, our findings further

suggested outer and inner retina respond differently to SF in the central region, while this characteristic is reduced in peripheral regions.

#### **5.4.1. Potential influence of edge effects as well as retinal lateral interactions on retinal activity**

The technique of electroretinogram (including ffERG and mfERG) was assumed to measure the potential difference from retinal cells of radially arranged within the retina, and the contribution from horizontal cells were assumed to be minimal. Some studies suggested the effects of lateral interactions in the retina were ignored, because they are known to be relatively small under the conventional mfERG paradigm (Gerth *et al.*, 2003), especially in subjects with clear optical media, as contrast attenuation at the stimulus borders is small (Sutter, 2001). Yet, by adding a global flash into the stimulation paradigm, the response to the global flash demonstrates the presence of retinal adaptation presumed to be of inner retinal origin and it has been suggested to represent the lateral interaction between cells (Chu *et al.*, 2006; Sutter *et al.*, 1999; Sutter and Tran, 1992) as well as temporal interaction. When the spatial frequency increases, the edges will increase. Lateral interaction may be accounted for the change in amplitude responses with respect to changing spatial frequencies. Seiple and colleagues (2001) demonstrated lateral interaction effect using mfERG. The response

amplitude and implicit time for the first-order kernel response significantly decreased when surrounding luminance increased (Seiple *et al.*, 2001). The DC response from the first-order kernel was found to be increased with spatial frequency in this experiment. It is likely related to lateral interaction. Lateral interaction at outer retinal level occurs at the level of horizontal cells that mediate inhibition in the form of spatially broad interconnections with other horizontal cells and acts as an inhibitory feedback onto cones (Werblin, 1974). While at inner retinal level, it is suggested lateral modification is carried out by amacrine cells (Werblin, 1972). Since refractive errors may affect the mfERG response, 12 age-matched subjects with spherical equivalent of  $-6.54 \pm 1.63D$ , underwent the same procedure. The general trend of DC and IC amplitudes against SF for the high myope group were similar to those from the low myope group

**(Appendix A).**

## **5.5. Conclusion**

In this study, mfERG measures showed that the outer and inner retina have different characteristics in processing spatial details.

**Chapter 6. Experiment 2. Human electroretinal  
responses to defocus under different spatial  
stimulus.**

(Modified from the manuscript published in: *PLoS One*, 10(4),  
pp. e0123480)

## **Abstract**

Twenty-three young adults were recruited for mfERG measurement. The retinal electrical responses for low (0.24cpd) and high (4.8cpd) SF under fully corrected conditions of short-term negative defocus (-2D) and short term positive defocus (+2D) conditions were measured. There was a sign-dependent response to defocus in the DC response, mainly in peripheral regions. The sign dependent response at low SF was more obvious than that at high SF, and was located more peripherally. The IC response showed no clear trends for either defocus condition. The human retina seems to have a decoding system for optical defocus, tuned for low spatial frequency, and located in the retinal near periphery.

## **6.1. Introduction**

The eye growth has been found to compensate for optically imposing defocus in animal studies. As a result, eye growth is thought to be guided by visual stimulus. The eye has been shown to regulate its growth locally. However, it is still controversial whether a higher centre is involved in decoding the visual stimulus for eye growth. Human electroretinal evidence of retinal ability to decode defocus comes a study by from Ho and co-workers (2011). The MOFO mfERG response was shown to be influenced

by optical defocus. The DC amplitude was reduced under hyperopic defocus while little change was seen under myopic defocus. In contrast, the IC amplitudes were shown to be increased with myopic defocus. In addition, such sign dependent mfERG response was shown to be more vigorous in the peripheral region. In addition, in Experiment 1, it was found that the DC and IC responded differently to spatial stimulus, thus spatial information was processed at retina level. In an animal study, Diether and Wildsoet (2005) showed that the compensation eye growth to myopic defocus was more efficient under a visual stimulus composed of middle to high SF, while there was no significant change observed in hyperopic defocus (Diether and Wildsoet, 2005). However, it is still not fully understood how the retina can decode signs of defocus based on Diether and Wildsoet (2005) study, decoding of defocus is possibly spatially tuned. In this study, MOFO mfERG was applied to examine the changes in retinal activities in human eye responding to specific SF under different defocus conditions.

## **6.2. Methods**

### **6.2.1. Experiment Setup**

The experiment setup was similar to Experiment 1. The spatial frequency (SFs) gratings were presented on a 22-inch colour liquid crystal display

monitor (Model: VX2260wm, ViewSonic, Hong Kong, China) during the mfERG stimulation. The mfERG stimulation (Refer to “Global flash mfERG stimulation” session) was performed using the Visual Evoked Response Imaging System software (VERIS Science 6.0.6d19; Electro-Diagnostic Imaging Inc., San Mateo, CA, USA). The stimulus array consisted of 103 non-scaled hexagons and the stimulus pattern subtended 33.7° vertically and 38.4° horizontally at a viewing distance of 40 cm. Non-scaled hexagons were used in this study to maintain the same SFs at different eccentricities.

### **6.2.2. Subject recruitment**

Twenty-three young adults aged from 20 to 27 years (mean =  $22 \pm 1.7$  years) were recruited. Two drops of 1% Tropicamide (Alcon Laboratories Inc., Fort Worth, TX, USA) were instilled with a 5-min interval to achieve the cycloplegic effect, and cycloplegia was evaluated as discussed below. Low and high SF gratings, 0.24cpd (low) and 4.8cpd (high), were selected, and the mfERG was then measured for each under various optical defocus conditions at the viewing distance of 40cm, including plano (fully corrected), positive defocus (+2D) and negative defocus (-2D). When imposing -2D defocus, the residual accommodation was compensated. For

example, if a subject possessed 0.5D residual accommodation, a -2.5D lens was used to impose -2D defocus. All subjects were reminded to report if they could manage to fixate the red-cross before and during recording. It has been shown that peripheral resolution was limited by neural sampling density, not by several diopters of defocus (Wang *et al.*, 1997), we assumed the gratings could be resolved by the retina with +/- 2D of defocus at all regions.

### **6.2.3. Evaluating the cycloplegic effect and residual accommodation**

The cycloplegic effect and the residual accommodation were assessed to ensure that they were constant throughout the experiment, as previously reported (Ho *et al.*, 2012b). The push-up method was employed to measure the residual accommodation of the tested eye of all subjects. For residual accommodation measurement, the subjects' refractive errors were corrected by adding +2D for near vision. A line of letters at their best acuity was gradually moved from a working distance of 50 cm towards the subject. The end point was reached when the line of letters was reported to blur. The residual accommodation was calculated by subtracting 2D (the near addition power given) from the amplitude of accommodation measured. This procedure was carried out three times 20 min after the instillation of the eye

drops, and immediately before and after the mfERG measurements by a masked examiner. The mfERG recordings were continued only if the difference in residual accommodation for three consecutive measurements, each separated by about 1 minute, was not more than 0.25D.

#### **6.2.4. Data analysis**

The direct (DC) and induced (IC) components of mfERG first-order kernel responses were extracted and pooled into six concentric rings for analysis (Figure. 5.3, left panel). For definition of DC and IC amplitude and implicit time, please refer to 5.2.6. Predictive Analytics SoftWare (PASW19.0, SPSS Inc., Chicago, IL, USA) was used for data analysis. Repeated measures analysis of variance (ANOVA) was applied to study the effect of SF with optical defocus on mfERG response for different retinal regions. Post hoc tests with Bonferroni adjustment were applied to correct the level of significance due to multiple comparisons of different retinal regions. The level of significance was set at 0.05.

### **6.3. Results**

The refractive errors (spherical-equivalent) of the recruited subjects ranged from +1.13D and -2.50D (mean =  $-0.48 \pm 0.89$ D) and astigmatism ranged from 0 to -1.00D (mean =  $-0.28 \pm 0.34$ D). The waveforms of MOFO

mfERG DC and IC responses under defocus conditions for 0.24cpd and 4.8cpd are shown in **Figure 6.1**. At low SF (0.24cpd), defocus with -2D lens broadened the DC response at all eccentricities, and reduced the amplitude of the response, especially in the retinal periphery. The IC response was diminished at all eccentricities (**Figure 6.1A**). Defocus with +2D lenses increased the DC response and decreased the IC response (**Figure 6.1C**). At high SF (4.8 cpd), defocus with -2D lens decreased both DC and IC response, while defocus with +2D lens appeared to have much smaller effects on either DC or IC responses at any eccentricity (**Figure 6.1 lower panels**).

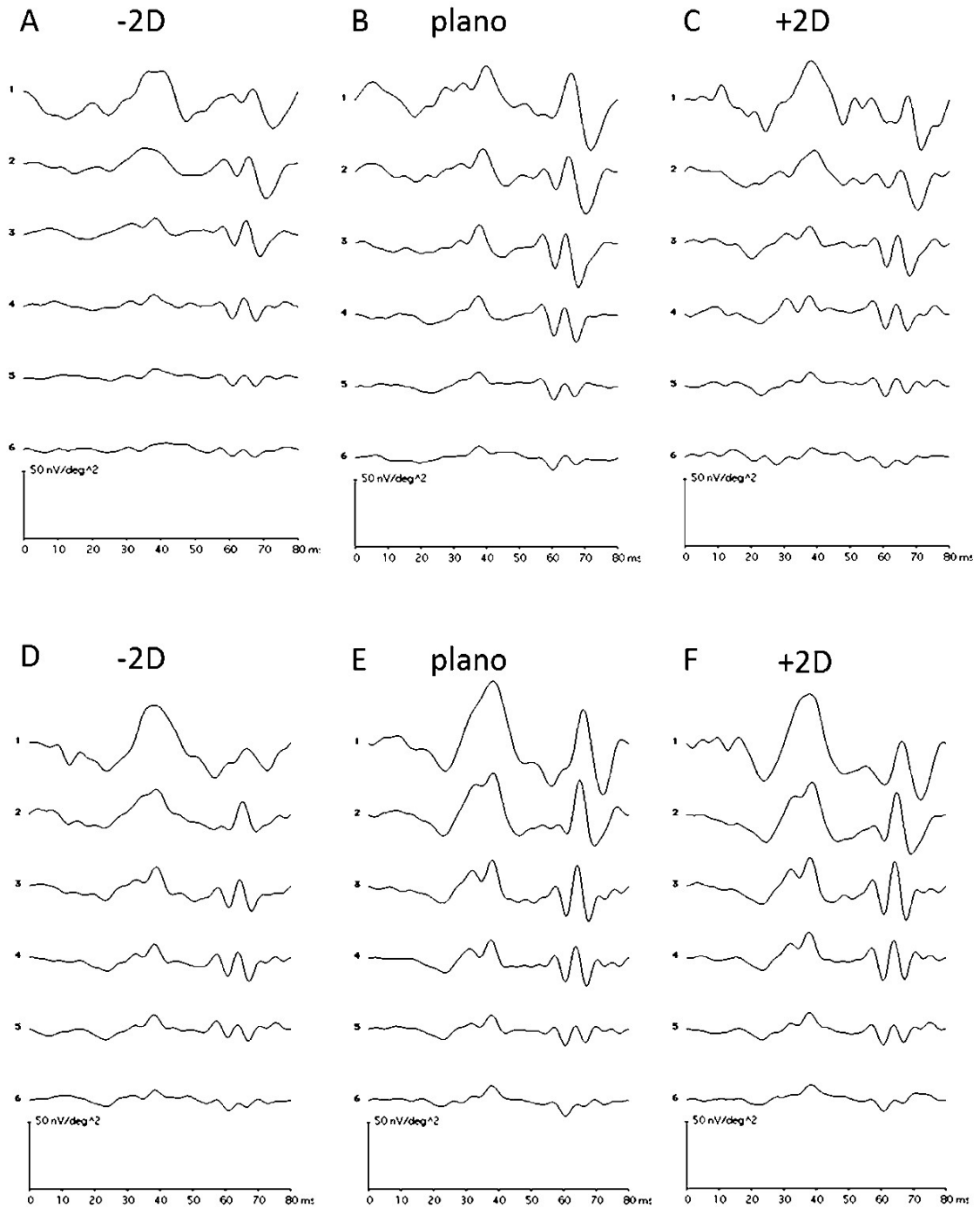


**Figure 6.1. The typical global flash mfERG waveform from one subject for high and low spatial frequency under different defocus. Upper panel: (A), (B) and (C) are responses from 0.24cpd under defocus of -2D, plano and +2D respectively. Lower panel: (D), (E) and (F) are response from 4.8cpd under defocus of -2D, plano and +2D respectively.**

**Table 6.1.** showed the average DC and IC amplitudes (mean  $\pm$  SEM) of ring regions when 0.24cpd and 4.8cpd stimuli are presented under different defocus conditions. The amplitude of both DC and IC decreased with increasing retinal eccentricity (from ring 1 to 6).

**Table 6.1.** Summary of amplitude (mean  $\pm$  SEM) of DC and IC from ring 1 to 6 under different defocus conditions with 0.24cpd or 4.8cpd.

	<b>DC amplitude (nV/degree<sup>2</sup>)</b>					
	<b>0.24cpd</b>			<b>4.8cpd</b>		
	<b>-2D</b>	<b>Plano</b>	<b>+2D</b>	<b>-2D</b>	<b>plano</b>	<b>+2D</b>
<b>Ring 1</b>	31.26 $\pm$ 2.13	27.21 $\pm$ 2.14	32.36 $\pm$ 1.77	32.76 $\pm$ 2.27	34.32 $\pm$ 2.27	35.90 $\pm$ 2.35
<b>Ring 2</b>	17.04 $\pm$ 1.22	14.87 $\pm$ 1.14	17.91 $\pm$ 1.10	18.77 $\pm$ 1.31	20.44 $\pm$ 1.53	22.17 $\pm$ 1.65
<b>Ring 3</b>	11.32 $\pm$ 0.70	11.47 $\pm$ 0.67	13.79 $\pm$ 0.67	13.84 $\pm$ 1.12	14.29 $\pm$ 1.13	17.35 $\pm$ 1.19
<b>Ring 4</b>	9.58 $\pm$ 0.71	10.49 $\pm$ 0.64	11.32 $\pm$ 0.60	11.73 $\pm$ 0.85	11.49 $\pm$ 0.93	13.41 $\pm$ 0.89
<b>Ring 5</b>	7.66 $\pm$ 0.44	8.91 $\pm$ 0.60	9.53 $\pm$ 0.53	9.93 $\pm$ 0.55	9.83 $\pm$ 0.66	10.61 $\pm$ 0.62
<b>Ring 6</b>	6.59 $\pm$ 0.47	7.46 $\pm$ 0.51	8.10 $\pm$ 0.49	8.31 $\pm$ 0.43	8.72 $\pm$ 0.62	8.92 $\pm$ 0.64
	<b>IC amplitude (nV/degree<sup>2</sup>)</b>					
	<b>0.24cpd</b>			<b>4.8cpd</b>		
	<b>-2D</b>	<b>Plano</b>	<b>+2D</b>	<b>-2D</b>	<b>plano</b>	<b>+2D</b>
<b>Ring 1</b>	28.95 $\pm$ 2.16	33.63 $\pm$ 2.54	31.65 $\pm$ 2.43	18.25 $\pm$ 1.78	22.29 $\pm$ 2.72	20.18 $\pm$ 2.91
<b>Ring 2</b>	21.72 $\pm$ 1.68	23.84 $\pm$ 1.77	24.97 $\pm$ 1.68	17.06 $\pm$ 1.52	21.62 $\pm$ 2.37	23.66 $\pm$ 2.54
<b>Ring 3</b>	19.05 $\pm$ 1.28	21.67 $\pm$ 1.87	23.02 $\pm$ 1.66	19.28 $\pm$ 1.77	20.83 $\pm$ 2.32	25.34 $\pm$ 2.62
<b>Ring 4</b>	15.23 $\pm$ 1.08	17.16 $\pm$ 1.44	17.56 $\pm$ 1.23	16.95 $\pm$ 1.67	17.30 $\pm$ 1.86	19.76 $\pm$ 2.04
<b>Ring 5</b>	9.67 $\pm$ 0.71	11.08 $\pm$ 0.88	10.64 $\pm$ 0.81	10.76 $\pm$ 1.01	10.99 $\pm$ 1.17	11.97 $\pm$ 1.13
<b>Ring 6</b>	6.44 $\pm$ 0.45	7.71 $\pm$ 0.61	6.11 $\pm$ 0.67	6.14 $\pm$ 0.64	6.24 $\pm$ 0.80	6.79 $\pm$ 0.69

Changes observed for defocus with SF interaction were more complex, and were best seen as differences from the ‘in focus’ condition. The individual percentage changes of DC and IC, with positive or negative optical defocus

compared to plano conditions for high and low SF were calculated and are shown in **Figure 6.2A and B** respectively. Although the eyes had mixed responses to defocus, the majority followed the pattern shown in **Figure 6.2**.

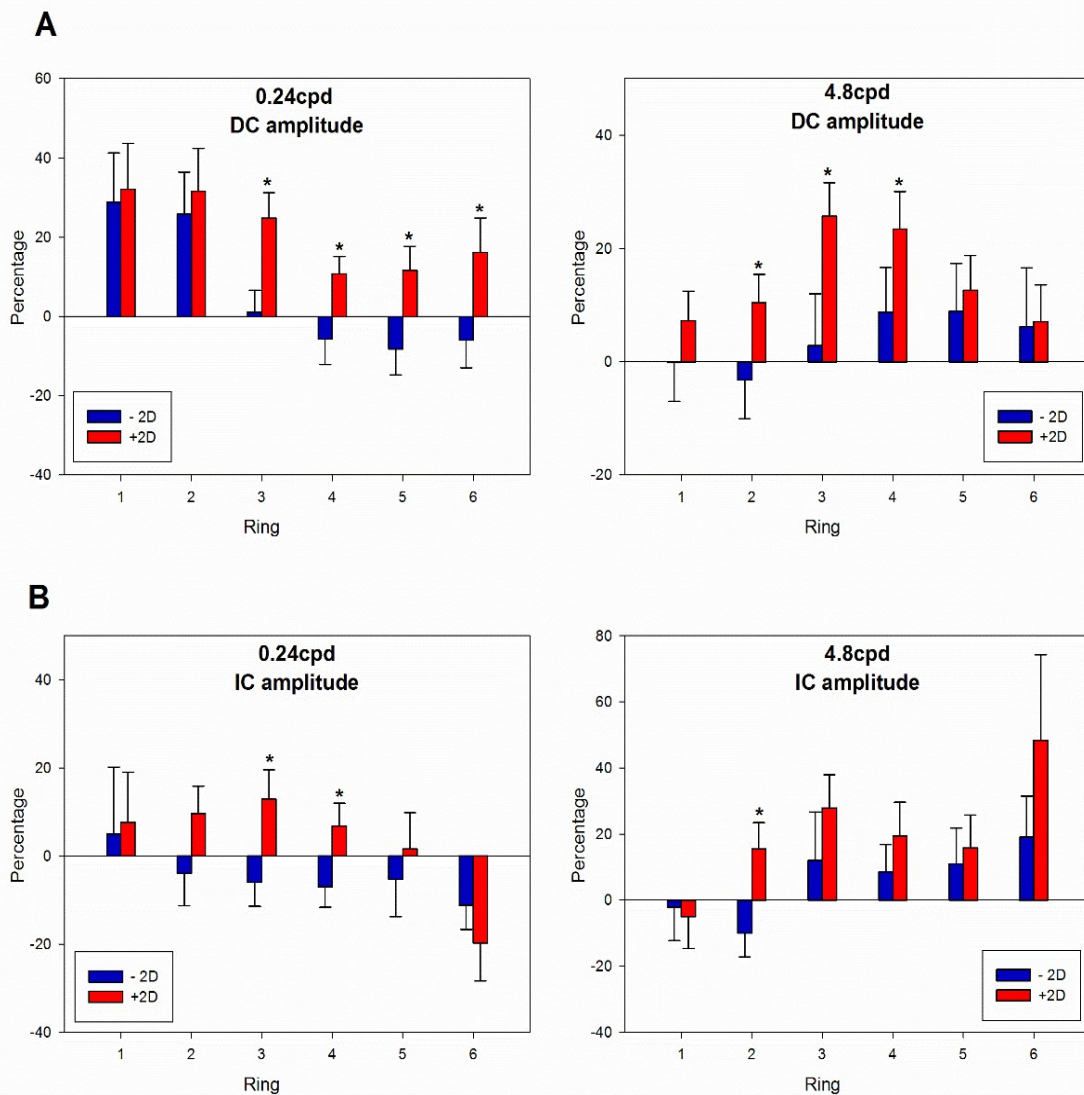


**Figure 6.2. Percentage change of DC and IC with imposing defocus under 0.24cpd or 4.8cpd.** (A) Percentage change of DC amplitudes (mean  $\pm$  SEM) with imposing defocus under 0.24cpd or 4.8cpd across the region. (B) Percentage change of IC amplitudes (mean  $\pm$  SEM) with imposing defocus under 0.24cpd or 4.8cpd across the region. Left panel is 0.24cpd and right panel is 4.8cd. Those marked with an asterisk “\*” are statistically different between +2D and -2D defocus.

For DC (**Figure 6.2A**), the trend of amplitude change with +2D defocus was significantly different from that for -2D defocus (3-way repeated measures ANOVA: ( $F = 17.99, p < 0.001$ )), while SF and region alone had no simple effect (SF:  $F = 0.06, p = 0.80$ ; Region:  $F = 1.63, p = 0.19$ ). There was no significant 3-way interaction (Region x SF x Defocus) for DC amplitude percentage change ( $F = 1.98, p = 0.13$ ). However, there was a significant interaction between region and SF ( $F = 3.94, p = 0.01$ ), indicating differing responses as eccentricity increased, as expected, but no interaction was found between region and defocus ( $F = 2.41, p = 0.07$ ). Further examination of the region and SF interaction by 2-way repeated measure ANOVA revealed a significant interaction when imposing -2D defocus ( $F = 4.83, p = 0.005$ ).

Imposing +2/-2D theoretically would produce the same magnitude of blur, and the retinal response should be the same if the retina responds only to blur and not to the sign of defocus. The results in this study demonstrated that imposing the same magnitude of defocus with different sign produces different retinal responses. At low SF (0.24cpd), +2D defocus produces 20-30% increase in response at all eccentricities (**Figure 6.2A, left panel**). In contrast to this, -2D defocus only gave increased amplitudes only centrally,

but reduced amplitudes from the mid-periphery to the far periphery. Under 0.24cpd (**Figure 6.2A left panel**), both +/-2D could trigger significant increase in DC amplitudes at ring 1 and 2 compared to the plano condition (one sample T test, +2D:  $p = 0.01$ ; -2D:  $p = 0.03$ ) but the sign of defocus was not differentiable. From ring 3 to 6, +/-2D triggered either increase or decrease in amplitude according to sign of defocus. This characteristic was reduced at higher SF (4.8cpd). At 4.8cpd, the +2D defocus produced an increased DC amplitude in the near and mid-periphery, while the -2D defocus had essentially no effect on amplitude of response (**Figure 6.2B, right panel**).

The IC response appeared to be more variable, but the +2D defocus at low SF showed increase response over the majority of the retina (excluding the far periphery), with strongest response in the mid-periphery. The -2D defocus showed a consistent decrease in amplitude of response across the peripheral retina (**Figure 6.2B, left panel**). Three-way repeated measures ANOVA of IC percentage change showed significant main effects of defocus ( $F = 7.60$ ,  $p = 0.01$ ), while region ( $F = 0.51$ ,  $p = 0.65$ ) and SF ( $F = 2.80$ ,  $p = 0.11$ ) did not show any main effect. There was a significant interaction between region and SF ( $F = 4.07$ ,  $p = 0.01$ ) but no significant 3-

way interaction (Region x SF x Defocus:  $F = 1.45$ ,  $p = 0.24$ ). At higher SF, the +2D defocus produced a consistent increase in IC amplitude across the peripheral retina, and smaller increases were seen with -2D defocus from ring 3 and beyond (**Figure 6.2B, right panel**).

**Table 6.2.** The DC and IC implicit time for high and low SF under defocus and plano conditions for different retinal regions.

DC implicit time (ms, mean $\pm$ SEM)						
	0.24cpd			4.8cpd		
	-2D	Plano	+2D	-2D	Plano	+2D
<b>Ring 1</b>	36.79 $\pm$ 0.36	37.01 $\pm$ 0.43	36.8 $\pm$ 0.40	37.51 $\pm$ 0.33	37.2 $\pm$ 0.39	37.09 $\pm$ 0.44
<b>Ring 2</b>	36.46 $\pm$ 0.32	36.91 $\pm$ 0.33	36.8 $\pm$ 0.32	37.46 $\pm$ 0.44	36.7 $\pm$ 0.52	37.21 $\pm$ 0.34
<b>Ring 3</b>	36.44 $\pm$ 0.22	36.3 $\pm$ 0.21	36.5 $\pm$ 0.30	37.22 $\pm$ 0.35	36.8 $\pm$ 0.45	36.62 $\pm$ 0.27
<b>Ring 4</b>	36.22 $\pm$ 0.23	36.03 $\pm$ 0.17	36.2 $\pm$ 0.30	36.56 $\pm$ 0.19	36.1 $\pm$ 0.21	36.44 $\pm$ 0.21
<b>Ring 5</b>	36.35 $\pm$ 0.21	36.39 $\pm$ 0.19	36.2 $\pm$ 0.27	36.49 $\pm$ 0.20	36.1 $\pm$ 0.21	36.32 $\pm$ 0.18
<b>Ring 6</b>	37.11 $\pm$ 0.33	36.5 $\pm$ 0.20	36.7 $\pm$ 0.32	36.57 $\pm$ 0.34	36.6 $\pm$ 0.26	36.85 $\pm$ 0.29

IC implicit time (ms, mean $\pm$ SEM)						
	0.24cpd			4.8cpd		
	-2D	Plano	+2D	-2D	Plano	+2D
<b>Ring 1</b>	38.96 $\pm$ 0.32	38.44 $\pm$ 0.31	38.6 $\pm$ 0.30	38.93 $\pm$ 0.46	38.1 $\pm$ 0.52	38.21 $\pm$ 0.41
<b>Ring 2</b>	37.48 $\pm$ 0.24	37.2 $\pm$ 0.23	37.1 $\pm$ 0.20	37.78 $\pm$ 0.40	37.5 $\pm$ 0.35	37.05 $\pm$ 0.26
<b>Ring 3</b>	36.47 $\pm$ 0.20	36.61 $\pm$ 0.29	36.4 $\pm$ 0.24	36.81 $\pm$ 0.36	36.8 $\pm$ 0.36	36.32 $\pm$ 0.21
<b>Ring 4</b>	36.04 $\pm$ 0.18	35.96 $\pm$ 0.21	36 $\pm$ 0.22	36.15 $\pm$ 0.33	36 $\pm$ 0.26	35.88 $\pm$ 0.20
<b>Ring 5</b>	36.09 $\pm$ 0.20	35.96 $\pm$ 0.18	35.7 $\pm$ 0.20	36.01 $\pm$ 0.36	36 $\pm$ 0.32	35.91 $\pm$ 0.37
<b>Ring 6</b>	36.11 $\pm$ 0.20	35.78 $\pm$ 0.34	35.8 $\pm$ 0.23	35.4 $\pm$ 0.44	36.2 $\pm$ 0.39	36.31 $\pm$ 0.43

The DC and IC implicit time for high and low SF under defocus and plano condition was summarized in Table 6.2. For the DC implicit time, both SF and region had significant main effects (SF:  $F = 5.55$ ,  $p = 0.003$ ; Region:  $F = 6.29$ ,  $p = 0.003$ ) and there was no significant 3-way interaction (Region x SF x Defocus:  $F = 1.56$ ,  $p = 0.19$ ). For IC implicit time, both defocus and

region had significant main effects (Defocus:  $F = 4.66$ ,  $p = 0.03$ ; Region:  $F = 72.28$ ,  $<0.0001$ ) but there was no significant 3-way interaction ( $F = 0.74$ ,  $p = 0.48$ ).

## **6.4. Discussion**

### **6.4.1. Regional sensitivity to defocus**

In Experiment 2, the DC responses to +2D and -2D differ mainly in the peripheral regions. For the 0.24cpd stimulus, the DC responses for rings 1 and 2 were less differentiable during stimulation with positive or negative defocus. In peripheral regions (ring 3 to 6), the DC responses were different with positive or negative defocus, suggesting that the peripheral region may be the site for the decoding of optical defocus. A similar hypothesis has been proposed in animal studies, suggesting that the retina may be able to decode defocus and that the eye grows according to the sign of defocus (Park *et al.*, 2003; Schaefel and Diether, 1999). Subsequent studies have shown that peripheral defocus can influence overall refractive error development in chicks (Liu and Wildsoet, 2012) or in monkeys (Smith *et al.*, 2009; Smith *et al.*, 2010), highlighting the dominant role of the peripheral retina in the regulation of ocular growth. In addition, it has been demonstrated that in clinical studies, myopic progression can be slowed by wearing

orthokeratology lenses. It has been speculated that the presence of myopic defocus on the peripheral retina may be the critical factor in slowing myopia development (Cho and Cheung, 2012; Mok and Chung, 2011). In this study, IC percentage change in differentiating optical defocus in the peripheral retina was observed in the 0.24cpd condition, but is not in the 4.8 cpd condition. This indicates that sign-dependent responses to defocus are mainly from the peripheral regions rather than the central retina. Ho *et al.* (2012b) used MOFO mfERG in human eyes and showed that DC and IC demonstrated different trends of changes with various levels of defocus from -4D to +4D (Ho *et al.*, 2012b). The peripheral retinal response to defocus was more vigorous than that of the central retina, a finding which is in agreement with the present study. Furthermore, although the subjects in this cohort and those in the study of Ho *et al.* (2012b) were mainly low stable myopes, the sign-dependent retinal characteristics were still present even though the myopia is stable. It has previously been noted that inner retinal function differs between stable myopes and progressing myopes (Chen *et al.*, 2006a). It would be of interest to determine whether progressing myopes have similar regional retinal response characteristics to defocus and SF as those reported here.

In the current study, the +2D defocus stimulus generally triggered higher mfERG responses than -2D defocus, suggesting that the retina responds more vigorously to myopic defocus. Previous animal studies have demonstrated that eye growth is more responsive to myopic defocus than to hyperopic defocus (Winawer and Wallman, 2002; Winawer *et al.*, 2005; Zhu *et al.*, 2003). In addition, Zhong and colleagues (2004) have shown that different conditions of optical focus can affect the activity of ON-bipolar as well as GABAergic amacrine cells in the primate retina (Zhong *et al.*, 2004). They used immunocytochemical markers to illustrate cellular activity which increased when images were in focus or had positive defocus; the response decreased for images with negative defocus. These findings match our findings, that the mfERG responses, in both DC and IC amplitudes, are higher with +2D defocus than with -2D defocus over the regions under stimulation.

#### **6.4.2. Spatial frequencies and defocus**

Spatial frequency was found to be a significant factor, even with the same amount of defocus in the same region. This finding showed sign dependent characteristic were present in the peripheral regions for both SF, and that DC reacted more vigorously under 0.24cpd (low SF) at ring 1 and 2 than if

under 4.8cpd (high SF). It is important to note that the low and high SF in this study were relative to each other, rather than the resolution threshold of the retina. The vertical grating resolution limit of the retina is about 5cpd at 20° (Atchison *et al.*, 2006; Rovamo *et al.*, 1982). All the subjects were able to detect the gratings when presented under focus and defocus conditions both centrally and in the peripheral retina.

In addition, the mfERG response of imposing +2/-2D defocus from central up to 20° in the periphery was investigated. There was concern that peripheral regions should receive the same amount of imposed defocus as the central retina. Previous studies have demonstrated that emmetropic or hyperopic eyes showed myopic shifts whereas most myopes have hyperopic shifts in the peripheral retina (Atchison *et al.*, 2006). Yet, it was noticed that the refractive errors from central to peripheral 20° for low myopes (less than 2D) are relatively stable within the central 20° of the visual field (Atchison *et al.*, 2006; Chen *et al.*, 2010). We were aware of the individual variation of peripheral refractive error beyond 20° of the visual field, but assumed the retina was experiencing roughly the same amount of defocus from ring 1 (1.75°) to ring 6 (19.2°) in our study.

The sign-dependent retinal activity was observed for the 0.24cpd stimulus in

the peripheral regions but was not as obvious for the 4.8cpd stimulus. If the retina possesses a mechanism to differentiate the sign of defocus, there must be some cues for the retina to extract the sign of defocus. The results suggest that the retina is more effective in extracting defocus under low SF than under high SF in the peripheral regions rather than in the central region. Anatomically, the receptive field size increases with eccentricity, and the peripheral retina cannot resolve spatial details with very high SF. It is reasonable to infer that the defocus decoding mechanism can respond to spatial stimuli with low SF rather than high SF. However, from the findings, it cannot be ascertained how the various defocus levels interact with the spatial details. That is, the defocus decoding mechanism may have preference for different SF under different optical defocus conditions. In terms of IC response to defocus, the trend was not as obvious as for DC for the two SFs. A general trend of increased amplitude with +2D defocus and reduced amplitude with -2D defocus was observed for the 0.24cpd condition for rings 2 to 5.

Imposing defocus reduces the contrast of the retinal image and reduction in image contrast may potentially decrease the amplitude of the mfERG response. A previous study has shown imposing myopic defocus could

reduce contrast sensitivity, especially at high SF (Green and Campbell, 1965). In addition, the mfERG amplitude is decreased with a decrease of stimulus contrast without imposed optical defocus (Brown and Yap, 1996; Chu *et al.*, 2006). Brown and Yap (1996) showed that reductions of amplitude are linear with little deviation in both foveal and peripheral regions (Brown and Yap, 1996). Yet our results showed some regions had increase in amplitudes after imposition of defocus. Both DC and IC amplitudes of MOFO mfERG were shown to be decreased with reducing contrast in previous studies (Chu *et al.*, 2007; Chu *et al.*, 2008; Chu *et al.*, 2006). Therefore, contrast reduction of the image after imposing defocus cannot fully account for the trend of mfERG amplitude response in low and high SF with +2/-2D defocus which should produce the same contrast reduction in terms of optical properties. Furthermore, the DC and IC amplitude responses of low SF across the retinal regions are comparable with the findings of Ho *et al.* (2012b). Our data confirms their low SF data (regarding each hexagon as stimulus with very low SF) and extends their findings to high SF data, which in this study behaves differently to low SF stimuli.

### **6.4.3. Does retinal image at different spatial frequency and retinal defocus affect myopia?**

Results from animal studies have shown that emmetropization is spatial-frequency tuned (Diether and Wildsoet, 2005; Hess *et al.*, 2006; Schmid and Wildsoet, 1997; Tran *et al.*, 2008; Zhi *et al.*, 2013) and myopia progression is related to exposure of hyperopic defocus (Read *et al.*, 2010; Smith *et al.*, 2009; Smith *et al.*, 2010; Winawer *et al.*, 2005). Both human and animal studies have shown that the eye can decode sign and magnitude of defocus (Day and Duffy, 2011), this still leaves the question of how the retina decodes the defocus. Our findings indicate that the retina respond to defocus more vigorously in lower spatial frequencies. Recent studies suggested non-central retina is corresponding to eye growth (Smith *et al.*, 2009; Smith *et al.*, 2010). While the foveal region provides good spatial vision because of its high resolution, peripheral retina has lower resolution which would be insensitive to defocus in high spatial frequency as it cannot “resolve” the defocus. As the emmetropization is a local regulatory mechanism to manipulate eye growth achieving a clear retinal image according to the visual signals, our findings provide evidence the human retina can differentiate sign of optical defocus at the peripheral region, while it is more sensitive in lower spatial frequency in order to compensate for

environmental influence. Further study is needed to confirm whether rate of eye growth is affected by spatial stimulus, given that the amount of defocus signal is kept the same.

#### **6.4.4. The consideration of aliasing effect in the experimental design**

The selection of spatial frequency in human experiment was based on the spatial resolution of human retina. At central retina, image sampling is neural limited by cone photoreceptor density (Green, 1970; Williams, 1985), whereas ganglion cell density limited peripheral resolution (Anderson *et al.*, 1991; Chui *et al.*, 2005). The resolution is highest at fovea and decrease when retinal eccentricity increase. The resolution acuity was about 5 cpd at retinal eccentricity of 20° horizontally and 13° vertically retinal eccentricity (Wilkinson *et al.*, 2016). The upper limit of SF selected in human study was 4.8cpd, so it is within the resolution limit and avoid potential aliasing effect.

#### **6.4.5. The pros and cons of using non-scaled stimulus patterns in human study**

When the hexagons are scaled, the sizes of the hexagons get larger as they extend peripherally, the average magnitude of response per hexagon would be roughly constant across rings. In addition, the signal-to-noise ratio is maintained more or less the same across the whole stimulated area (Sutter

and Tran, 1992). However, the scaling is approximated and depends on individuals and displays, which would be difficult for comparison between studies, especially in case of various protocols. Another consideration for the current human study was that the overall luminance within each hexagon was tried to maintain the same for all spatial frequencies. Thus, non-scaled hexagons are better to control the overall luminance of each hexagon with different spatial frequency across the retina and it is adopted to be used. In addition, as the amount (area) of defocus (signal) would be affected by the stimulus size if scaled hexagons were used, the use of the non-scaled hexagon allows direct comparison between defocus conditions against control (plano) condition at different eccentricities in Experiment 2.

## **6.5. Conclusion**

In this experiment, it was shown that the peripheral retina can differentiate positive and negative defocus more effectively for low spatial frequencies than the central retina. The human retina seems to have a decoding system for optical defocus, which is tuned for low spatial frequency, and is located in the retinal near periphery.

**Chapter 7. Experiment 3. Spatial dependency of  
myopia development in chick**

## **Abstract**

**PURPOSE:** Eye growth is a self-regulated local process relying on visual feedback. Chicks were chosen to investigate how the eye responds to hyperopic defocus under different spatial visual stimuli.

**METHODS:** One eye of normal chicks (10-11 days old) was fitted with a lens-cone device (40mm in length) monocularly and the fellow eye acted as a control. At the proximal end of the cone, lenses with powers of +25D, +20D, +15D and +10D were placed. At the distal end of the cone, a high spatial frequency (SF) visual patterns (0.4mm x 0.4mm black and white checks, 0.9 cpd) and a low SF visual patterns (1.2mm x 1.2mm black and white checks, 0.3 cpd) were used as visual stimuli. On-axis ocular refraction and axial ocular component dimensions were measured before wearing the device, and on day 4 and day 7 after lens-cone wearing.

**RESULTS:** Both spatial stimulus and defocus had a significant main effects on interocular vitreous chamber depth (VCD) and on refractive error (RE) on day 4 and day 7. Eye growth was significantly faster and more myopic for chicks wearing the device with low SF visual stimuli than those with high SF stimuli.

**CONCLUSION:** In chicks, the myopia development induced by hyperopic

defocus was shown to be dependent on spatial stimulus. The rate of compensation to induced hyperopic defocus was higher with low SF stimulus.

## **7.1. Introduction**

The eye is similar to other organs in the body having a self-regulated growth process and this process is called emmetropization. During emmetropization, the components of the eye develop in a coordinated manner, and the axial length of eyeball is matched to the focal length to achieve clear vision. This eye growth process has been shown to be dependent on visual stimulation in many studies (Refer to Chapter 2). In animal models, it has been shown that eye growth can compensate for the sign of the induced defocus in various vertebrate species such as chicks (Irving *et al.*, 1992; Schaeffel *et al.*, 1990; Wildsoet and Schmid, 2001; Wildsoet and Wallman, 1995), guinea pigs (Howlett and McFadden, 2009; McFadden *et al.*, 2014; McFadden and Wildsoet, 2009), tree shrews (Norton *et al.*, 2006; Shaikh *et al.*, 1999), and primates (Smith and Hung, 1999; Smith *et al.*, 2010). The retina is believed to have a local mechanism to detect defocus and to convert the visual stimulation provided by the image to a growth signal which is the basis of the emmetropization process (Miles

and Wallman, 1990; Norton and Siegwart, 1991; Smith *et al.*, 2010; Wallman *et al.*, 1987). Diether and Wildsoet (2005) showed that compensation to myopic defocus was more effective with inclusion of higher spatial frequencies. However, the physiological mechanism to detect the sign of defocus in the retina is still not clear. In humans, electroretinal activity was shown to have sign-dependent changes in defocus (Ho *et al.*, 2012b), implying the retina can locally decode defocus. Furthermore, in Experiment 2, it was found that there was a SF preference for human retina in responding to defocus (Chin et al 2015). It is possible that the signal of defocus can be extracted by a specific type of retinal neuron which are spatially tuned. In the experiment by Diether and Wildsoet (2005), the SF dependency could be seen in compensation to myopic defocus but no particular spatial preference was reported on hyperopic defocus (Diether and Wildsoet, 2005). As hyperopic defocus is believed to be important in myopia development, the influence of high and low SF in compensation of hyperopic defocus would be re-visited in this study. In Experiment 3, the spatial influence on emmetropization set-points with various levels of hyperopic defocus was investigated.

## **7.2. Methods**

### **7.2.1. Animals**

White Leghorn chick (*Gallus gallus*) pathogen-free fertilized eggs were hatched in the University's central animal facilities. They were housed in an enclosure made of metal mesh (distant viewing was assumed unrestricted for the control eye) under a 12-hour light/12-hour dark cycle (from 7am to 7pm). Food and water were given ad libitum. Chicks were 10 to 11 days old at the start of experiment. Adaptation of the 10 to 11 day old chicks to the lens-cone treatment was determined (see Lens-cone system below). These chicks adapted faster than younger animals and returned to normal feeding behavior in a day (**Figure 7.1D**). All the rearing and experimental procedures were approved by the Animal Ethics Committee of The Hong Kong Polytechnic University and were in compliance with the ARVO Statement for the Use of Animals in Ophthalmic and Vision Research. The room lighting ranging from 700-1000 lux (measured at different locations at the level of the food containers).

### **7.2.2. Lens-cone system**

The right eye of the chicks was fitted with a modified lens-cone system of a similar design as has been described in previous studies (Diether and

Wildsoet, 2005; Hess *et al.*, 2006; Nevin *et al.*, 1998; Schmid *et al.*, 2006; Tse and To, 2011; Wildsoet and Schmid, 2001). The cones were made of a translucent plastic material. Epoxy resin was used to assemble the parts and secure the cone onto a Velcro ring, which attached the cone to the eye surround of the chick. A PMMA lens was embedded at the proximal end of the cone, limiting the vision of chick to the distal end of the cone which provided the spatial stimulus (**Figure 7.1A**). The distance from the lens to the target plane was 40mm, which is equivalent to 25D of vergence. Thus, using a +25D lens, by the thin lens formula, gives 0D (plano) of defocus at the target. Using the thick lens formula yields very mild hyperopic defocus at the corneal plane of the chick eye (Schmid *et al.*, 2006). In addition, the central and peripheral defocus may be slightly different as the focal plane of the lens is curved (Tse and To, 2011). Since the same set of cones was used for the whole experiment, it was assumed that the errors caused by the lens and the slight fluctuation in target position would be very similar even if different spatial stimuli were presented. The back vertex powers of lenses were +25D, +20D, +15D, +10D (optical zone diameter 10.0 mm, back surface radius 12.0 mm), which gave 0D, -5D, -10D and -15D hyperopic defocus respectively (using the thin lens formula (**Table 7.1**)). The cones

were attached by Velcro rings as shown in **Figure 7.1B** and **C**. Lenses were cleaned and checked daily to minimize decentration or dislocation.

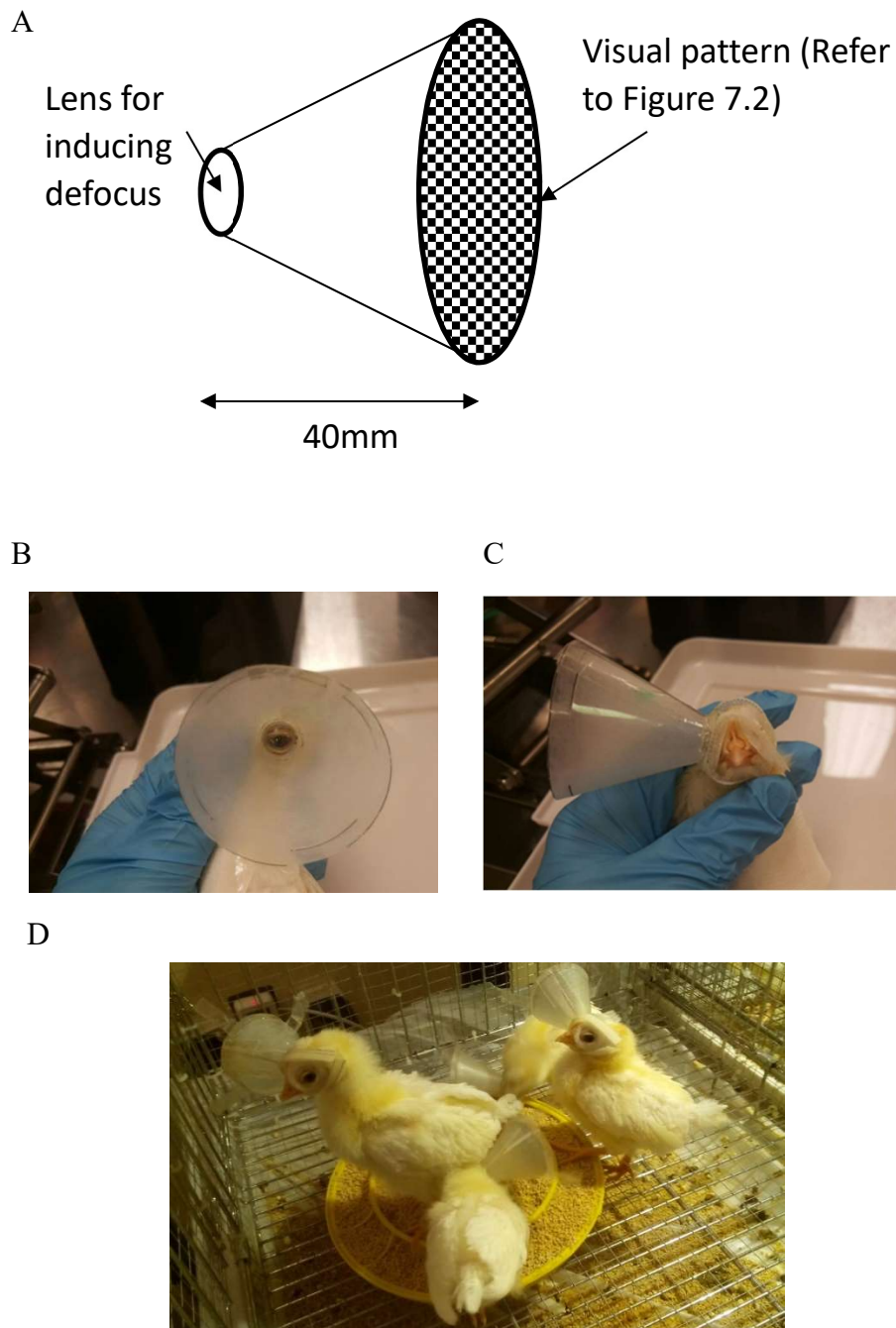


**Figure 7.1. Lens-cone device and animal preparation.** (A) Schematic diagram of a lens-cone device. A lens was placed at proximal end of the device. A visual target with different spatial patterns was positioned at the distal side of the device. (B) and (C) Attachment of the lens-cone device on the chick's right eye. The eye was tried to position at the centre of the lens and the device was stabled by Velcro. (D). 10 to 11 days old chicks were used as they adapted to the lens-cone device quicker and returned to normal feeding behavior in a day.

### 7.2.3. Visual target

Visual targets were constructed using Corel Draw (CorelDraw; Corel Corporation, Ottawa, Canada). The diameter of the target plane was 44.85mm, so field of view was 52.8 °. Schematic diagrams of visual stimuli are shown in **Figure 7.2**. High contrast black and white checks were used as targets. The stimuli were composed of spatial checks of uniform size (**Figure 7.2A and B**). The sizes of the small checks (relatively high SF, **Figure 7.2A**) and the large checks (relatively low SF, **Figure 7.2B**) were 0.4mm x 0.4mm (0.9 cpd at 40mm) and 1.2mm x 1.2mm (0.3 cpd at 40mm) respectively. The spatial patterns used were within the acuity limit of the chick eye with reported ranging from 1.5cpd (Over and Moore, 1981) to 8.6cpd (Schmid and Wildsoet, 1998). Thus, chicks should be able to resolve the visual patterns used in this experiment. It is appreciated that the patterns were trimmed at the stimulus margin. This would induce a small error in the ratio of the high and low spatial patterns. It was assumed that the small error would not affect the modulation of eye growth. A high-resolution (up to 600 x 600 dpi) printer (LaserJet Pro 200 color Printer M251nw; Hewlett-Packard, Avondale, PA, USA.) was used to print out the targets for the experiment.

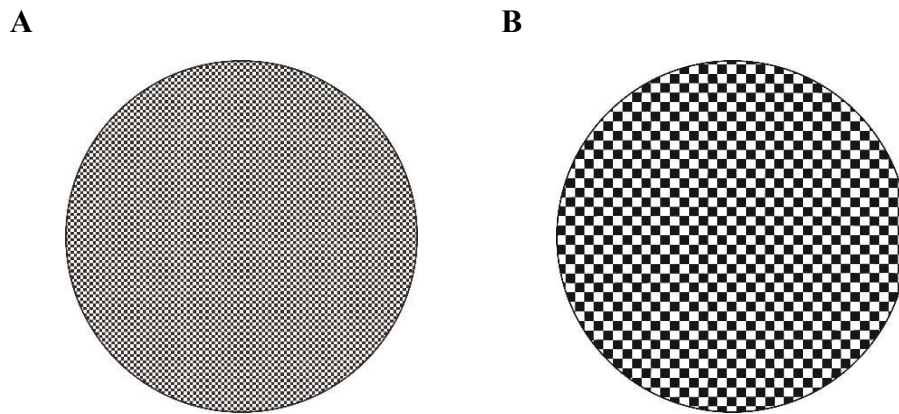


**Figure 7.2. Schematic diagrams of high contrast black and white checkers as visual stimulus. (A)** Uniform small checkers as high spatial content. The size of the check was 0.4mmX0.4mm (0.9 cpd at 4 cm). **(B)** Uniform checkers as low spatial content. The size of the check was 1.2mmX1.2mm (0.3 cpd at 4 cm).

#### 7.2.4. Measurement

Biometric and refractive data were collected before application of the lens-cone device, on day 4 and on day 7 of the experiment. The refractive status was measured along the pupillary axis using a modified Hartinger refractometer (Jena Coincidence Refractometer, Model 110, Carl Zeiss Meditec, Jena, Germany) (Chu and Kee, 2015) in anaesthetized chicks. The chicks were anaesthetized by 1.0% isoflurane in oxygen for low complication (Furtado and Andrade, 2013). Axial ocular dimensions were obtained using A-scan ultrasonography (Refer to 7.2.4.1. A-scan ultrasonography). Chicks with the following conditions were excluded from the experiment: the lens-cone device being detached, the device being

dislocated in which the eye not aligned with the optical zone of the lens, abnormal eye conditions such as inflammation, excessive tearing, etc., and the chick eye not opening freely when the lens-cone device was attached. Ocular parameters that beyond 3 standard deviations of individual group means would be regarded as outlier and excluded. There are 15 chicks (12%) were excluded. The lens-cone device was placed on the right eye of chicks and the fellow eye was used as a control.

#### **7.2.4.1. A-scan ultrasonography**

The setting of A-scan ultrasound system in Experiment 3 and 4 was described in previous study (Prashar *et al.*, 2009). It was consisted of a 25 MHz transducer probe of focal length 25 mm. The probe (Panametrics, model 5073PR) was fitted with a 15mm saline stand-off at 0.1 ml/min perfusion rate, and a personal computer fitted with a digital acquisition card (model DP110, Acqiris, Switzerland). The waveforms were sampled at 100 MHz. Distinct peaks that corresponding to ocular components of eyeball of a sample trace is shown in **Figure 7.3**. Clear and distinct peaks for corresponding ocular components were regarded with accepted measurement and average of three measurements were calculated. The ultrasound traces were assumed the velocities of 1608m/s in the lens and

1534m/s in other ocular components. Post-acquisition analysis was carried out on the waveform ‘peak assignments’ to identify the components including anterior chamber depth (ACD), lens thickness (LT), vitreous chamber depth (VCD) and axial length (AXL) (Figure 7.3).

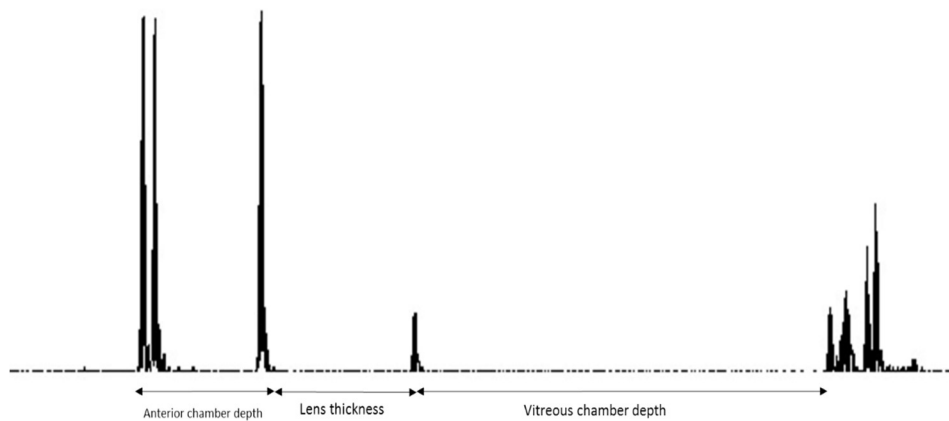


**Figure 7.3. Ultrasound waveforms generated from a chick eye.** The major peaks corresponding to the cornea, anterior lens surface, posterior lens surface and posterior segment are visible (from left to right). Post-acquisition analysis was carried out on the waveform ‘peak assignments’ to identify the components including anterior chamber depth (ACD), lens thickness (LT), vitreous chamber depth (VCD) and axial length (AXL).

### 7.2.5. Experimental Groups and Treatment Protocol

Table 7.1 summarizes the treatment conditions including spatial frequencies, magnitude of imposed defocus and numbers of chicks in different conditions. Animals were divided into eight groups based on the levels of induced defocus magnitude (plano (0D), -5D, -10D and -15D) and different spatial stimulus patterns (H: high SF; L: low SF).

**Table 7.1.** Treatment condition for each group of chicks.

<b>Treatment</b>		<b>number of chicks</b>
<b>Induced Defocus</b>	<b>Spatial Stimulus</b>	
0D	H	16
0D	L	15
-5D	H	11
-5D	L	12
-10D	H	11
-10D	L	9
-15D	H	17
-15D	L	22

### **7.3. Data analysis**

Interocular differences (right eye minus left eye) as mean ( $\pm$  SEM) were presented. The overall effects of SF and defocus were tested with two-way ANOVA using the Predictive Analytics SoftWare (PASW19.0, SPSS Inc., Chicago, IL, USA). Planned comparison was carried out to investigate the effect of SF in each defocus condition. Near all the groups had passed the normality test ( $p > 0.05$ ). Bonferroni post hoc testing was applied if it was appropriate between treatment groups. The level of significance was set at 0.05.

### **7.4. Results**

Although there was significant difference in ACD and LT in some groups, the interocular difference for the baseline ocular parameters overall was close to zero, which means the right eye and left eye were symmetrical

before applying the lens-cone devices. In this study, either high SF or low SF checks were presented to groups of chicks under various magnitudes of hyperopic defocus. The interocular changes and the number of chicks in each group on day 4 and 7 were showed in **Table 7.2** and **7.3** respectively.

**Table 7.2.** Interocular differences in response to monocular lens-cone device wear on day 4. Statistical significances between H and L spatial group for each defocus group. Asterisk denotes  $p < 0.05$ . Abbreviations: N = Number of animals in group.

<b>Interocular difference in vitreous chamber depth (mm)</b>							
<b>Defocus</b>	<b>L</b>			<b>H</b>			<b>Statistical significance</b>
	<b>Mean</b>	<b>SEM</b>	<b>N</b>	<b>Mean</b>	<b>SEM</b>	<b>N</b>	
<b>-15.00</b>	0.45	0.03	22	0.34	0.04	17	*
<b>-10.00</b>	0.27	0.04	9	0.22	0.04	11	*
<b>-5.00</b>	0.26	0.03	11	0.22	0.02	12	
<b>Plano</b>	0.31	0.04	15	0.18	0.04	17	*

<b>Interocular difference in axial length (mm)</b>							
<b>Defocus</b>	<b>L</b>			<b>H</b>			<b>Statistical significance</b>
	<b>Mean</b>	<b>SEM</b>	<b>N</b>	<b>Mean</b>	<b>SEM</b>	<b>N</b>	
<b>-15.00</b>	0.49	0.03	22	0.41	0.05	17	
<b>-10.00</b>	0.33	0.04	9	0.25	0.03	11	
<b>-5.00</b>	0.30	0.03	11	0.30	0.02	12	
<b>Plano</b>	0.35	0.05	15	0.25	0.04	17	

<b>Interocular difference in refractive error (D)</b>							
<b>Defocus</b>	<b>L</b>			<b>H</b>			<b>Statistical significance</b>
	<b>Mean</b>	<b>SEM</b>	<b>N</b>	<b>Mean</b>	<b>SEM</b>	<b>N</b>	
<b>-15.00</b>	-7.25	0.55	18	-5.14	0.97	14	
<b>-10.00</b>	-6.07	0.94	9	-2.07	0.64	11	*
<b>-5.00</b>	-3.56	0.41	11	-3.03	0.68	12	
<b>Plano</b>	-3.27	0.99	7	0.13	1.07	7	*

**Table 7.3.** Interocular differences in response to monocular lens-cone device wear on day 7. Statistical significances between H and L spatial group for each defocus group. Asterisk denotes  $p < 0.05$ . Abbreviations: N = Number of animals in group.

<b>Interocular difference in vitreous chamber depth (mm)</b>							<b>Statistical significance</b>
	<b>L</b>			<b>H</b>			
<b>Defocus</b>	<b>Mean</b>	<b>SEM</b>	<b>N</b>	<b>Mean</b>	<b>SEM</b>	<b>N</b>	
<b>-15</b>	0.64	0.06	12	0.43	0.07	8	*
<b>-10</b>	0.43	0.08	5	0.43	0.11	6	*
<b>-5</b>	0.28	0.06	11	0.21	0.05	9	
<b>Plano</b>	0.24	0.09	9	-0.02	0.08	6	

<b>Interocular difference in axial length (mm)</b>							<b>Statistical significance</b>
	<b>L</b>			<b>H</b>			
<b>Defocus</b>	<b>Mean</b>	<b>SEM</b>	<b>N</b>	<b>Mean</b>	<b>SEM</b>	<b>N</b>	
<b>-15</b>	0.88	0.06	12	0.64	0.06	8	*
<b>-10</b>	0.66	0.10	5	0.55	0.10	6	
<b>-5</b>	0.44	0.04	11	0.38	0.04	9	
<b>Plano</b>	0.35	0.13	9	0.18	0.04	6	

<b>Interocular difference in refractive error (D)</b>							<b>Statistical significance</b>
	<b>L</b>			<b>H</b>			
<b>Defocus</b>	<b>Mean</b>	<b>SEM</b>	<b>N</b>	<b>Mean</b>	<b>SEM</b>	<b>N</b>	
<b>-15</b>	-13.11	0.90	11	-6.87	0.83	7	*
<b>-10</b>	-10.56	1.03	5	-5.97	1.01	6	
<b>-5</b>	-5.65	0.47	11	-5.05	0.69	9	
<b>Plano</b>	-2.50	1.30	5	0.00	0.99	3	

The rate of compensatory eye growth to defocus was found to be faster for low SFs.

### 7.4.1. Refractive Error

**Figure 7.4A to C** showed interocular refractive error (RE) differences (spherical equivalent (SE)) before treatment with cone devices with myopia-inducing lenses and either high or low SF stimuli, and on days 4 and 7 of the experiment.

Before application of the lens-cone devices, the mean interocular SEs were close to zero at the beginning of the experiment and there was no significant difference between groups (2-way ANOVA, SF:  $F(1,89) = 0.06, p=0.80$ ; defocus:  $F(3,89) = 0.48, p=0.70$ ) (**Figure 7.4A**).

On day 4, all the groups with hyperopic defocus lens-cone devices became myopic (**Figure 7.4B**). Chick eyes with low SF stimuli were more myopic compared to those with high SF stimuli. There were significant main effects of SF and defocus (2-way ANOVA, SF:  $F(1,89) = 19.2.0, p<0.0001$ ; Defocus:  $F(3,89) = 12.1, p<0.0001$ ). The interaction (SF x defocus) was not statistically significant ( $F(3,89) = 1.8, p=0.15$ ). Under the -15D defocus condition, the interocular SE mean was -7.2D at low SF, in contrast, it was -5.1D at high SF. The mean interocular SE for low SF under -10D defocus was -6.1D, and high SF effect was significantly less. On day 4, even without defocus, chick eyes with low SF stimulation were significantly myopic with interocular SE mean of -3.3D (One sample t-test comparing to 0,  $t=-3.31$ ,

p=0.02). In contrast, chicks with high SF visual input did not have obvious SE change, with interocular SE mean of 0.1D (One sample t-test comparing to 0,  $t=-0.118$ ,  $p=0.91$ ).

After 7 days of treatment, all trends were similar to those on day 4 (**Figure 7.4C**). Both SF and defocus also had significant main effects on the mean of intraocular SE (2-way ANOVA, SF:  $F(1,57) = 26.6$ ,  $p<0.0001$ ; defocus:  $F(3,57) = 28.6$ ,  $p<0.0001$ ). In addition, SF and defocus had a significant interaction ( $F(3,62) = 4.7$ ,  $p=0.005$ ). For low SF stimulation, there was more accurate compensation to induced hyperopic defocus than for high SF stimulation, especially for the groups with induction of higher magnitude of defocus.

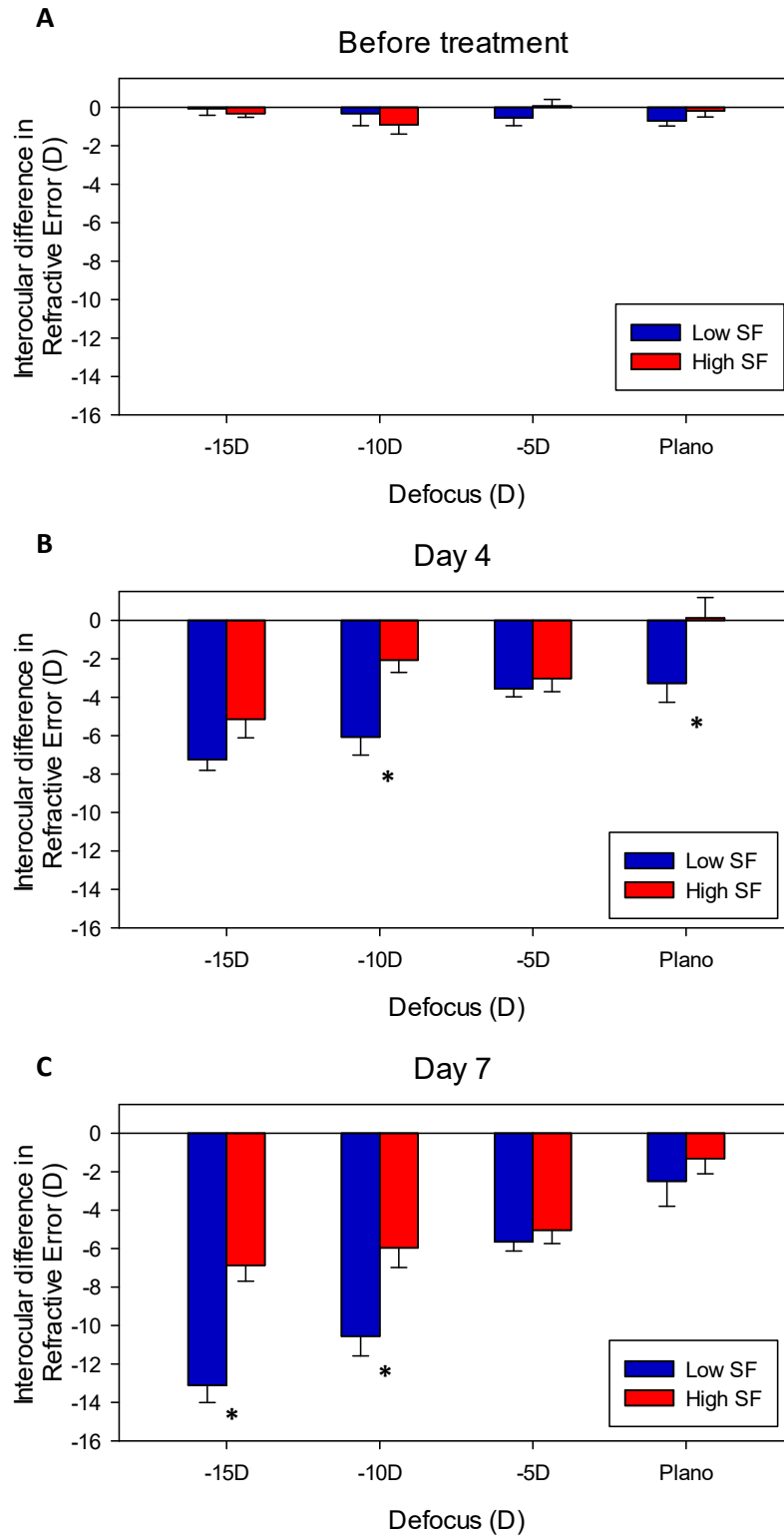


**Figure 7.4.** The interocular difference in refractive error from before treatment (A), after 4 days (B) and 7 days (C) of monocular treatment using lens-cone device. X-axis represents the magnitude of defocus applied to the right eye. Y-axis represents the interocular refractive error (treatment minus control). Blue bar and red bar represent the low and high SF content respectively. Error bars represent standard error of mean. Asterisks denote statistical significance with  $p < 0.05$ .

### 7.4.2. Axial length

The interocular difference (right eye minus left eye) in axial length (AXL) before treatment, on day 4 and day 7 is illustrated in **Figure 7.5A to C**. After application of the lens-cone device for 4 days, the eye started to elongate.

Both SF and defocus produced significant main effects on day 4 (SF: 2-way ANOVA,  $F(1,114) = 5.20$ ,  $p = 0.024$ ; defocus: 2-way ANOVA,  $F(3,114) = 8.67$ ,  $p < 0.0001$ ). On day 7, both SF and defocus also had significantly increased the length of the chick eyes (SF: 2-way ANOVA,  $F(1,66) = 6.68$ ,  $p = 0.012$ ; defocus: 2-way ANOVA,  $F(3,66) = 16.55$ ,  $p < 0.0001$ ).

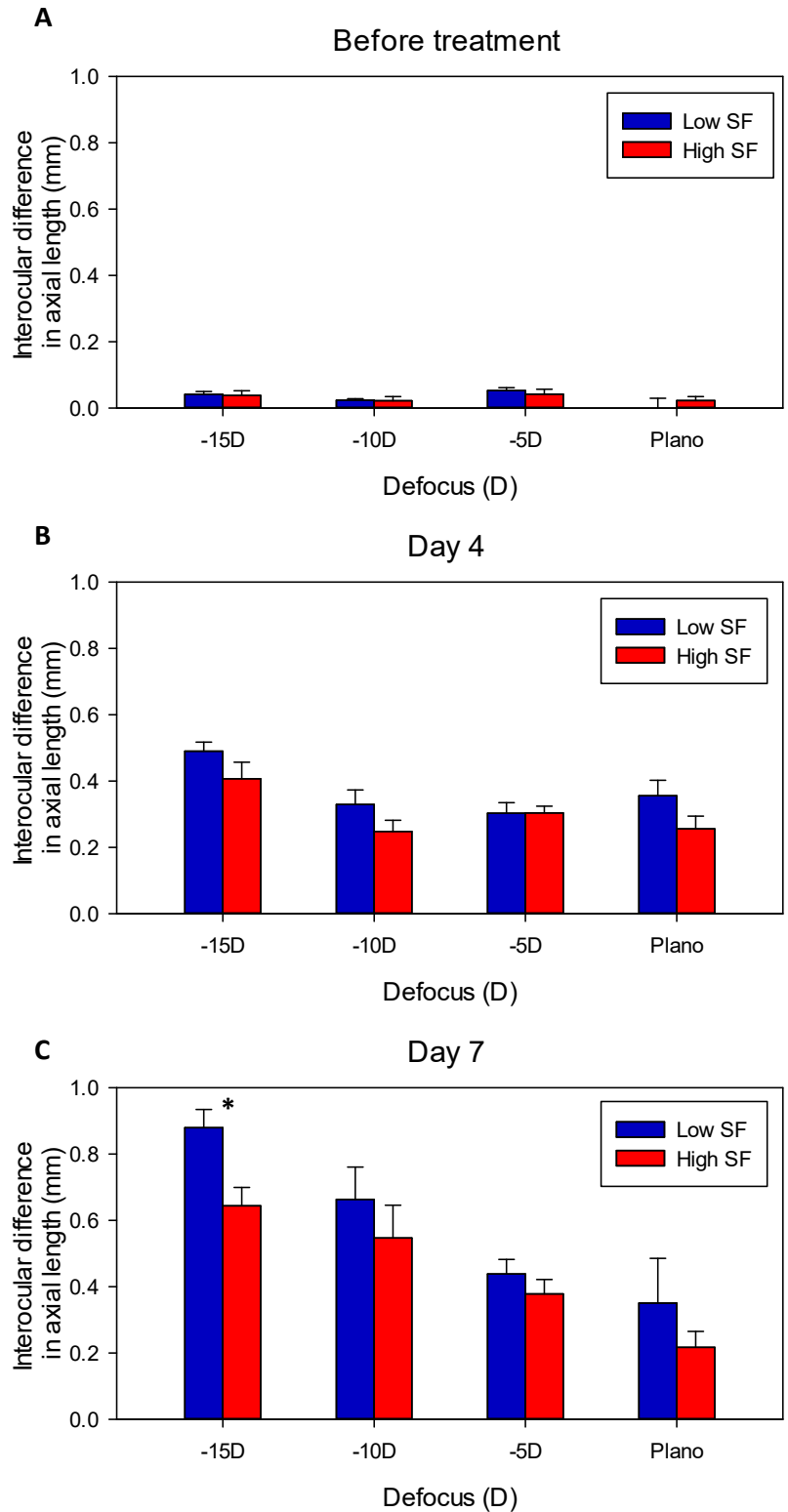


**Figure 7.5.** The interocular differences in axial lengths from before treatment (A), after 4 days (B) and 7 days (C) of monocular treatment using a lens-cone device. X-axis represents the amount of defocus applied. Y-axis represents the interocular axial length (treatment minus control). Blue and red bars represent the low and high SF content respectively. Error bars represent standard error of the mean. Asterisks denote statistical significance with  $p < 0.05$ .

### 7.4.3. Vitreous chamber depth

The interocular differences (right eye minus left eye) in vitreous chamber depth (VCD) before treatment, on day 4 and day 7 are illustrated in **Figure 7.6A to C**.

Before treatment, the interocular VCD difference was close to zero among groups (**Figure 7.6A**).

On day 4, graded response to hyperopic defocus was observed as there was increasing VCD difference from -5D to -15D defocus. In addition, the VCD elongation was faster with the low SF stimulation than that with the high SF stimulation. Defocus (2-way ANOVA,  $F(3,114) = 8.6, p < 0.0001$ ) and SF (2-way ANOVA,  $F(1,114) = 7.8, p < 0.0001$ ) both produced a significant main effect. The trend of VCD change was correlated with interocular refractive error change (see below). Interestingly, it was observed that under the plano (0D) condition, the VCD (mean $\pm$ SEM) also elongated at an increased pace (high SF:  $0.18 \pm 0.04$ mm; low SF:  $0.31 \pm 0.04$ mm over 4 days). As in the hyperopic defocus conditions, the high SF stimulus produced slower VCD elongation than the lower SF conditions.

On day 7, both SF and defocus had significant influence on interocular VCD difference (SF: 2-way ANOVA,  $F(1,66) = 6.5, p = 0.014$ ; defocus: 2-way ANOVA,  $F(3,66) = 13.4, p < 0.0001$ ). There was further increase in

interocular VCD difference for the level of -15D defocus. The VCD was elongated significantly under the low SF condition (**Figure 7.6C**) ( $p=0.045$ ). For -5D and -10D hyperopic defocus, no statistical difference in the elongation of VCD was observed between high and low SF stimulation ( $p>0.05$ ), although the trend was clear.

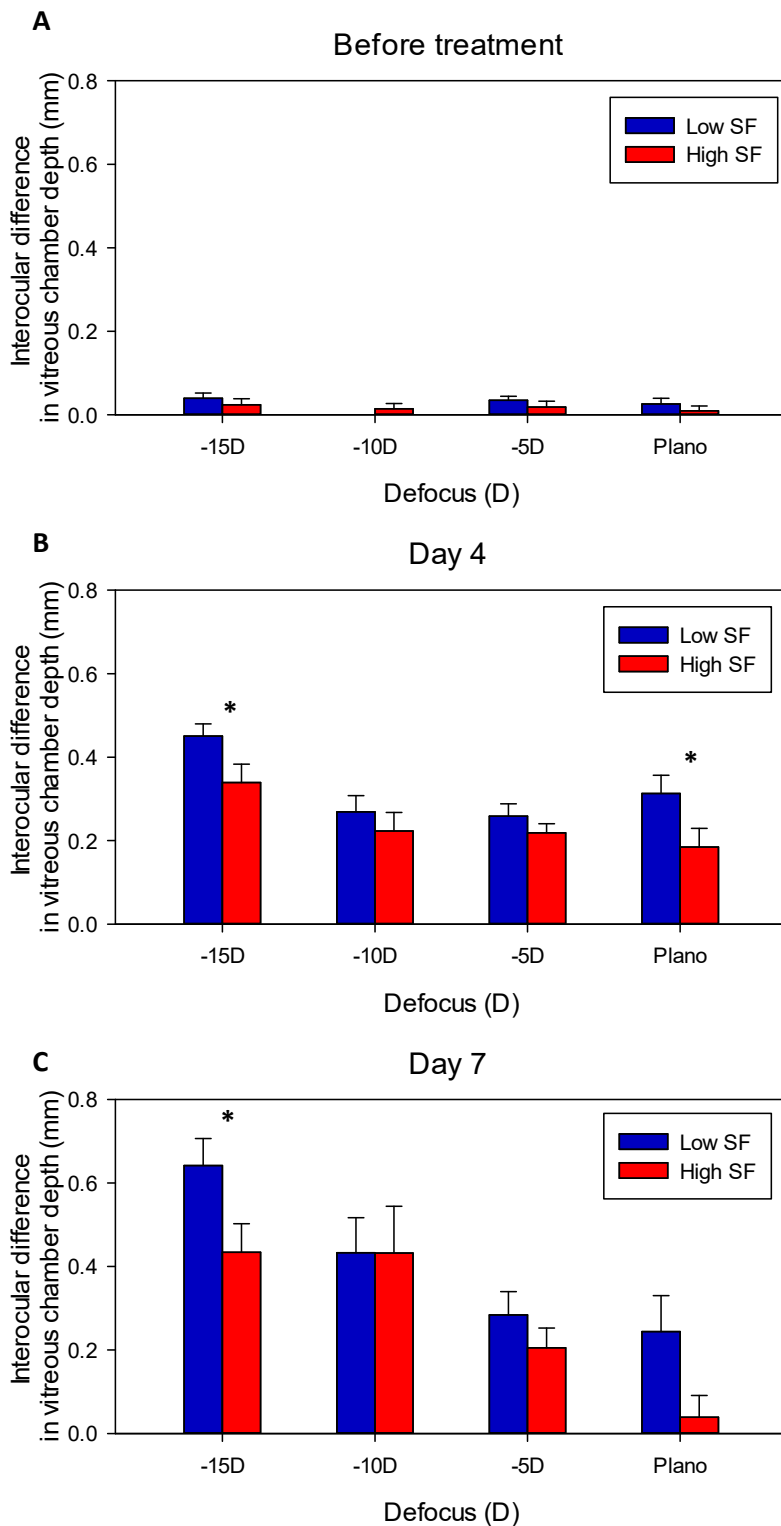


**Figure 7.6. The interocular differences in vitreous chamber depth from before treatment (A), after 4 days (B) and 7 days (C) of monocular treatment using lens-cone device. X-axis represents the magnitude of defocus applied on the right eye. Y-axis represents the interocular vitreous chamber depth (treatment minus control). Blue and red bars represent the low and high SF content respectively. Error bars represent standard error of the mean. Asterisks denote statistical significance with  $p < 0.05$**

#### 7.4.4. Eyeball elongation and refractive errors

The Pearson's correlation between refractive errors and ocular parameters are summarized in **Table 7.4**.

**Table 7.4.** Pearson's correlation and its significance between refractive error and ocular biometric parameters (ACD, LT, VCD and AXL).

RE		ACD	LT	VCD	AXL
Day 0	Pearson's correlation	0.06	0.02	-0.12	-0.07
	Statistical significance	0.56	0.86	0.24	0.51
Day 4	Pearson's correlation	-0.16	-0.02	-0.6	-0.63
	Statistical significance	0.13	0.84	0.0001	0.0001
Day 7	Pearson's correlation	-0.3	0.05	-0.69	-0.76
	Statistical significance	0.01	0.64	0.0001	0.0001

The interocular RE difference was strongly correlated with the interocular VCD and AXL difference on both day 4 and day 7. **Figure 7.7A and B** show the correlations of interocular RE difference to interocular VCD difference on days 4 and 7. The refractive error change was mainly due to axial change. The linear correlations indicate that the eyeball elongated to compensate for the defocus induced from lens-cone device, and this was mainly at the posterior part of the eye. Interestingly, on day 7, ACD

elongation also showed significant correlation with RE (Pearson's correlation:  $R=0.30$ ,  $p=0.01$ , suggesting that it also contributed partly to the development of compensatory myopia (Table 7.4).

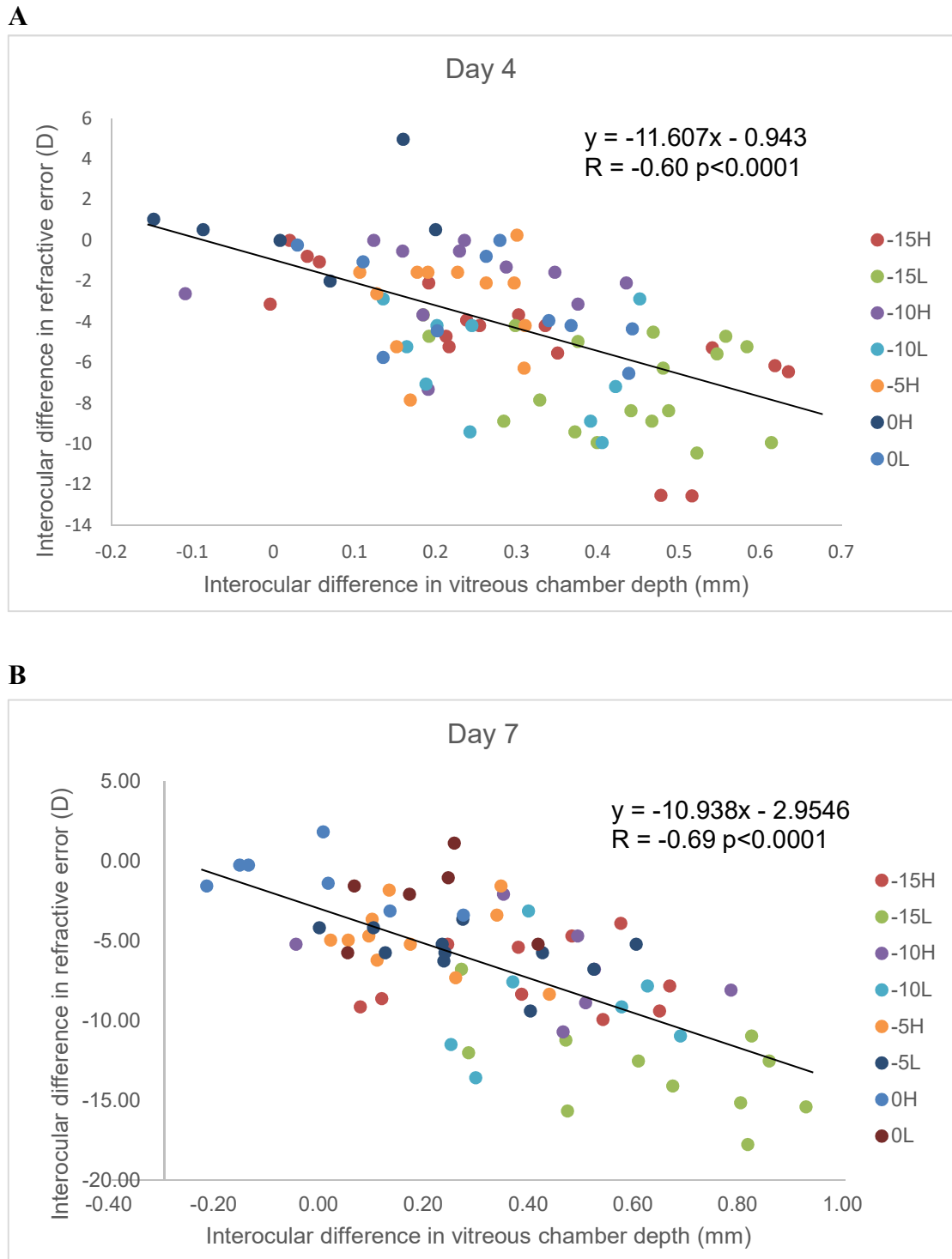


**Figure 7.7.** Interocular VCD difference versus interocular RE difference on (A) day 4 and (B) day 7.

## 7.5. Discussion

### 7.5.1. Emmetropization with and without hyperopic defocus

Our results show that the eye under hyperopic defocus, they respond differently when receiving visual stimulation with different spatial details.

This helps to gain new insight into the mechanisms how the eye grows to become myopic or “functionally” emmetropic under different spatial stimuli. In the study of Hess and colleagues (2006), the visual stimuli were adjusted without defocus, varying from  $1/f^{0.5}$  (more contribution from higher SF) to  $1/f^2$  (more contribution from lower SF). Hyperopia was resulted with  $1/f^{0.5}$  stimuli and the eye became myopic with  $1/f^2$  stimulus.

The findings under plano condition in this study that eyes exposed to lower SF grew faster than those exposed to higher SF, which match with their results.

In addition, the eye has long been shown to grow according to the sign of defocus (Irving *et al.*, 1991; Wildsoet and Schmid, 2001). However, it is not clear what cue the retina uses for decoding defocus. Wildsoet and Schmid (2001) used a similar lens-cone system to explore the emmetropization mechanism. They suggested the eye utilized optical vergence to guide emmetropization. When the visual information was restricted to one plane,

i.e. the visual pattern at the distal end of the cone, the incident optical vergence was shown to guide emmetropization (Wildsoet and Schmid, 2001). In their study, when the carrier for the visual patterns was made transparent, thus providing two focal planes for retinal stimulation, the emmetropization set point was shifted to the hyperopic side. It is no surprise that more myopic defocus was experienced by the eye when the carrier for the visual pattern was transparent. Tse and To (2007) later showed that the eye can locally compute the amount of myopia and hyperopic defocus signals what the eye experiences and emmetropize to the integrated set-point (Tse *et al.*, 2007; Tse and To, 2011).

In the current study, only a single plane of visual stimulus was presented and so the eye was exposed to single optical vergence. With the induction of -5D to -15D lenses, it was observed that the chick eyes compensated for the particular induced hyperopic defocus as in previous studies (Irving *et al.*, 1991). In addition, the effectiveness of compensation depended on the details of the visual pattern at the distal end of the lens-cone device. The compensation to hyperopic defocus was more accurate with inclusion of a relatively more low SF stimulus, and thus the refractive error was closer to the power of lens induced (**Figure 7.5**). The results of this experiment

indicated the mechanism of decoding defocus for the eye is spatially tuned. Previous studies have investigated the effect of spatial frequency on emmetropization. For instance, Schmid and Wildsoet (1997) demonstrated that exposing chicks for 20 mins a day with mid-range SF (from 0.09 to 4.3 cpd) could inhibit form-deprivation myopia. In addition, Tran and colleagues (2008) used various Bangerter filters with various levels of image degradation and found that form-deprivation myopia was triggered when the image quality was seriously reduced (<0.1 Bangerter filters). Both studies suggested emmetropization is tuned to respond to mid-range SF. Yet, the mechanisms mediating form-deprivation and lens-induced myopia are suggested to be different (Morgan *et al.*, 2013). Diether and Wildsoet (2005) used Maltese cross targets with a striped filler pattern compared to a solid black Maltese cross as visual targets for the lens-cone device, and a defocus range of  $\pm 7D$ . The treatment period in their experiment was 4 days. In contrast to the current study, they found that no spatial preference for the eye growth compensating to hyperopic defocus. On the other hand, compensation to myopic defocus was shown to be more accurate with inclusion of middle and high SF. By comparing the spectral analysis for the Maltese cross in the study of

Diether and Wildsoet (2005) and the stimulus patterns in this experiment (**Figure 7.8**), the striped and solid Maltese crosses used in their study are mainly differed in increased composition of higher SF for the striped target, while the low SF regions are similar in both crosses (**Figure 7.8E**). In contrast, distinct peaks for relative low and relative high SF were seen in spectrum analysis of the patterns used in this experiment (**Figure 7.8F**). Our results suggest that the compensation for induced hyperopic defocus would be more accurate with inclusion of a relatively low SF stimulus. Combining the results from Diether and Wildsoet (2005) and this experiment, it is possible that the retina decodes hyperopic defocus and myopic defocus utilizing stimuli with different ranges of SF.

In Experiment 2, the human retina was shown to have a more vigorous activity under visual stimulation with relatively low SF than relatively high SF (Chin et al., 2015). And the current study also demonstrated similar results in myopic development. It is possible that the detection of hyperopic defocus is being tuned to relatively low SF. Images from natural scenes is abundance of low SF (Millane *et al.*, 2003; Ruderman, 1994; Ruderman and Bialek, 1994). If emmetropization is spatially tuned, low spatial frequencies are believed to be the main contributor in term of natural

abundance and drivers of physiological response.

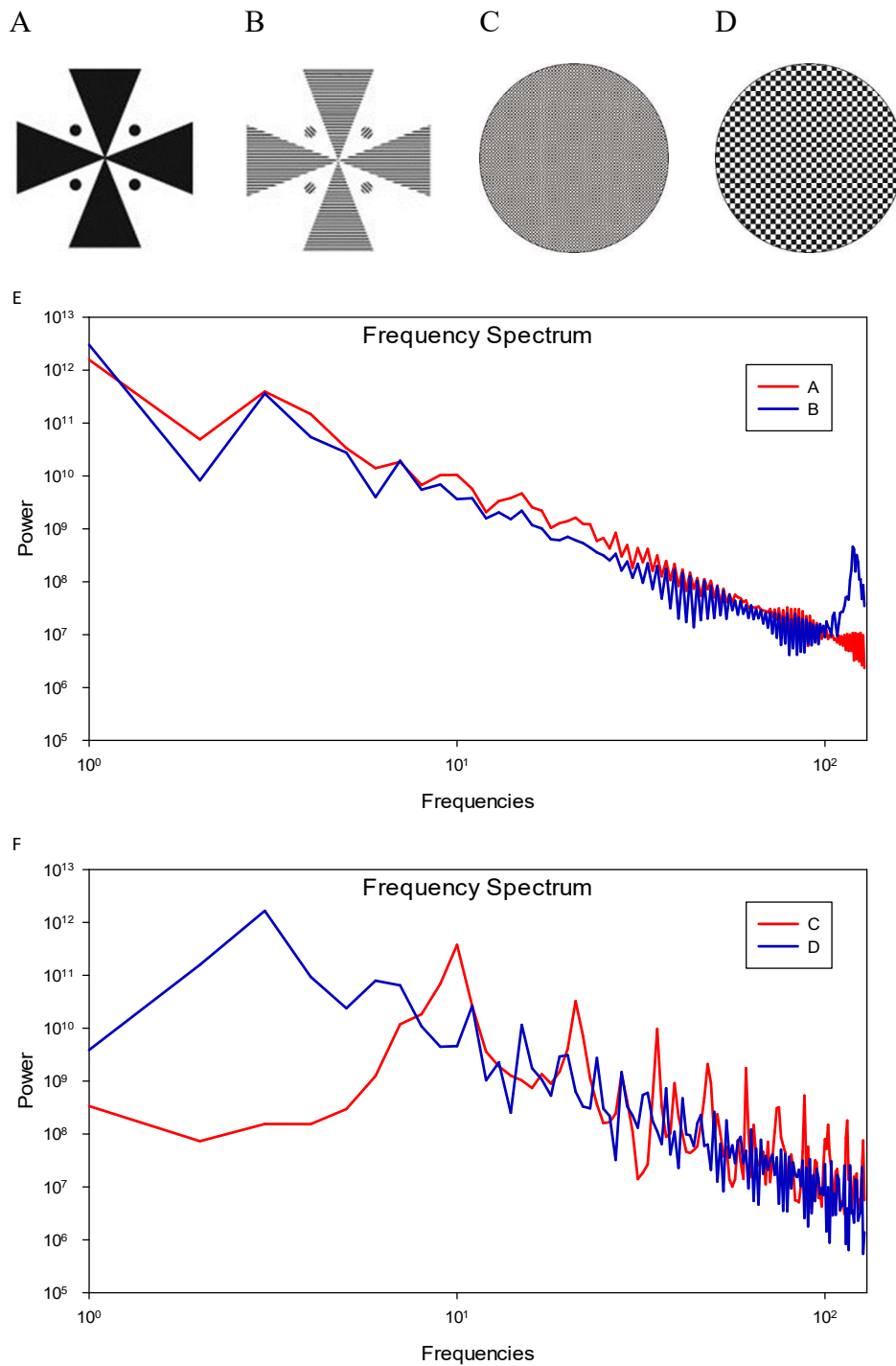


**Figure 7.8.** The Maltese crosses (**A** and **B**) and visual patterns used in the current experiment (**C** and **D**) and their respective spatial energy spectrums are shown in (**E**) and (**F**). It is noted that, in both Maltese crosses, the contributions from lower range of SFs are rather similar and there is an increase of high SFs for the striped Maltese cross (**B**). For the patterns in (**C**) and (**D**), the contributions from high and low SF are very different. (Figure 7.8A and B were adapted from Diether and Wildsoet (2005) study.)

### **7.5.2. Response to magnitude of defocus**

The maximum magnitude of defocus that the eye can decode correctly is limited and varies from species to species. Chicks have been widely used as a model for myopia and they have a wide range of defocus compensation (Irving *et al.*, 1992; Nevin *et al.*, 1998). Previous studies have shown that the chick eye can compensate accurately for refractive errors between -10D and +15D (Irving *et al.*, 1992; Nevin *et al.*, 1998). When the absolute magnitude of induced defocus increases, some potential cues for decoding are rendered increasingly insignificant (Wallman and Winawer, 2004). The details of image are reduced as the defocus increases. As the main effect of defocus is to attenuate high spatial frequencies, with less effect on the lower the spatial frequency (Westheimer, 1964). Higher SF becomes more attenuated as defocus magnitude increases. The image quality reduces and becoming no stimulus at all apart from a luminance signal and thus form deprivation myopia would be the result. Our results showed however that eyeball growth rate for high SF under defocus was slowed. To further examine this finding, another batch of chicks was exposed to -25D of defocus to study if a very blurred visual image would trigger form-deprivation myopia instead of compensatory eye growth. The eye growth rate was also shown to follow on the characteristics of stimulus SF and

hyperopic defocus and this relationship extends to -25D of defocus

**(Appendix B).** With the lens-cone device, since the visual stimuli were limited and controlled, it is surprising that the eye can still decode the sign of hyperopic defocus beyond -15D without causing form deprivation myopia. Aliasing of stimulus may be a possible explanation. However, form deprivation myopia was observed in myopic defocus experiment with +20D hyperopic defocus (Nevin *et al.*, 1998). In our study, the trend of accurate compensation under lower SF is maintained from low (-5D) to high (-25D) magnitude of defocus.

The limitations of this experiment are the magnification effect of the visual image induced by the amount of defocus used. Although the checks appear to be bigger with higher magnitude of defocus, the discrepancy was minimized as the eye growth rate between high and low SF with the same magnitude of defocus was compared. In addition, as a short viewing distance and high power lenses were used for the lens-cone device, small errors in fixing the device on the eye may alter the amount of defocus induced. Yet, this error would be expected to have equal effects for the visual image of both SFs. In addition, owing to the size of the lens-cone device, only black and white checks, instead of sinusoidal stimulus, were

used in this study. There were some high spatial frequencies within the stimuli (**Figure 7.8F**), which may confound the result. As the highest acuity of chick is limited to 8.6cpd (Schmid and Wildsoet, 1998), the high SF component may be beyond the resolution of chick retina.

## **7.6. Conclusion**

In this experiment, axial emmetropization responses to hyperopic defocus was shown to be dependent on spatial stimuli. Under low spatial stimulus, the chick eye emmetropizes more accurate to lens-induced hyperopic defocus. The development of myopia, apart from optical defocus, is also highly related to the spatial details of the visual stimuli received.

**Chapter 8. Experiment 4. Compensation to  
constant hyperopic defocus is locally spatial  
sensitive**

## **Abstract**

**PURPOSE:** In lens compensation myopia, the eye grows in response to induced hyperopic defocus. In this experiment, the rate of compensation associated with varying spatial composition under constant magnitude of hyperopic defocus was investigated using chicks.

**METHODS:** One eye of normal chicks (10-11 days old) was fitted with a lens-cone device monocularly and the fellow eye was used as control. At the proximal end of the device, a constant hyperopic defocus of -15D would be induced. At the distal end, visual patterns were made by varying the composition of high (**H**) spatial frequency stimulus (0.4mmx0.4mm black and white checks) and low (**L**) spatial frequency stimulus (1.2mmx1.2mm black and white checks) with different occupying ratios (3H:1L, 1H:1L, 1H:3L). On-axial ocular refraction and axial ocular component dimensions were measured before wearing the device, and on day 4 and day 7 after lens-cone wear. The results were compared with those having only high and low SF objects in Experiment 3.

**RESULTS:** On day 4, there was a trend indicating that increasing the low SF ratio would result in more myopia. On day 7, the effect became more obvious and significant (1-way ANOVA,  $F(4,47) = 6.18, p=0.001$ ).

Corresponding eyeball elongation was observed as the ratio of low SF increased, but the variations of some groups were large and it was statistically just insignificant.

CONCLUSION: Under the same magnitude of hyperopic defocus, trends of increased myopia and ocular elongation were observed when the spatial composition was gradually increased from higher to lower SF. Various combinations of spatial details influence eye growth even at the same levels of hyperopic defocus. Interactive mechanisms between spatial details and optical defocus on myopia development may be useful in control of myopia.

## **8.1. Introduction**

Emmetropization is a visually guided local feedback process for regulating eye growth (Miles and Wallman, 1990; Norton and Siegwart, 1991; Wallman *et al.*, 1987). The eye is hypothesized as being able to decode and differentiate the sign of defocus. In chick experiments, eyes wearing positive lenses and negative lenses slow down and speed up the ocular elongation respectively (Norton *et al.*, 2006; Smith and Hung, 1999; Smith *et al.*, 2009; Zhu *et al.*, 2003). Most experiments investigated emmetropization by imposing lens-induced myopic defocus and hyperopic defocus without controlling the visual stimulus. Previous studies have

shown that different visual cues were involved in emmetropization such as chromatic aberrations (Wildsoet *et al.*, 1993), luminance levels (Ashby *et al.*, 2009; Ashby and Schaeffel, 2010; Norton and Siegwart, 2013; Siegwart *et al.*, 2012), contrast levels (Diether *et al.*, 2001; Diether and Wildsoet, 2005; Schmid *et al.*, 2006; Schmid and Wildsoet, 1997) and spatial details (Diether and Wildsoet, 2005; Hess *et al.*, 2006; Schmid and Wildsoet, 1997; Tran *et al.*, 2008). However, it remains unclear how the eye decodes information from the visual environment to regulate its growth.

To investigate the contribution of SFs in relation to emmetropization, the visual environment was controlled by putting a lens-cone device on chick eyes. It was shown that by adjusting the relative spectrum level, the characteristics of eye growth were altered (Hess *et al.*, 2006). A follow up question is that when the eye is exposed to defocus, how does the eye emmetropize to the sign of defocus in response to spatial details?

In addition, Diether and Wildsoet (2005) demonstrated, with the inclusion of higher SFs in visual stimulus that the chick eye compensated to myopic defocus more accurately, while compensation to hyperopic defocus was independent of spatial stimulus (Diether and Wildsoet, 2005). However, the results in Experiment 3 was different from what Diether and Wildsoet

(2005) reported. The chick eye was found to compensate better with lower SFs when hyperopic defocus was induced.

Another important aspect of emmetropization is that both decoding and compensation growth can occur locally and regionally in the eyes. Local refractive changes can be observed when visual stimulus was defocused or deprived regionally (Fitzke *et al.*, 1985; Hodos and Erichsen, 1990; Miles and Wallman, 1990; Norton and Siegwart, 1991). Those studies implied that the retina is capable of decoding visual stimulus and to regulate eye growth regionally. In addition, globally, the overall refractive status was shifted according to “summation” of exposure to the amount of hyperopic and myopic defocus area (McFadden *et al.*, 2014; Tse *et al.*, 2007; Tse and To, 2011). As the chick eye growth response to hyperopic defocus was shown to be spatially tuned in Experiment 3, this experiment is to testify whether changing the composition of SFs within the visual image would have impact on eye growth compensation to hyperopic defocus which is related to myopia development.

## **8.2. Methods**

The setup is similar to that in Experiment 3.

### **8.2.1. Animals**

White Leghorn chick (*Gallus gallus*) pathogen-free fertilized eggs were

hatched in the University Central Animal Facilities. They were housed in an enclosure made of fine metal mesh (distant viewing was assumed unrestricted for the control eye) under a 12-hour light/12-hour dark cycle (from 7am to 7pm). Food and water were given ad libitum. All the rearing and experimental procedures were approved by the Animal Ethics Committee of The Hong Kong Polytechnic University and were in compliance with the ARVO Statement for the Use of Animals in Ophthalmic and Vision Research.

### **8.2.2. Lens-cone system**

The right eyes of white leghorn chicks were fitted with a modified lens-cone system which had a similar design to that described in Experiment 3 and previous studies (Diether and Wildsoet, 2005; Hess *et al.*, 2006; Nevin *et al.*, 1998; Schmid *et al.*, 2006; Tse and To, 2011; Wildsoet and Schmid, 2001). The dimensions of the cone were constructed using a graphics software package (CorelDraw; Corel Corporation, Ottawa, Canada). The cones were made of translucent material. Epoxy resin was used to assemble the parts and secure the cone onto the Velcro. At the proximal end of the cone, a PMMA lens with back vertex power of +10D was embedded and the vision of the chick was limited to the distal end of spatial stimulus (**Figure**

**8.1).** The distance from the lens side to target plane was 40mm, which is equivalent to 25D of vergence. This gave a hyperopic defocus of -15D to the eye, using thin lens formulae. Lenses were cleaned and checked daily to minimize decentration or dislocation.

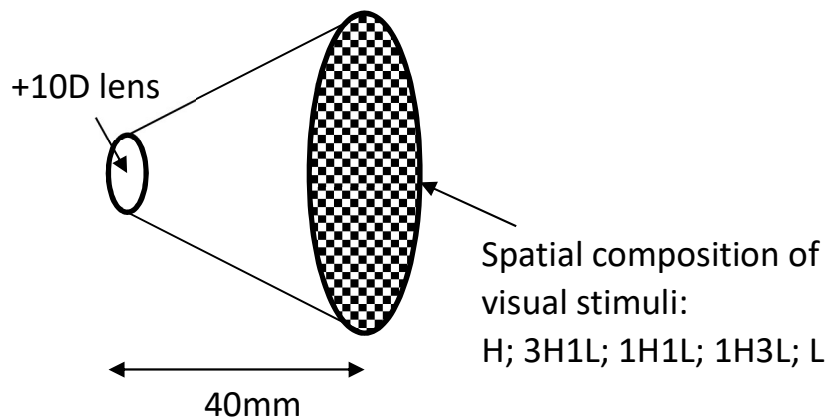


**Figure 8.1. Schematic diagram of a lens-cone device.** The lens was placed at proximal end of the device. Visual target with different spatial patterns was positioned at the distal side of the device. Refer to Section 8.2.3 for the description of spatial composition of visual stimuli (H; 3H1L; 1H1L; 1H3L; L).

### **8.2.3. Visual target**

Visual targets were constructed using Corel Draw. (CorelDraw; Corel

Corporation, Ottawa, Canada). The diameter of the target plane was

44.85mm, so the visual angle subtended was 52.8°. **Figure 8.2A** and **8.2E**

are the stimuli composed of spatial checkers of uniform sizes that were used

in Experiment 3. The stimuli shown in **Figure 8.2B** to **8.2D** were composed

of checks with different compositions of high SF and low SF. A 75:25 ratio

by area of high to low SF pattern was denoted as 3H1L (**Figure 8.2B**), a 50:50 ratio of high to low SF pattern was denoted as 1H1L (**Figure 8.2C**), and a 25:75 ratio of high to low SF pattern was denoted as 1H3L (**Figure 8.2D**). It is appreciated that the patterns were trimmed at the stimulus margin. This would induce a small errors in the ratio of the high and low spatial patterns. It was assumed that the small error would not affect the modulation of eye growth. A high-resolution (up to 600 x 600 dpi) printer (LaserJet Pro 200 color Printer M251nw; Hewlett-Packard, Avondale, PA, USA.) was used to print out the targets for the experiment.

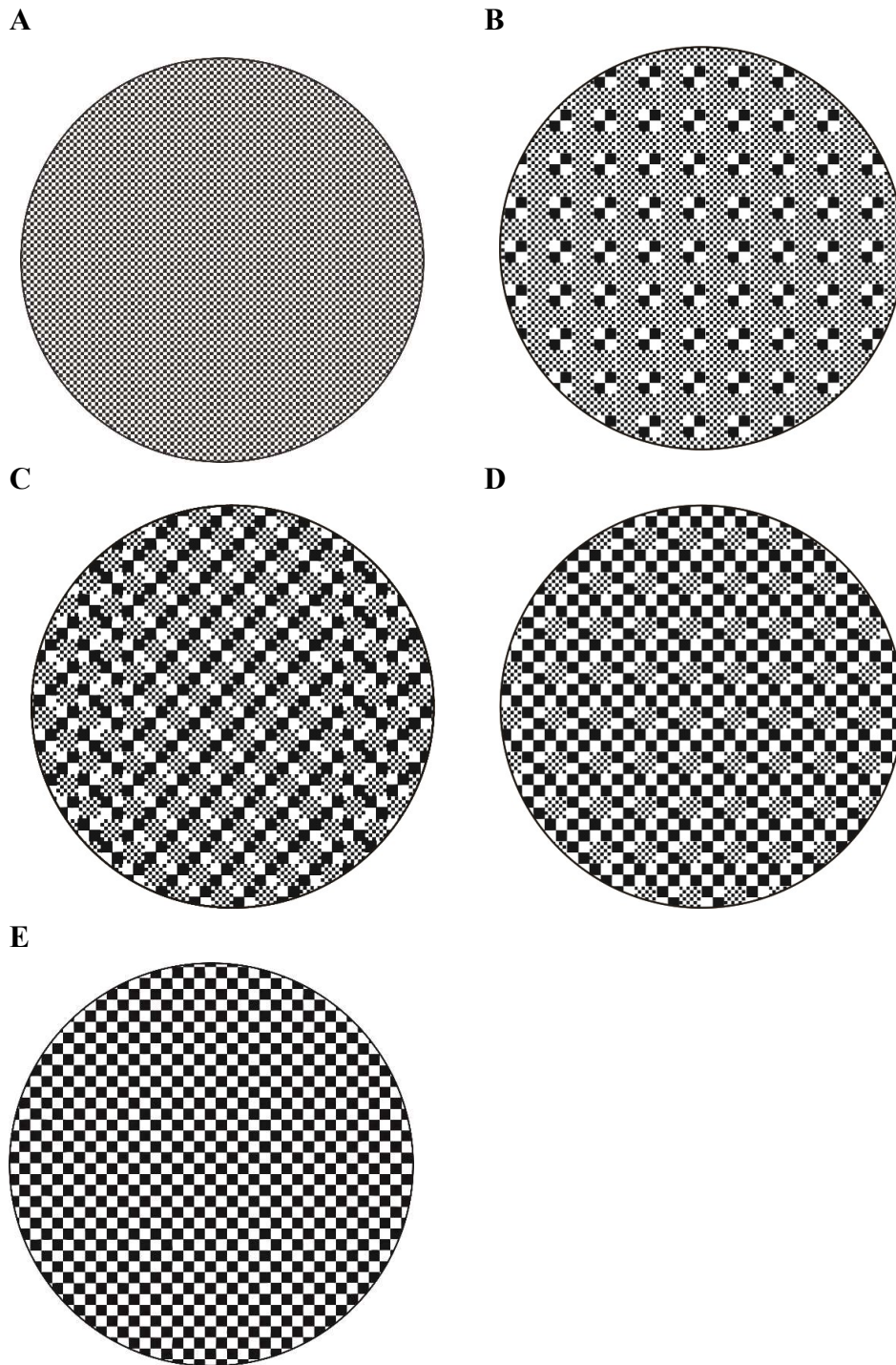


**Figure 8.2. The patterns of visual stimuli used in the experiment. (A)** and **(E)** Uniform checkers of high and low SF which were used in Experiment 3. **(B)**, **(C)** and **(D)** were the patterns composed of checker mixtures of high and low SF. **(B)** 3H1L: One area unit of large checkers with 3 area units of small checkers. **(C)** 1H1L: One area unit of large checkers with one area unit of small checkers. **(D)** 1H3L: One area unit of small checkers with 3 area units of large checkers.

#### **8.2.4. Measurement**

Biometric and refractive data were collected before application of the lens-cone device, on day 4, and day 7 of the experiment. The refractive status was measured along the pupillary axis using a modified Hartinger refractometer (Jena Coincidence Refractometer, Model 110, Carl Zeiss Meditec, Jena, Germany) in anaesthetized chicks (isoflurane inhalation, 1.0% to 1.5% in oxygen for rapid induction and low percentage of possible complications) (Furtado and Andrade, 2013). Axial ocular dimensions including anterior chamber depth (ACD), lens thickness (LT), vitreous chamber depth (VCD), and axial length (AXL) were obtained using A-scan ultrasound (Refer to 7.2.4.1.). The data was excluded if the following conditions occurred. The lens-cone device was detached, the device was dislocated so that the eye was not aligned with the optical zone of the lens, abnormal eye conditions such as inflammation, excessive tearing, or the eye could not open freely when the lens-cone device was attached. The lens-cone device was on right eye of the chicks and the fellow eyes acted as controls. Ocular parameters that beyond 3 standard deviations of individual group means would be regarded as outlier and excluded. There are 25 chicks (20%) were excluded.

### 8.2.5. Experimental Groups and Treatment Protocol

**Table 8.1** summarizes the treatment conditions including visual patterns of various ratios of high to low SF and numbers of chicks in each group. A constant magnitude of -15D hyperopic defocus was induced in all groups of chicks. The data of high and low SF groups were from Experiment 3.

**Table 8.1.** Treatment condition for each group of chicks. H=100 % high SF; 3H1L=75% high SF: 25% low SF; 1H1L=50% high SF:50% low SF; 1H3L= 25% high SF:75% low SF; L= 100% low SF.

Treatment		number of chicks
Induced Defocus	Visual pattern	
-15D	H	17
-15D	3H1L	22
-15D	1H1L	19
-15D	1H3L	18
-15D	L	22

### 8.3. Data analysis

The data was presented as mean ( $\pm$  SEM) of interocular difference (right eye minus left eye). Nearly all the groups had passed the normality test ( $p>0.05$ ). The overall effects of SF were tested with one-way ANOVA with Predictive Analytics SoftWare (PASW19.0, SPSS Inc., Chicago, IL, USA). Bonferroni post hoc testing was applied if it was appropriate between treatment groups. Trend analysis by one-way ANOVA was carried out to investigate how varying the spatial composition ratio effect on interocular ocular growth and refractive error change. The level of significance was set

at 0.05.

#### **8.4. Results**

In this experiment, chick eyes were exposed to the same magnitude of hyperopic defocus (-15D) while the spatial composition of the stimulus was varied. The longitudinal changes of interocular differences in ocular parameters were presented in **Table 8.2**. Noted that there were sacrifice of chicks throughout the treatment periods. The reason of lower successful rate in using the lens-cone device (40mm in height) is its weight as compared with a single lens attached to the eye. In current experiments, as 10 days old chicks were used in the beginning of the experiment for 7 days. Most failure was due to the lens-cone device detachment accidentally during the experiment period. It was found that the device tended to detach easily after four to five days into the experiment. We had tried to use a cone with 30mm height to reduce the chance of device being torn off. Yet, the required working lens would have more plus addition. There is a technical issue in production of this high power lenses. Additionally, a slightly deviation of back vertex distance would produce greater error during the experiments. Finally, we decided to use 40mm height lens-cone device.

**Table 8.2.** Interocular differences in response to monocular lens-cone device wear. Abbreviations: N = Number of animals in group.

Spatial composition	Interocular difference in anterior chamber depth (mm)					
	Day 4			Day 7		
	Mean	Standard error	N	Mean	Standard error	N
L	0.08	0.01	22	0.64	0.06	12
3L1H	0.08	0.01	18	0.49	0.05	14
1L1H	0.08	0.01	18	0.51	0.11	8
1L3H	0.08	0.01	19	0.38	0.09	8
H	0.10	0.02	17	0.43	0.07	8

Spatial composition	Interocular difference in lens thickness (mm)					
	Day 4			Day 7		
	Mean	Standard error	N	Mean	Standard error	N
L	-0.04	0.02	22	-0.03	0.01	12
3L1H	0.00	0.01	18	0.01	0.01	14
1L1H	-0.01	0.01	18	-0.05	0.02	8
1L3H	-0.01	0.01	19	-0.03	0.02	8
H	-0.04	0.02	17	0.00	0.02	8

Spatial composition	Interocular difference in vitreous chamber depth (mm)					
	Day 4			Day 7		
	Mean	Standard error	N	Mean	Standard error	N
L	0.45	0.03	22	0.64	0.06	12
3L1H	0.27	0.02	18	0.49	0.05	14
1L1H	0.33	0.04	18	0.51	0.11	8
1L3H	0.29	0.03	19	0.38	0.09	8
H	0.34	0.04	17	0.43	0.07	8

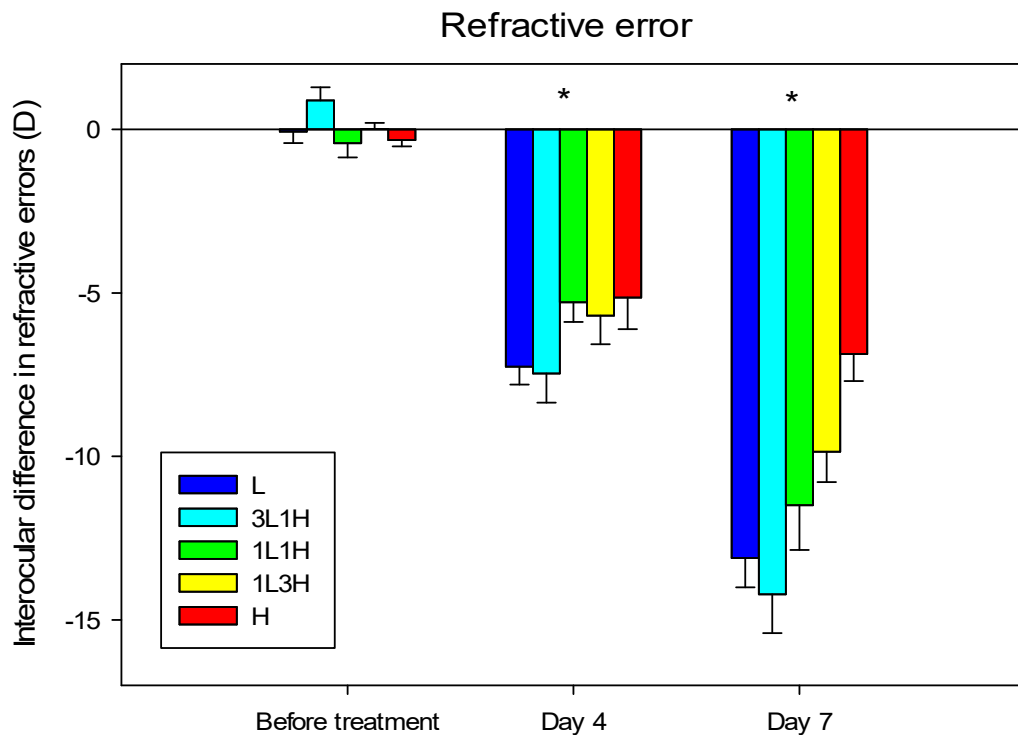
Spatial composition	Interocular difference in axial length (mm)					
	Day 4			Day 7		
	Mean	Standard error	N	Mean	Standard error	N
L	0.49	0.03	22	0.88	0.06	12
3L1H	0.35	0.03	18	0.77	0.05	14
1L1H	0.40	0.03	18	0.75	0.10	8
1L3H	0.37	0.03	19	0.58	0.09	8
H	0.41	0.05	17	0.64	0.06	8

Spatial composition	Interocular difference in refractive error (D)					
	Day 4			Day 7		
	Mean	Standard error	N	Mean	Standard error	N
L	-7.25	0.55	18	-13.11	0.90	11
3L1H	-7.46	0.89	18	-14.22	1.18	14
1L1H	-5.28	0.60	18	-11.50	1.37	8
1L3H	-5.69	0.88	19	-9.86	0.93	8
H	-5.14	0.97	14	-6.87	0.83	7

### 8.4.1. Refractive Error

To illustrate the effect of increasing the proportions of low spatial frequency checks in the visual stimulus on eye growth, the interocular RE difference (Mean±SEM) in each SF ratio group is shown in **Figure 8.3**. All groups started with interocular RE difference close to zero. On day 4, an effect of SF ratio was observed on myopia development. As low SF ratio increased, the eyes developed higher myopia. On day 7, the effect became more obvious and became significant (1-way ANOVA,  $F(4,47) = 6.18, p=0.001$ ). For the visual stimulus composed of only high SF, the compensation to -15D of defocus was not as effective as those stimuli including low SF. Post hoc showed that chicks wearing 100% high SF lens-cone device were significantly less myopic compared with other SF ratio with more low SFs (H vs L: mean difference  $6.2\pm 1.7D, p=0.006$ ; H vs 3L1H: mean difference  $7.4\pm 1.6D, p<0.0001$ ).



**Figure 8.3.** The interocular differences in refractive error from before treatment, after 4 days and after 7 days with monocular treatment with lens-cone device. X-axis represents the time points of the measurements. Y-axis represents the interocular difference in refractive error (treatment minus control). Error bars represent the standard error of the mean. Asterisks denote ANOVA trend analysis with statistical significance with  $p < 0.05$ .

#### 8.4.2. Vitreous chamber depth and axial length

The interocular differences (Mean $\pm$ SEM) for VCD and AXL for different

SF ratio groups are shown in **Figures 8.4A and B** respectively. At the

baseline, the interocular differences of VCD and AXL were close to zero

(VCD: 1-way ANOVA,  $F(4,107) = 1.9$ ,  $p = 0.11$ ; AXL: 1-way ANOVA,  $F$

$(4,107) = 0.6$ ,  $p = 0.63$ ). On day 4, there was an increase in both interocular

difference of VCD and AXL when reducing the proportion of high SF from

100% to 50% (i.e. 1H1L) (VCD: 1-way ANOVA,  $F(4,93) = 5.1, p = 0.001$ ;

AXL: 1-way ANOVA,  $F(4,93) = 2.66, p = 0.04$ ). A significant increasing

trend was observed for VCD elongation from high to low SF ( $F(1,91) =$

$8.59, p = 0.004$ ).

On day 7, reduction in the proportion of high SF in the stimulus increased

the interocular difference of VCD and AXL (VCD: 1-way ANOVA,  $F(4,49)$

$= 1.9, p = 0.12$ ; AXL: 1-way ANOVA,  $F(4,49) = 2.9, p = 0.32$ ). Significant

linear increasing trends were observed for both VCD ( $F(1,49) = 5.5,$

$p = 0.02$ ) and AXL ( $F(1,49) = 9.7, p = 0.003$ ).

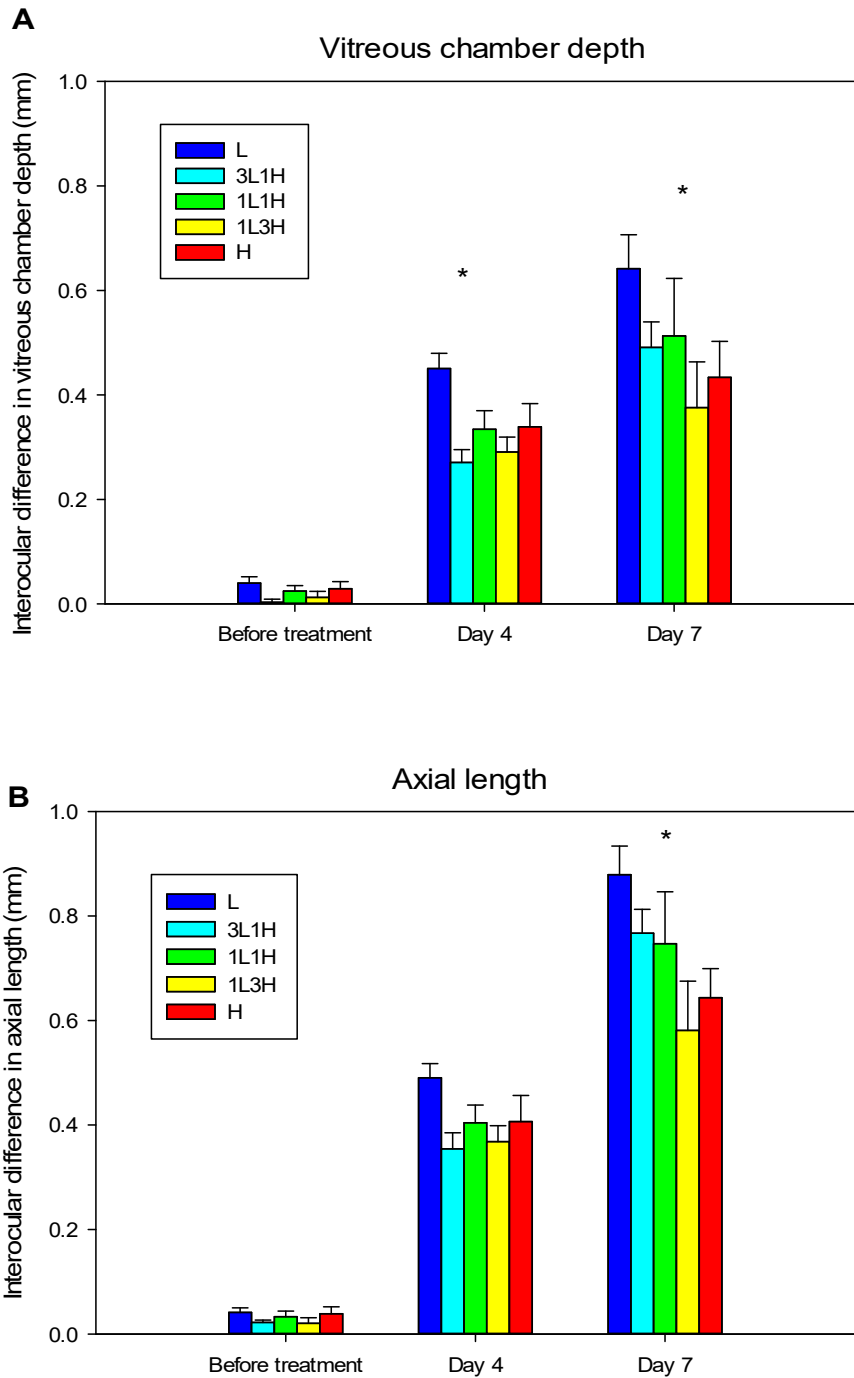


**Figure 8.4.** The interocular differences in refractive error from before treatment, after 4 days and after 7 days with monocular treatment with lens-cone device. X-axis represents the time points of the measurements. The Y-axis represents the interocular difference in VCD (A) and AXL (B) (treatment minus control). Error bars represent the standard error of the mean. Asterisks denote ANOVA trend analysis with statistical significance with  $p < 0.05$ .

### 8.4.3. Anterior chamber depth and lens thickness

The interocular differences (Mean±SEM) for ACD and LT for different SF ratio groups are shown in **Figures 8.5A and B** respectively. The anterior eye growth was as expected to be less influenced by visual stimuli. There was consistent growth of ACD on day 4 across the groups (**Figure 8.5A**) and on day 7, a greater variability was seen. There was trend that slower ACD growth with increased high SF ratio, although it was not significant ( $F(1,49) = 1.4, p=0.24$ ). The interocular LT maintained similar growth pace across different SF ratio groups.

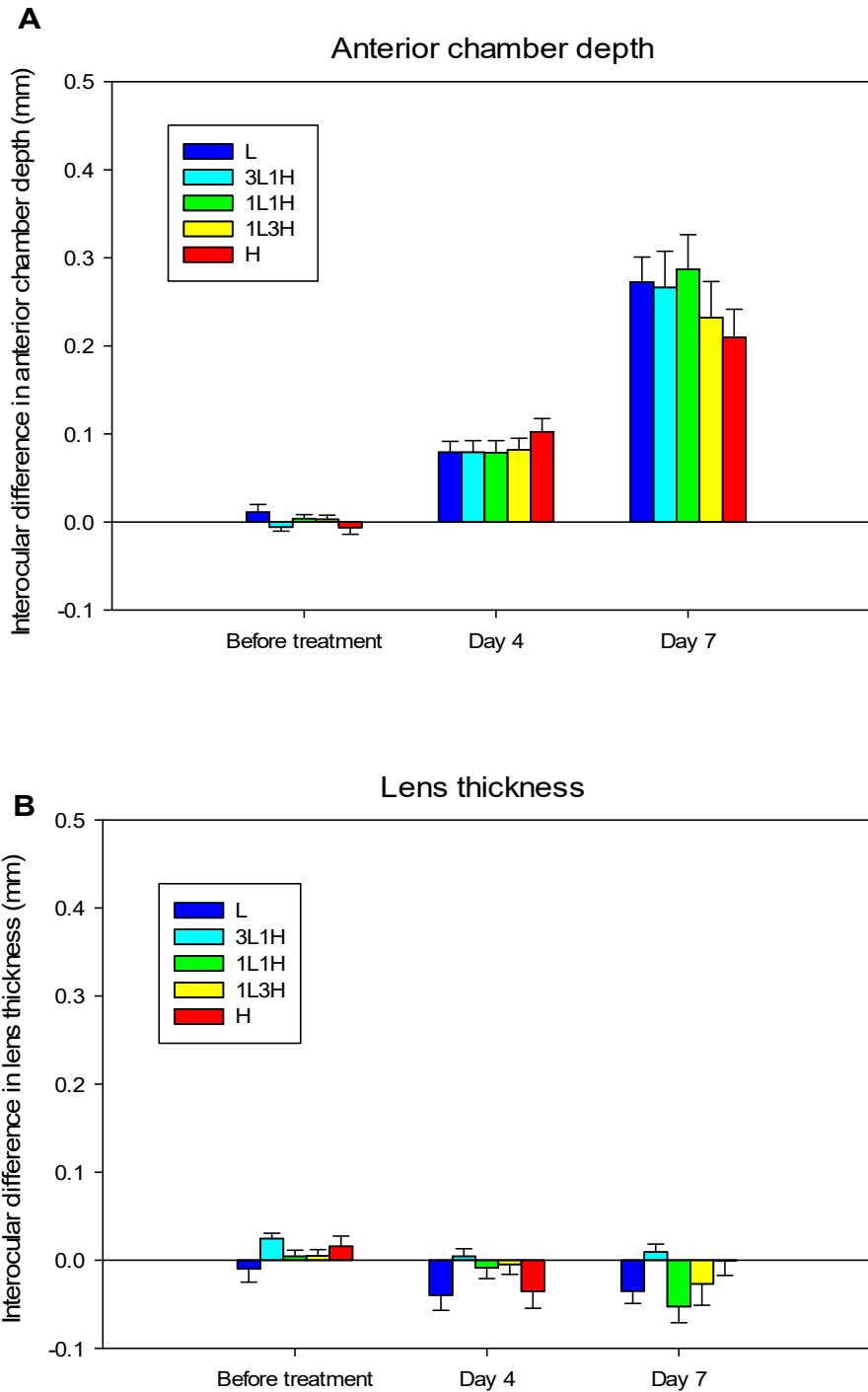


**Figure 8.5.** The interocular differences in refractive error from before treatment, after 4 days and after 7 days with monocular treatment with lens-cone device. X-axis represents the time points of the measurements. The Y-axis represents the interocular difference in VCD (A) and AXL (B) (treatment minus control). Error bars represent the standard error of the mean. Asterisks denote ANOVA trend analysis with statistical significance with  $p < 0.05$

## 8.5. Discussion

In most previous studies using a lens-induced myopia models, animals were fitted with a concave lens to induce myopia, but the visual environment was usually not controlled. In this experiment, the right eye of the chicks was exposed constantly to -15D of hyperopic defocus. Based on the hypothesis of emmetropization, all the eyes should grow and compensate to become “functionally” emmetropic for the induced defocus. Our results demonstrate that changing the spatial frequency composition in the visual stimulus affects the decoding characteristic for hyperopic defocus and thus influences the emmetropization process. Previous studies found that the eye can decode and grow regionally in response to hyperopic and myopic defocus (Miles and Wallman, 1990). In addition, when two levels of defocus were presented at the same time in the retinal image, an integration mechanism within the eye can compute the amount of defocus input and guide the corresponding growth (McFadden *et al.*, 2014; Tse *et al.*, 2007; Tse and To, 2011). The emmetropization end-point is then thought to be set according to the magnitude of defocus induced (McFadden *et al.*, 2014; Tse *et al.*, 2007; Tse and To, 2011). The results in this experiment suggest there is an interaction between spatial stimuli and defocus to influence the emmetropization set-

point.

### **8.5.1. Could accommodation compensate differently to the imposed defocus under different spatial frequency?**

It has been shown that human accommodation is spatially tuned to mid-spatial frequencies (3-5cpd) (Mathews and Kruger, 1994; Owens and Wolfe, 1985). It is plausible that chick's accommodation behaves similarly to human, and thus the pattern containing more high spatial frequency information may reflect more sustained accommodation, thereby attenuating the imposed defocus. The chick accommodative amplitude was about 15-20D (Schaeffel *et al.*, 1986; Troilo and Wallman, 1987). In Experiment 3, the induced defocus ranged from -5D to 15D, the amount of defocus imposed maybe relative unstable for -5D since it is well within the accommodative amplitude of young chicks (Wildsoet, 2003). In contrast, lesser concern about accommodation in Experiment 4. Since, imposing -15D defocus was expected to be relatively stable as previous studies indicated that accommodation activity is only poorly sustained for high powered hyperopic defocus (-15D)(Nau *et al.*, 1999; Wildsoet, 2003). In addition, the high contrast checkers used in the experiments were not extremely high (0.9cpd) or low (0.3cpd), and both spatial frequencies thus

should be within the spatial resolution of chick.

### **8.5.2. Possible mechanism for spatial tuning in decoding defocus**

The results showed that as the contribution of low spatial frequency stimulus increased from 0% to 100%, the eye refractive errors shifted to match with the induced defocus (-15D). The difference between Experiment 3 and this experiment is that the eye was globally experiencing -15D of defocus together with different spatial information. This suggests within the eye, there is a mechanism for decoding defocus with spatial selectivity and this selective signal processing from the retina is to execute emmetropization. The underlying physiological mechanism to modulate and integrate the spatial signals for emmetropization is not known. In Experiment 2, sign dependent retinal responses to defocus (DC and IC amplitudes) were shown to be more obvious in peripheral regions under low spatial frequency in humans (Refer to Chapter 6). This is also further evidence for retina decoding optical defocus which is spatially tuned. A previous study suggested that amacrine cells are responsible for controlling the eye growth, with their complexity and variety of cell types (Masland, 2012). They come in all shapes, sizes and stratification patterns. With such complexities, the amacrine cells are hypothesized to possess the ability to

receive signals from different layers and regions in the retina. In Sinclair et al. (2004) study, it was found that amacrine cells played a key role in spatial frequency tuning for ganglion cells (Sinclair *et al.*, 2004). If amacrine cells are involved in decoding optical defocus, it is possible that amacrine cells with a larger receptive field, are more sensitive for decoding defocus at lower spatial frequencies. Some preliminary evidence from Zhong and colleagues (2004) also demonstrated that the activity of amacrine cells and bipolar cells could be modulated by defocus (Zhong *et al.*, 2004). It is speculated that these neurons are spatially tuned to respond to defocus as a control of emmetropization as well as being involved in the myopia development.

## **8.6. Conclusion**

In this experiment, under the same magnitude of hyperopic defocus, trends of increased myopia and ocular elongation were observed when the spatial frequency composition was gradually changed from higher SF to lower SF. This suggests decoding of hyperopic defocus within the eye is spatially tuned. Further studies are needed to investigate the interaction of spatial effect and myopia defocus and how the mechanism can be employed in myopia control.

## **Chapter 9. General Discussion and Future**

### **Directions**

In this Chapter, the results from Experiment 1 (Chapter 5) to Experiment 4 (Chapter 8) will be combined and further discussed. For human subjects, the retinal response to spatial frequency and retinal response to defocus under spatial frequency will be discussed. In addition, by using chicks as a myopia model, the eye “response” to defocus with spatial frequency stimulation in relation to eye growth will be discussed. Furthermore, the mechanism of spatial effect in our visual environment on myopia development will also be proposed.

#### **9.1. Spatial vision and spatial frequency**

Spatial frequency is one of the important “key elements” in this spatial vision. Irrespective of which scenes or objects are viewed, the visual stimuli contain information with many different spatial characteristics, from very fine to very coarse. Spatial vision, is the ability of the visual system to resolve and discriminate features in space. Spatial frequency is a fundamental attribute for visual stimulus. Considerable amount of work has been done to investigating how eyes “see” (Hubel and Wiesel, eds., *Brain and Visual Perception*, 2005, Oxford University Press, Oxford) In brief,

previous studies have proved there are many spatial channels (**Figure 9.1A**) in the visual system. Each channel has its individual sensitivity function and all channels contribute to an overall visual contrast sensitivity function (**Figure 9.1B**) (Campbell and Robson, 1968; Graham, 1972). This hypothesis is also supported by the observation that the receptive fields of retinal neurons vary in size. They are responsible for decoding the stimuli with varying spatial frequencies. Visual stimulus has been shown to be segregated firstly in a layer-by-layer manner within the retina (Pang *et al.*, 2002). The results of Experiment 1 provide electrophysiological evidence that spatial segregation of visual image starts at the retinal level of human eye (Refer to Chapter 5).

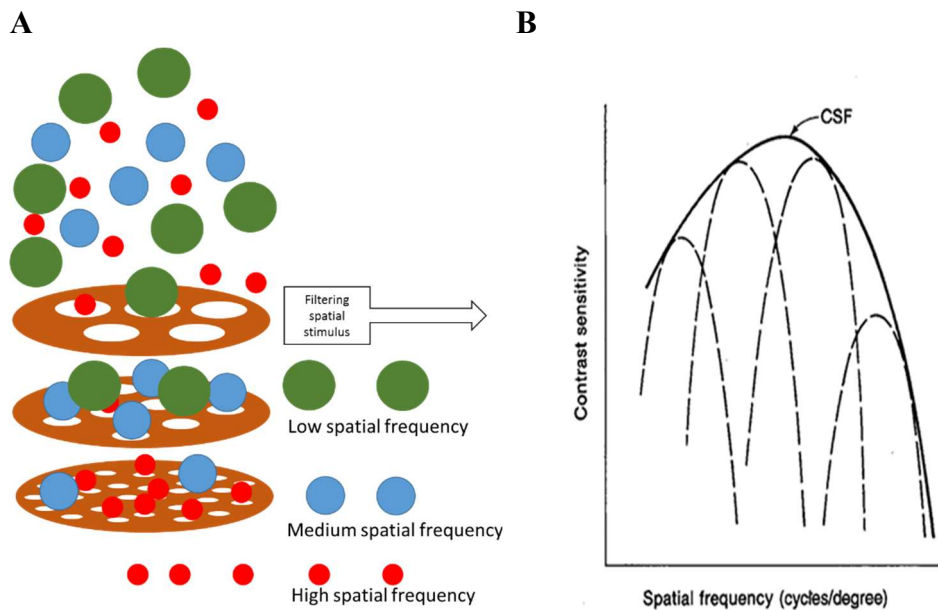


**Figure 9.1. Visual processing in the retina.** (A) Schematic diagram for channeling spatial information in retina. Visual stimulus is composed of a range of spatial frequencies. The retina is hypothesized to possess various channels acting as filters for different spatial frequencies. (B) Contrast sensitivity function (CSF, solid line) is formed by combining numerous individual channels (dashed lines) (Billock, 2000; Billock and Harding, 1996; Sekuler *et al.*, 1984).

## 9.2. Spatial vision and optical defocus

The eye is known to regulate its own growth in accordance with the characteristics of visual stimulus received. One of the most important characteristics is optical defocus. Since the image of an object further from the plane of focus should be blurred as much as that of an object closer than the plane of focus, the blurriness caused by defocus solely in an aberration-free eye could not provide any direction/sign information to guide the eye growth. It has long been debated how the eye can decode defocus to guide

the eye growth. Ho et al. (2012) found that human retinal activity had sign-dependent variation on defocus. Taking this step further, we hypothesized that the eye itself is fundamentally for resolving spatial details of the environment, it is possible that the eye may use spatial details as cues for detecting decoding defocus. If it is the case, the spatial frequencies and the defocus should have certain interactive effects to guide the eye on decoding, and the retina should respond differently for different spatial frequencies under various conditions of defocus. Thus, in Experiment 2, the human retinal response to defocus under different SFs was investigated. It was found that sign dependent retinal response to defocus was more obvious under low spatial frequency presentation. In addition, the results showed that such sign dependent retinal response to defocus was occurred dominantly in the peripheral retina rather than the central region, echoing studies carried out by Smith and colleagues suggested the peripheral retina has an important role in emmetropization (Smith *et al.*, 2009; Smith *et al.*, 2005; Smith *et al.*, 2007). In humans, the spatial resolution in the peripheral retina is lower than that in fovea. Thus, from our ERG results, if the detection of defocus is spatially preferred to lower SF, the peripheral retina is capable of performing this function. The concept of spatial tuning for

detecting defocus (Experiment 2) was tested to determine if there is spatial tuning for eye growth responding to optical defocus (Experiment 3 and 4).

### **9.3. Retinal site for detecting defocus**

The mfERG results in Experiment 2 was found that the outer retinal response (direct component) showed more obvious sign dependent change to defocus than the inner retinal response (induced component). Most studies have suggested that the inner retina detects defocus and generates growth control signals, due to visual processing and complexity of the inner retina (amacrine cells, ganglion cells). Only a few considered the role of the outer retina in regulating eye growth. As photoreceptors were shown to have preference in light direction, known as the Stiles-Crawford effect (Stiles and Crawford, 1933), a previous study hypothesized that Stiles-Crawford effect can be used in defocus detection (Crewther, 2000). On the other hand, in further studying the characteristics of the direct component in MOFO mfERG response in human and animal studies, the oscillation-like wavelets in the direct component were shown to be contributed from inner retinal activity (Chu *et al.*, 2008; Chu *et al.*, 2006). Hence, the involvement of the inner retina in detecting/decoding defocus cannot be ruled out. As the induced component in mfERG response was shown to be a TTX-sensitive

component activity (Chu *et al.*, 2008; Chu *et al.*, 2006), it is highly related to the action potential from retinal ganglion cells which may not be directly contributed to defocus detection. Based on the findings in this thesis, we speculate that the activity from the inner plexiform layer may also be the possible site for detecting defocus.

#### **9.4. From retinal activity to eye growth**

In Experiment 3 and 4, it was found that the eye growth response to hyperopic defocus was dependent on visual stimulus. The chick eye compensates to induced defocus more accurately with increased spatial frequency component. The results of Experiment 3 and 4 are highly correlated with the findings of human retinal activity to spatial frequency and defocus shown in Experiment 2. Owing to ocular anatomical differences in humans and bird, and indeed the mfERG waveform of chick is not exactly the same as human (Schmid *et al.*, 2013), the human mfERG response of spatial details and defocus may not fully account for the response of eye growth in the chick eye. However, based on many previous myopia studies using chick eye as a model and the experiments in this thesis, it has been shown that increase in vitreous chamber depth in chicks resulting in myopia was similar to the etiology of myopia progression in

human. We believe that the chick retina is similar to the human retina as the major contributor to the response to defocus with different spatial details in myopia development.

### **9.5. Emmetropization end-point**

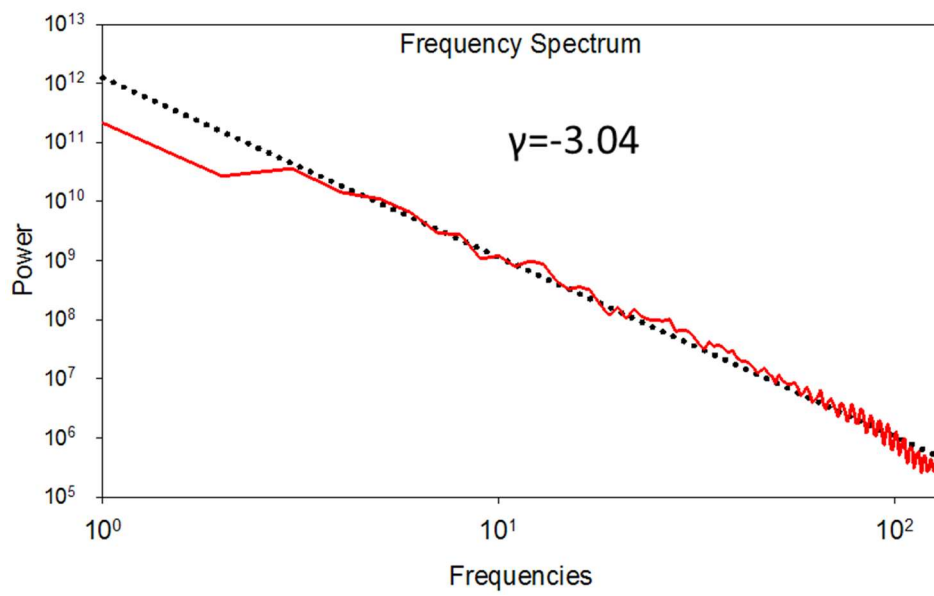
Base on the results of Experiment 3 and 4, spatial stimulus is important to guide eye growth. In many species, deprivation of spatial stimulus would cause uncontrolled eye elongation resulting in severe myopia. Hess and colleagues (2006) presented a hypothesis that images composed of higher spatial frequencies ( $1/f$ ) were more effective to achieve emmetropization, Thus, no myopia development. In their study, a blank stimulus would be equivalent to a form-deprived condition which results in high myopia development, that is, no emmetropization end-point. Adjusting the spatial composition to a higher contribution from low SF ( $1/f^2$ ), resulted in the eyes still becoming myopic. In contrast, with more contribution from high SF ( $1/f^{0.5}$ ), the eyes become less myopic (more hyperopia). Thus, Hess et al. (2006) suggested spatial composition with high SF was important for emmetropization.

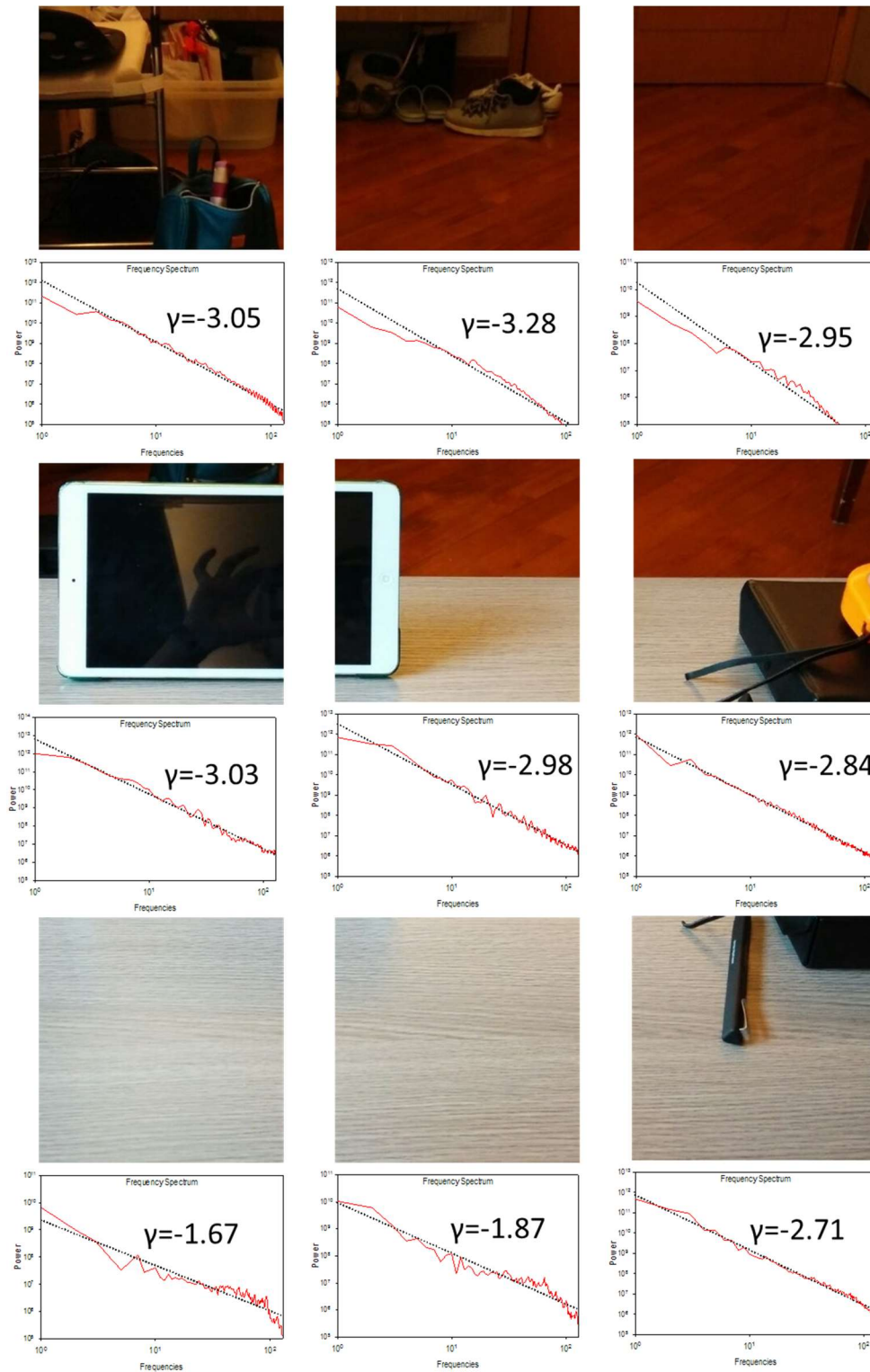
Even though Hess and colleagues (2006) showed eye growth can be modulated by adjusting spatial composition. Numerous studies have shown

that power spectra of natural images share similar characteristics as  $1/f^\gamma$  and, low spatial frequencies in natural images are generally more dominant which would be myopigenic as suggested by Hess's model of emmetropization (without defocus). In Experiment 3 and 4, when the eye is under hyperopic defocus, as a directional signal for compensation, we however showed that the compensation executed better under lower SF. Moreover, the spatial spectra within a carpentered environment can be anisotropic. For example, in **Figure 9.2**, the overall spatial spectrum of the image was broken into nine individual visual images with their own spatial spectra. There was a large variation in the value of  $\gamma$  in indoor scenes. Some parts of the indoor environment would be more myopigenic ( $\gamma=3.28$ ) than other ( $\gamma=1.67$ ). This raises a question whether the eye, is behaved as a single global sensor, detects the overall characteristics of spatial stimulus to emmetropize. Or, does the eye possess multiple sensors on the retina, to detect various retinal images simultaneously. Tse and To (2011) suggested that the emmetropization set-points were graded according to summation of different retinal areas receiving hyperopic and myopic levels of defocus. Our results highlight the possibility that the retina possesses multiple sensors and integrate all these spatial signals for global emmetropization.

We have shown that eye growth responds differently to defocus under different spatial stimuli. The result may shed light on how the retina detects defocus in emmetropization. In Experiment 2, the mfERG response to defocus (Chin *et al.*, 2015a) is also spatially and regionally tuned. The detection of defocus in emmetropization may tune to low SF. In Experiment 4, a constant -15D hyperopic defocus to be induced, the emmetropization set-point should be close to -15D. Instead, the emmetropization response varied according to the ratio of low and high SF in the visual stimulus, with eyes becoming less myopic with a lower ratio of low spatial frequency. This suggests the spatial composition of visual stimulus at individual retinal areas would affect the global emmetropization response.

A



**B**

**Figure 9.2. Images and respective spatial spectra.** The full picture and its spatial spectrum are shown in (A). The image in (A) is broken down into nine individual images and their spatial spectra were shown in (B). Note that the profile of the images is similar, obeying  $1/f^\gamma$  function while the slopes are varied.

## 9.6. Future Directions

### 9.6.1. Interactive retinal tuning to spatial frequency and defocus

Previous studies have all concluded that the retina can decode sign and magnitude of optical defocus locally (Miles and Wallman, 1990; Norton and Siegwart, 1991; Wallman *et al.*, 1987). The results of our studies preliminarily show that such detection of defocus mechanism possesses different spatial sensitivity. Since the spatial resolution of vision is correlated inversely with the size of the receptive field (Watson, 2014), we speculate, based on our findings, that the retinal neurons, with large-receptive field size, may be relatively more responsible for the detection of defocus on the retina. To complicate matters, as the receptive field size in humans is increased with retinal eccentricity, what particular receptive field size of what particular retinal cell that is more sensitive to optical defocus for triggering eye growth. In addition, our vision system has been suggested to adapt to the visual environment (Billock, 2000; Knill *et al.*, 1990; Laughlin, 1983; Parraga *et al.*, 2000). For example, children less than 10 years old, their visual system is not yet optimally tuned for detecting natural images (Elleberg *et al.*, 2012). This implied that the younger eyes are adapting themselves to the environment during the growth process. More

work is needed to carry out for manipulating environmental factors in regulating the eye growth.

### **9.6.2. Clinical implication of spatial frequency in myopia control**

Based on the current understanding of eye growth, previous studies have attempted various methods to reduce the progression of myopia. Utilizing the spectacle method includes under-correction of myopic refractive error (Adler and Millodot, 2006; Chung *et al.*, 2002), bifocal (Cheng *et al.*, 2014; Fulk *et al.*, 2000) or progressive addition spectacles (Berntsen *et al.*, 2012; Gwiazda *et al.*, 2003). Contact lens method includes rigid gas permeable (Katz *et al.*, 2003), soft bifocal lenses (Lam *et al.*, 2013; Sankaridurg *et al.*, 2011; Walline *et al.*, 2013) and orthokeratology (Charm and Cho, 2013; Chen *et al.*, 2013; Cho and Cheung, 2012). Topical pharmaceutical agent includes atropine (Bedrossian, 1979; Chia *et al.*, 2012; Chua *et al.*, 2006). It is highlighted that no current myopia control methods can halt myopia progression completely, and the overall about 50% of slowing the myopia progression rate was reported. Thus, we speculate that it should have other factors that can be incorporated into myopia control with current strategies to further halt the rest of 50% of progression. From my findings, it showed that there is an interactive effect of spatial and defocus in myopia

development. It is possible for incorporating spatial frequency as a new contributor into myopia control. In addition, spending more time outdoors has been shown to decrease the likelihood of becoming myopic. The major attributional difference highlighted between outdoor and indoor are light intensity (Sherwin *et al.*, 2012a), ultraviolet radiation (Williams *et al.*, 2017). Yet little was mentioned about the difference in the spatial compositions of visual scene between outdoor and indoor. According to the findings from Hansen and co-workers (Hansen and Essock, 2005), more carpentered settings were found in indoor than outdoor environment. Empirical experience from indoor is that even more low SF components, such as plain wall, which can be myopicgenic. The relationship of the spatial composition within the environment and myopia progression may be one of the future directions in applying controlled visual stimuli, together with defocus manipulation, in myopia control.

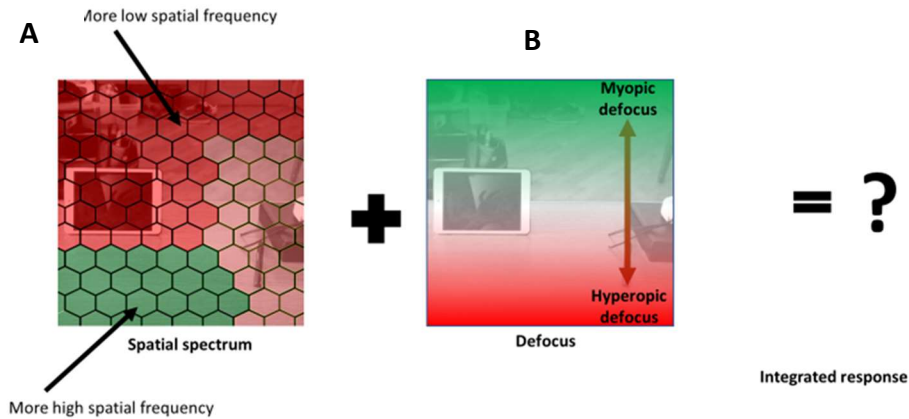


**Figure 9.3. Visual environment characterizing different profiles of spatial composition and defocus.** (A) Spatial composition, green: more high spatial frequency; red: more low spatial frequency. (B) Defocus, green: myopic defocus; red: hyperopic defocus. Saturation of the colours represents relative strength.

## 9.7. Limitations

### 9.7.1. Square-wave spatial frequencies were used in the experiments

In current experiments, high contrast black and white square-wave spatial frequency was used. By Fourier analysis, a square-wave spatial frequency is made up by adding the fundamental frequency together with pure harmonics of sine waves (Campbell and Robson, 1968). Some may challenge there are numerous components of high spatial frequency within the square-wave gratings/checks. For square-wave grating on human vision, Blakemore and Campbell (1969) found that adaptation to a high contrast square-wave grating produced marked threshold elevation in the fundamental frequency

and its third harmonic only (Blakemore and Campbell, 1969b). Hence, we assumed the signal of spatial frequencies beyond the third harmonic of fundamental frequency only cause neglectable noise to the fundamental spatial frequency perceived by the retina. When the existence of channels in the human visual system was proposed (Campbell and Robson, 1968), and the channels are sensitive to a narrow range of spatial frequency. The fundamental spatial frequencies selected in human studies (0.24, 1.2, 2.4, 4.8cpd) and chick studies (0.3 and 0.9cpd) should have sufficient separation between each other to avoid overlapping of response.

### **9.7.2. Adopting the relatively low spatial frequency in the experiments**

The spatial frequency selected in either human (0.24 to 4.8cpd) or chick (0.3 and 0.9cpd) studies was relative low according to maximum resolution of human (about 30cpd) and chick (about 12cpd). The selection of spatial frequency of human studies was limited by the maximum resolution at human peripheral retina. At the eccentricity of  $20^\circ$ , the resolution was about 5cpd. While the selection of spatial frequency for chick studies was limited by the working distance (40mm) of the lens-cone device as well as the resolution of printing. In the preliminary stage of the experiment, the size of the lens-cone device was tested out. It was noticed that if a bigger cone

(50mm height) was used, the lens-cone device was easily torn away by the 2 weeks old chick. On the other hand, using a cone with 30mm height reduced the chance of device being torn off. However, the working lens required had more plus addition. It was concerned about the slightly deviation of back vertex distance which would produce greater error. Although relatively low spatial frequency was chosen in the experiments, it was believed that the experimental setup was valid as high spatial frequencies are infrequent in the typical natural scenes. We suggest if peripheral region can decode defocus and the mechanism is spatial tuned, low SF stimuli may be the main contributor in terms of resolution at the peripheral retina and the availability of low SF in natural scene.

### **9.7.3. Effect of magnification factor**

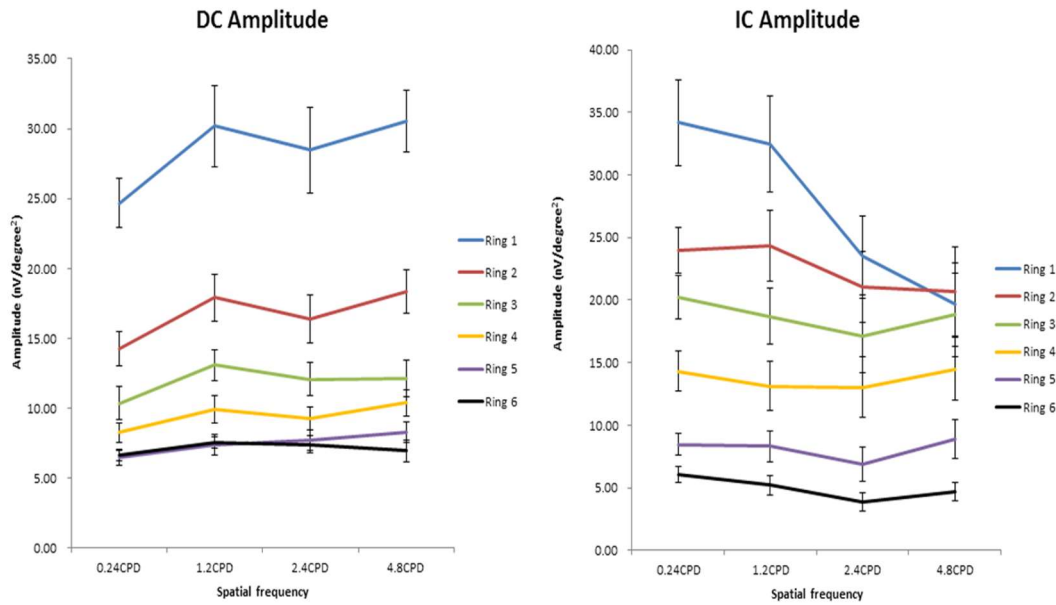
In human studies, the hexagons of mfERG stimulus was projected onto the retina and the retinal image size was influenced by the magnitude of subjects' refractive errors and the sign of defocus induced. Inevitably, the correction of refractive error by spectacle lenses causes different retinal image sizes for subject with different refractive errors. In both experiments, the spectacle magnification was tried to be controlled by limiting the range of refractive errors of all subjects. In Experiment 2, retinal image of

hexagonal array under positive defocus is expected to be magnified and larger than in-focus retinal image. This could lead to an increase in mfERG response. By estimation, +2D magnified the image by 1-2%. The magnification effect solely cannot explain the increase in amplitude response as much as 20% in some retinal regions. In addition, sign dependent changes were observed regionally. These suggested that the result was unlikely due to magnification effect of spectacle lenses. In chick studies, the limitation of applying different magnitudes of induced defocus was the various degrees of magnification of spatial checks. Inter-ocular differences in magnification could be a cue used in eye growth. Curry and colleagues (1999) tested out that a significant difference in magnification would induced eye growth. When the eye was treated with afocal lens with magnification produced close to that of a 10D convex inducing lens, the eye was barely and slightly more myopic than its fellow untreated eye (Curry *et al.*, 1999). This implies the spectacle magnification of image itself was not the main cue for decoding the defocus. Furthermore, Schmid and colleagues (1999) demonstrated that manipulating the retinal image size has no effect on chick ability to compensate the imposed hyperopia defocus (Schmid *et al.*, 1999). The difference between the rates of eye growth in the current

experiments was unlikely due to the difference in the spectacle magnification factor.

# APPENDICES

## APPENDIX A



**Appendix A.** Global flash mfERG response for spatial frequency in high myopic subjects. DC amplitude and IC amplitude of 12 age-matched subjects with spherical equivalent of  $-6.54 \pm 1.63D$ , are shown. The general trends of DC and IC amplitudes against spatial frequency for the high myope group were similar to those from the low myope group (Refer to **Figure 5.6.**).

## APPENDIX B

**Appendix B.** The interocular difference of vitreous chamber depth in response to different lens powers and different spatial frequency patterns. With induction of -25D defocus, chick eyes with low SF stimulus elongated faster than with high SF stimulus, similar to the trend shown in other defocus conditions.

Interocular difference in vitreous chamber depth (mm) (Day 4)						
Lens power (D)	Defocus (D)	High SF		Low SF		Statistical significance
		Mean	(S.E.M)	Mean	(S.E.M)	
25	0	0.19	(0.04)	0.31	(0.04)	0.046
20	-5	0.22	(0.02)	0.26	(0.03)	0.304
15	-10	0.22	(0.04)	0.28	(0.04)	0.318
10	-15	0.33	(0.05)	0.45	(0.03)	0.032
0	-25	0.30	(0.08)	0.64	(0.08)	0.006

Interocular difference in vitreous chamber depth (mm) (Day 7)						
Lens power (D)	Defocus (D)	High SF		Low SF		Statistical significance
		Mean	(S.E.M)	Mean	(S.E.M)	
25	0	0.02	(0.05)	0.24	(0.08)	0.028
20	-5	0.18	(0.04)	0.28	(0.06)	0.161
15	-10	0.44	(0.09)	0.45	(0.06)	0.893
10	-15	0.43	(0.07)	0.64	(0.06)	0.045
0	-25	0.28	(0.10)	0.83	(0.07)	0.001

## REFERENCES

- Adams, A. J. (1987). Axial length elongation, not corneal curvature, as a basis of adult onset myopia. *American Journal of Optometry and Physiological Optics*, 64(2), 150-152.
- Adler, D., & Millodot, M. (2006). The possible effect of undercorrection on myopic progression in children. *Clinical and Experimental Optometry*, 89(5), 315-321. doi:10.1111/j.1444-0938.2006.00055.x
- Anderson, S. J., Mullen, K. T., & Hess, R. F. (1991). Human peripheral spatial resolution for achromatic and chromatic stimuli: limits imposed by optical and retinal factors. *The Journal of physiology*, 442, 47-64.
- Andison, M. E., Sivak, J. G., & Bird, D. M. (1992). The refractive development of the eye of the American kestrel (*Falco sparverius*): a new avian model. *Journal of Comparative Physiology A*, 170(5), 565-574.
- Angle, J., & Wissmann, D. A. (1980). The epidemiology of myopia. *Am J Epidemiol*, 111(2), 220-228.
- Arden, G. B. (1987). Effect of pattern luminance profile on the pattern ERG in man and pigeon. *Vision Res*, 27(6), 883-892.
- Ashby, R. S., Kozulin, P., Megaw, P. L., & Morgan, I. G. (2010). Alterations in ZENK and glucagon RNA transcript expression during increased ocular growth in chickens. *Molecular Vision*, 16, 639-649.
- Ashby, R. S., Ohlendorf, A., & Schaeffel, F. (2009). The effect of ambient illuminance on the development of deprivation myopia in chicks. *Investigative Ophthalmology and Visual Science*, 50(11), 5348-5354. doi:10.1167/iovs.09-3419; 10.1167/iovs.09-3419
- Ashby, R. S., & Schaeffel, F. (2010). The effect of bright light on lens compensation in chicks. *Investigative Ophthalmology and Visual Science*, 51(10), 5247-5253. doi:10.1167/iovs.09-4689; 10.1167/iovs.09-4689
- Atchison, D. A., Pritchard, N., & Schmid, K. L. (2006). Peripheral refraction along the horizontal and vertical visual fields in myopia. *Vision Res*, 46(8), 1450-1458.
- Baird, P. N., Schache, M., & Dirani, M. (2010). The GENes in Myopia (GEM) study in understanding the aetiology of refractive errors. *Progress in Retinal and Eye Research*, 29(6), 520-542. doi:10.1016/j.preteyeres.2010.05.004

- Baldwin, W. R. (1990). Refractive status of infants and children. *Principles and Practice of Pediatric Optometry*. Philadelphia, PA: Lippincott, 104-152.
- Barathi, V. A., Boopathi, V. G., Yap, E. P. H., & Beuerman, R. W. (2008). Two models of experimental myopia in the mouse. *Vision Res*, 48(7), 904-916.
- Bartmann, M., & Schaeffel, F. (1994). A simple mechanism for emmetropization without cues from accommodation or colour. *Vision Res*, 34(7), 873-876.
- Bedrossian, R. H. (1979). The effect of atropine on myopia. *Ophthalmology*, 86(5), 713-717.
- Belkin, M., Yinon, U., Rose, L., & Reiser, I. (1977). Effect of visual environment on refractive error of cats. *Documenta ophthalmologica*, 42(2), 433-437.
- Beresford, J. A., Crewther, S. G., & Crewther, D. P. (1998). Anatomical correlates of experimentally induced myopia. *Australian and New Zealand journal of ophthalmology*, 26(S1), S84-S87.
- Berninger, T., & Schuurmans, R. P. (1985). Spatial tuning of the pattern ERG across temporal frequency. *Documenta ophthalmologica*, 61(1), 17-25.
- Berntsen, D. A., Sinnott, L. T., Mutti, D. O., & Zadnik, K. (2012). A randomized trial using progressive addition lenses to evaluate theories of myopia progression in children with a high lag of accommodation. *Investigative Ophthalmology and Visual Science*, 53(2), 640-649.
- Billock, V. A. (2000). Neural acclimation to 1/f spatial frequency spectra in natural images transduced by the human visual system. *Physica D: Nonlinear Phenomena*, 137(3-4), 379-391.  
doi:[http://dx.doi.org/10.1016/S0167-2789\(99\)00197-9](http://dx.doi.org/10.1016/S0167-2789(99)00197-9)
- Billock, V. A., & Harding, T. H. (1996). Evidence of spatial and temporal channels in the correlational structure of human spatiotemporal contrast sensitivity. *The Journal of physiology*, 490(Pt 2), 509-517.
- Birch, D. G., & Fish, G. E. (1988). Focal cone electroretinograms: aging and macular disease. *Documenta ophthalmologica*, 69(3), 211-220.
- Bitzer, M., & Schaeffel, F. (2002). Defocus-induced changes in ZENK expression in the chicken retina. *Investigative Ophthalmology and Visual Science*, 43(1), 246-252.
- Blakemore, C., & Campbell, F. W. (1969a). Adaptation to spatial stimuli.

- The Journal of physiology*, 200(1), 11P-13P.
- Blakemore, C. T., & Campbell, F. W. (1969b). On the existence of neurones in the human visual system selectively sensitive to the orientation and size of retinal images. *The Journal of physiology*, 203(1), 237-260.
- Boothe, R. G. (2001). *Perception of the visual environment*: Springer Science and Business Media.
- Bowrey, H. E., Metse, A. P., Leotta, A. J., Zeng, G., & McFadden, S. A. (2015). The relationship between image degradation and myopia in the mammalian eye. *Clinical and Experimental Optometry*, 98(6), 555-563.
- Brodstein, R. S., Brodstein, D. E., Olson, R. J., Hunt, S. C., & Williams, R. R. (1984). The treatment of myopia with atropine and bifocals: a long-term prospective study. *Ophthalmology*, 91(11), 1373-1378.
- Brown, B., & Yap, M. K. H. (1996). Contrast and luminance as parameters defining the output of the VERIS topographical ERG. *Ophthalmic and Physiological Optics*, 16(1), 42-48.
- Buck, C., Schaeffel, F., Simon, P., & Feldkaemper, M. (2004). Effects of positive and negative lens treatment on retinal and choroidal glucagon and glucagon receptor mRNA levels in the chicken. *Investigative Ophthalmology and Visual Science*, 45(2), 402-409.
- Campbell, F. W., & Robson, J. G. (1968). Application of Fourier analysis to the visibility of gratings. *The Journal of physiology*, 197(3), 551.
- Chan, H. L., & Mohidin, N. (2003). Variation of multifocal electroretinogram with axial length. *Ophthalmic and Physiological Optics*, 23(2), 133-140.
- Charm, J., & Cho, P. (2013). High Myopia–Partial Reduction Ortho-k: A 2-Year Randomized Study. *Optometry and Vision Science*, 90(6), 530-539.
- Charman, W. N. (1999). Near vision, lags of accommodation and myopia. *Ophthalmic and Physiological Optics*, 19(2), 126-133.
- Chen, C., Cheung, S. W., & Cho, P. (2013). Myopia Control Using Toric Orthokeratology (TO-SEE Study) Myopia Control Using Toric Orthokeratology. *Investigative Ophthalmology and Visual Science*, 54(10), 6510-6517.
- Chen, J. C., Brown, B., & Schmid, K. L. (2006a). Evaluation of inner retinal function in myopia using oscillatory potentials of the multifocal electroretinogram. *Vision Res*, 46(24), 4096-4103.

- Chen, J. C., Brown, B., & Schmid, K. L. (2006b). Retinal adaptation responses revealed by global flash multifocal electroretinogram are dependent on the degree of myopic refractive error. *Vision Res*, *46*(20), 3413-3421. doi:10.1016/j.visres.2006.03.013
- Chen, J. F., Elsner, A. E., Burns, S. A., Hansen, R. M., Lou, P. L., Kwong, K. K., & Fulton, A. B. (1992). The effect of eye shape on retinal responses. *Clinical vision sciences*, *7*(6), 521-530.
- Chen, X., Sankaridurg, P., Donovan, L., Lin, Z., Li, L., Martinez, A., . . . Ge, J. (2010). Characteristics of peripheral refractive errors of myopic and non-myopic Chinese eyes. *Vision Res*, *50*(1), 31-35.
- Cheng, D., Woo, G. C., Drobe, B., & Schmid, K. L. (2014). Effect of bifocal and prismatic bifocal spectacles on myopia progression in children: three-year results of a randomized clinical trial. *Jama ophthalmology*, *132*(3), 258-264.
- Chia, A., Chua, W. H., Cheung, Y. B., Wong, W. L., Lingham, A., Fong, A., & Tan, D. (2012). Atropine for the treatment of childhood myopia: safety and efficacy of 0.5%, 0.1%, and 0.01% doses (Atropine for the Treatment of Myopia 2). *Ophthalmology*, *119*(2), 347-354.
- Chin, M. P., Chu, P. H., Cheong, A. M., & Chan, H. H. (2015a). Human electroretinal responses to grating patterns and defocus changes by global flash multifocal electroretinogram. *PLoS One*, *10*(4), e0123480. doi:10.1371/journal.pone.0123480
- Chin, M. P., Siong, K. H., Chan, K. H., Do, C. W., Chan, H. H., & Cheong, A. M. (2015b). Prevalence of visual impairment and refractive errors among different ethnic groups in schoolchildren in Turpan, China. *Ophthalmic and Physiological Optics*, *35*(3), 263-270. doi:10.1111/opo.12193
- Cho, P., & Cheung, S. W. (2012). Retardation of Myopia in Orthokeratology (ROMIO) Study: A 2-Year Randomized Clinical Trial Retardation of Myopia in Orthokeratology Study. *Investigative Ophthalmology and Visual Science*, *53*(11), 7077-7085.
- Choh, V., Lew, M. Y., Nadel, M. W., & Wildsoet, C. F. (2006). Effects of interchanging hyperopic defocus and form deprivation stimuli in normal and optic nerve-sectioned chicks. *Vision Res*, *46*(6-7), 1070-1079. doi:10.1016/j.visres.2005.08.020
- Chu, C. H., & Kee, C. S. (2015). Effects of optically imposed astigmatism on early eye growth in chicks. *PLoS One*, *10*(2), e0117729. doi:10.1371/journal.pone.0117729

- Chu, P. H., Chan, H. H., & Brown, B. (2007). Luminance-modulated adaptation of global flash mfERG: fellow eye losses in asymmetric glaucoma. *Investigative Ophthalmology and Visual Science*, *48*(6), 2626-2633. doi:10.1167/iovs.06-0962
- Chu, P. H., Chan, H. H., Ng, Y. F., Brown, B., Siu, A. W., Beale, B. A., . . . Wong, F. (2008). Porcine global flash multifocal electroretinogram: possible mechanisms for the glaucomatous changes in contrast response function. *Vision Res*, *48*(16), 1726-1734. doi:10.1016/j.visres.2008.05.006; 10.1016/j.visres.2008.05.006
- Chu, P. H., Chan, H. H. L., & Brown, B. (2006). Glaucoma detection is facilitated by luminance modulation of the global flash multifocal electroretinogram. *Investigative Ophthalmology and Visual Science*, *47*(3), 929-937.
- Chu, P. H., Ng, Y. F., & Chan, H. H. (2011). Forward and backward adaptive effects in global flash multifocal electroretinogram stimulation. *Clinical and Experimental Optometry*, *94*(3), 259-267. doi:10.1111/j.1444-0938.2011.00583.x
- Chua, W. H., Balakrishnan, V., Chan, Y. H., Tong, L., Ling, Y., Quah, B. L., & Tan, D. (2006). Atropine for the treatment of childhood myopia. *Ophthalmology*, *113*(12), 2285-2291.
- Chui, T. Y., Yap, M. K., Chan, H. H., & Thibos, L. N. (2005). Retinal stretching limits peripheral visual acuity in myopia. *Vision Res*, *45*(5), 593-605. doi:10.1016/j.visres.2004.09.016
- Chung, K., Mohidin, N., & O'Leary, D. J. (2002). Undercorrection of myopia enhances rather than inhibits myopia progression. *Vision Res*, *42*(22), 2555-2559.
- Cook, P. B., & McReynolds, J. S. (1998). Lateral inhibition in the inner retina is important for spatial tuning of ganglion cells. *Nature neuroscience*, *1*(8), 714-719.
- Cottrill, C. L., & McBrien, N. A. (1996). The M1 muscarinic antagonist pirenzepine reduces myopia and eye enlargement in the tree shrew. *Investigative Ophthalmology and Visual Science*, *37*(7), 1368-1379.
- Crewther, D. P. (2000). The role of photoreceptors in the control of refractive state. *Progress in retinal and eye research*, *19*(4), 421-457.
- Curry, T. A., Sivak, J. G., Callender, M. G., & Irving, E. L. (1999). Afocal magnification does not influence chick eye development. *Optometry and Vision Science*, *76*(5), 316-319.
- Czepita, D., Mojsa, A., & Zejmo, M. (2008). Prevalence of myopia and

- hyperopia among urban and rural schoolchildren in Poland. *Ann Acad Med Stetin*, 54(1), 17-21.
- Day, M., & Duffy, L. A. (2011). Myopia and defocus: the current understanding. *Scandinavian Journal of Optometry and Visual Science*, 4(1), 1-14.
- Deller, J. F., O'Connor, A. D., & Sorsby, A. (1947). X-ray measurement of the diameters of the living eye. *Proceedings of the Royal Society of Medicine*, 134(877), 456-467.
- Diether, S., Gekeler, F., & Schaeffel, F. (2001). Changes in contrast sensitivity induced by defocus and their possible relations to emmetropization in the chicken. *Investigative Ophthalmology and Visual Science*, 42(12), 3072-3079.
- Diether, S., & Schaeffel, F. (1997). Local changes in eye growth induced by imposed local refractive error despite active accommodation. *Vision Res*, 37(6), 659-668.
- Diether, S., & Wildsoet, C. F. (2005). Stimulus requirements for the decoding of myopic and hyperopic defocus under single and competing defocus conditions in the chicken. *Investigative Ophthalmology and Visual Science*, 46(7), 2242-2252.  
doi:10.1167/iovs.04-1200
- Dirani, M., Chamberlain, M., Shekar, S. N., Islam, A. F., Garoufalis, P., Chen, C. Y., . . . Baird, P. N. (2006). Heritability of refractive error and ocular biometrics: the Genes in Myopia (GEM) twin study. *Investigative Ophthalmology and Visual Science*, 47(11), 4756-4761.  
doi:10.1167/iovs.06-0270
- Dirani, M., Tong, L., Gazzard, G., Zhang, X., Chia, A., Young, T. L., . . . Saw, S. M. (2009). Outdoor activity and myopia in Singapore teenage children. *Br J Ophthalmol*, 93(8), 997-1000.  
doi:10.1136/bjo.2008.150979; 10.1136/bjo.2008.150979
- Donders, F. C., & Moore, W. D. (1864). *On the anomalies of accommodation and refraction of the eye: With a preliminary essay on physiological dioptrics* (Vol. 22): The New Sydenham Society.
- Ehrlich, D. L., Braddick, O. J., Atkinson, J., Anker, S., Weeks, F., Hartley, T., . . . Rudenski, A. (1997). Infant emmetropization: longitudinal changes in refraction components from nine to twenty months of age. *Optometry and Vision Science*, 74(10), 822-843.
- Enroth-Cugell, C., & Robson, J. G. (1966). The contrast sensitivity of retinal ganglion cells of the cat. *The Journal of physiology*, 187(3), 517-

552.

- Falsini, B., Porciatti, V., Bolzani, R., & Marchionni, A. (1991). Spatial-frequency-dependent changes in the human pattern electroretinogram after acute acetyl-L-carnitine administration. *Graefe's Archive for Clinical and Experimental Ophthalmology*, 229(3), 262-266.
- Feldkaemper, M. P., Burkhardt, E., & Schaeffel, F. (2004). Localization and regulation of glucagon receptors in the chick eye and preproglucagon and glucagon receptor expression in the mouse eye. *Experimental eye research*, 79(3), 321-329.
- Feldkaemper, M. P., & Schaeffel, F. (2002). Evidence for a potential role of glucagon during eye growth regulation in chicks. *Visual neuroscience*, 19(06), 755-766.
- Fischer, A. J., McGuire, J. J., Schaeffel, F., & Stell, W. K. (1999). Light- and focus-dependent expression of the transcription factor ZENK in the chick retina. *Nature neuroscience*, 2(8), 706-712. doi:10.1038/11167
- Fischer, A. J., Ritchey, E. R., Scott, M. A., & Wynne, A. (2008). Bullwhip neurons in the retina regulate the size and shape of the eye. *Developmental biology*, 317(1), 196-212. doi:10.1016/j.ydbio.2008.02.023
- Fischer, A. J., Seltner, R. L., & Stell, W. K. (1997). N-methyl-D-aspartate-induced excitotoxicity causes myopia in hatched chicks. *Canadian Journal of Ophthalmology*, 32(6), 373-377.
- Fitzke, F. W., Hayes, B. P., Hodos, W., Holden, A. L., & Low, J. C. (1985). Refractive sectors in the visual field of the pigeon eye. *The Journal of physiology*, 369(1), 33-44.
- Flores-Herr, N., Protti, D. A., & Wässle, H. (2001). Synaptic currents generating the inhibitory surround of ganglion cells in the mammalian retina. *The Journal of neuroscience*, 21(13), 4852-4863.
- Fortune, B., Bearse, M. A., Jr., Cioffi, G. A., & Johnson, C. A. (2002). Selective loss of an oscillatory component from temporal retinal multifocal ERG responses in glaucoma. *Investigative Ophthalmology and Visual Science*, 43(8), 2638-2647.
- Foulds, W. S., Barathi, V. A., & Luu, C. D. (2013). Progressive Myopia or Hyperopia Can Be Induced in Chicks and Reversed by Manipulation of the Chromaticity of Ambient Light. *Myopia, Hyperopia, and Ambient Light. Investigative Ophthalmology and Visual Science*, 54(13), 8004-8012.

- Fulk, G. W., Cyert, L. A., & Parker, D. E. (2000). A randomized trial of the effect of single-vision vs. bifocal lenses on myopia progression in children with esophoria. *Optometry and Vision Science*, 77(8), 395-401.
- Furtado, K. S., & Andrade, F. O. (2013). Comparison of the beneficial and adverse effects of inhaled and injectable anaesthetics: A mini-review. *OA Anaesthetics*, 1(2), 20-25.
- Gee, S. S., & Tabbara, K. F. (1988). Increase in ocular axial length in patients with corneal opacification. *Ophthalmology*, 95(9), 1276-1278.
- George, S., & Rosenfield, M. (2004). Blur adaptation and myopia. *Optometry and Vision Science*, 81(7), 543-547.
- Gerth, C., Sutter, E. E., & Werner, J. S. (2003). mfERG response dynamics of the aging retina. *Investigative Ophthalmology and Visual Science*, 44(10), 4443-4450.
- Goss, D. A., & Rainey, B. B. (1999). Relationship of accommodative response and nearpoint phoria in a sample of myopic children. *Optometry and Vision Science*, 76(5), 292-294.
- Goss, D. A., & Wickham, M. G. (1995). Retinal-image mediated ocular growth as a mechanism for juvenile onset myopia and for emmetropization. A literature review. *Documenta ophthalmologica*, 90(4), 341-375.
- Graham, B., & Judge, S. J. (1999). Normal development of refractive state and ocular component dimensions in the marmoset (*Callithrix jacchus*). *Vision Res*, 39(2), 177-187.
- Graham, N. (1972). Spatial frequency channels in the human visual system: Effects of luminance and pattern drift rate. *Vision Res*, 12(1), 53-68.
- Green, D. G. (1970). Regional variations in the visual acuity for interference fringes on the retina. *The Journal of physiology*, 207(2), 351-356.
- Green, D. G., & Campbell, F. W. (1965). Effect of focus on the visual response to a sinusoidally modulated spatial stimulus. *The Journal of the Optical Society of America*, 55(9), 1154-1157.
- Grosvenor, T. (2003). Why is there an epidemic of myopia? *Clinical and Experimental Optometry*, 86(5), 273-275.
- Guo, S. S., Sivak, J. G., Callender, M. G., & Diehl-Jones, B. (1995). Retinal dopamine and lens-induced refractive errors in chicks. *Current eye research*, 14(5), 385-389.
- Gusek-Schneider, G. C., & Martus, P. (2001). Stimulus deprivation myopia

- in human congenital ptosis: a study of 95 patients. *Journal of pediatric ophthalmology and strabismus*, 38(6), 340-348.
- Guyton, D. L., Greene, P. R., & Scholz, R. T. (1989). Dark-rearing interference with emmetropization in the rhesus monkey. *Investigative Ophthalmology and Visual Science*, 30(4), 761-764.
- Gwiazda, J., Hyman, L., Hussein, M., Everett, D., Norton, T. T., Kurtz, D., . . . Scheiman, M. (2003). A randomized clinical trial of progressive addition lenses versus single vision lenses on the progression of myopia in children. *Investigative Ophthalmology and Visual Science*, 44(4), 1492-1500.
- Hammond, C. J., Snieder, H., Gilbert, C. E., & Spector, T. D. (2001). Genes and environment in refractive error: the twin eye study. *Investigative Ophthalmology and Visual Science*, 42(6), 1232-1236.
- Hansen, B., & Essock, E. (2005). Influence of scale and orientation on the visual perception of natural scenes. *Visual Cognition*, 12(6), 1199-1234.
- Hare, W. A., & Ton, H. (2002). Effects of APB, PDA, and TTX on ERG responses recorded using both multifocal and conventional methods in monkey. *Documenta ophthalmologica*, 105(2), 189-222.
- Hart, N. S. (2001). The visual ecology of avian photoreceptors. *Progress in retinal and eye research*, 20(5), 675-703.
- He, M., Xiang, F., Zeng, Y., Mai, J., Chen, Q., Zhang, J., . . . Morgan, I. G. (2015). Effect of Time Spent Outdoors at School on the Development of Myopia Among Children in China: A Randomized Clinical Trial. *Journal of the American Medical Association*, 314(11), 1142-1148. doi:10.1001/jama.2015.10803
- He, M., Zheng, Y., & Xiang, F. (2009). Prevalence of myopia in urban and rural children in mainland China. *Optometry and Vision Science*, 86(1), 40-44. doi:10.1097/OPX.0b013e3181940719
- Heinrich, T. S., & Bach, M. (2001). Contrast adaptation in human retina and cortex. *Investigative Ophthalmology and Visual Science*, 42(11), 2721-2127.
- Heinrich, T. S., & Bach, M. (2002). Contrast adaptation in retinal and cortical evoked potentials: no adaptation to low spatial frequencies. *Visual neuroscience*, 19(05), 645-650.
- Hepsen, I. F., Evereklioglu, C., & Bayramlar, H. (2001). The effect of reading and near-work on the development of myopia in emmetropic boys: a prospective, controlled, three-year follow-up study. *Vision*

- Res*, 41(19), 2511-2520.
- Hess, R. F., Schmid, K. L., Dumoulin, S. O., Field, D. J., & Brinkworth, D. R. (2006). What image properties regulate eye growth? *Current Biology*, 16(7), 687-691. doi:10.1016/j.cub.2006.02.065
- Ho, W. C., Kee, C. S., & Chan, H. H. (2012a). Myopia progression in children is linked with reduced foveal mfERG response. *Investigative Ophthalmology and Visual Science*, 53(9), 5320-5325. doi:10.1167/iovs.12-10185 [doi]
- Ho, W. C., Ng, Y. F., Chu, P. H., Fong, Y. Y., Yip, K. S., Kee, C. S., & Chan, H. H. (2011). Impairment of retinal adaptive circuitry in the myopic eye. *Vision Res*, 51(3), 367-375. doi:10.1016/j.visres.2010.12.001; 10.1016/j.visres.2010.12.001
- Ho, W. C., Wong, O. Y., Chan, Y. C., Wong, S. W., Kee, C. S., & Chan, H. H. (2012b). Sign-dependent changes in retinal electrical activity with positive and negative defocus in the human eye. *Vision Res*, 52(1), 47-53. doi:10.1016/j.visres.2011.10.017
- Hodos, W., & Erichsen, J. T. (1990). Lower-field myopia in birds: an adaptation that keeps the ground in focus. *Vision Res*, 30(5), 653-657.
- Hodos, W., & Kuenzel, W. J. (1984). Retinal-image degradation produces ocular enlargement in chicks. *Investigative Ophthalmology and Visual Science*, 25(6), 652-659.
- Holden, B. A., Fricke, T. R., Wilson, D. A., Jong, M., Naidoo, K. S., Sankaridurg, P., . . . Resnikoff, S. (2016). Global Prevalence of Myopia and High Myopia and Temporal Trends from 2000 through 2050. *Ophthalmology*, 123(5), 1036-1042. doi:10.1016/j.ophtha.2016.01.006
- Hood, D. C. (2000). Assessing retinal function with the multifocal technique. *Progress in retinal and eye research*, 19(5), 607-646.
- Hood, D. C., Bach, M., Brigell, M., Keating, D., Kondo, M., Lyons, J. S., . . . International Society For Clinical Electrophysiology of, V. (2012). ISCEV standard for clinical multifocal electroretinography (mfERG) (2011 edition). *Documenta ophthalmologica*, 124(1), 1-13. doi:10.1007/s10633-011-9296-8
- Hood, D. C., Frishman, L. J., Saszik, S., & Viswanathan, S. (2002). Retinal origins of the primate multifocal ERG: implications for the human response. *Investigative Ophthalmology and Visual Science*, 43(5), 1673-1685.

- Hood, D. C., Odel, J. G., Chen, C. S., & Winn, B. J. (2003). The multifocal electroretinogram. *Journal of Neuro-Ophthalmology*, *23*(3), 225-235.
- Hood, D. C., Seiple, W., Holopigian, K., & Greenstein, V. (1997). A comparison of the components of the multifocal and full-field ERGs. *Visual neuroscience*, *14*(03), 533-544.
- Howlett, M. H., & McFadden, S. A. (2006). Form-deprivation myopia in the guinea pig (*Cavia porcellus*). *Vision Res*, *46*(1-2), 267-283. doi:10.1016/j.visres.2005.06.036
- Howlett, M. H., & McFadden, S. A. (2009). Spectacle lens compensation in the pigmented guinea pig. *Vision Res*, *49*(2), 219-227. doi:10.1016/j.visres.2008.10.008
- Hunziker, H. (2007). In the Eye of the Reader: Foveal and Peripheral Perception. *Germany: Staubli*.
- Ip, J. M., Rose, K. A., Morgan, I. G., Burlutsky, G., & Mitchell, P. (2008a). Myopia and the urban environment: findings in a sample of 12-year-old Australian school children. *Investigative Ophthalmology and Visual Science*, *49*(9), 3858-3863. doi:10.1167/iovs.07-1451
- Ip, J. M., Saw, S. M., Rose, K. A., Morgan, I. G., Kifley, A., Wang, J. J., & Mitchell, P. (2008b). Role of near work in myopia: findings in a sample of Australian school children. *Invest Ophthalmol Vis Sci*, *49*(7), 2903-2910. doi:10.1167/iovs.07-0804
- Irving, E. L., Callender, M. G., & Sivak, J. G. (1991). Inducing myopia, hyperopia, and astigmatism in chicks. *Optometry and Vision Science*, *68*(5), 364-368.
- Irving, E. L., Sivak, J. G., & Callender, M. G. (1992). Refractive plasticity of the developing chick eye. *Ophthalmic and Physiological Optics*, *12*(4), 448-456.
- Jacobs, G. H. (2009). Evolution of colour vision in mammals. *Philosophical Transactions of the Royal Society of London B: Biological Sciences*, *364*(1531), 2957-2967.
- Jiang, L., Schaeffel, F., Zhou, X., Zhang, S., Jin, X., Pan, M., . . . Qu, J. (2009). Spontaneous axial myopia and emmetropization in a strain of wild-type guinea pig (*Cavia porcellus*). *Investigative Ophthalmology and Visual Science*, *50*(3), 1013-1019. doi:10.1167/iovs.08-2463
- Jonas, J. B., Xu, L., Wang, Y. X., Bi, H. S., Wu, J. F., Jiang, W. J., . . . Panda-Jonas, S. (2016). Education-Related Parameters in High Myopia: Adults versus School Children. *PLoS One*, *11*(5), e0154554.

doi:10.1371/journal.pone.0154554

- Jones, L. A., Sinnott, L., Mitchell, G. L., Mutti, D. O., Moeschberger, M. L., & Zadnik, K. (2006). How Well Do Parental History and Near Work Predict Myopia? *Investigative Ophthalmology and Visual Science*, 47(13), 5452-5452.
- Jones, L. A., Sinnott, L. T., Mutti, D. O., Mitchell, G. L., Moeschberger, M. L., & Zadnik, K. (2007). Parental history of myopia, sports and outdoor activities, and future myopia. *Investigative Ophthalmology and Visual Science*, 48(8), 3524-3532. doi:10.1167/iovs.06-1118
- Katz, J., Schein, O. D., Levy, B., Cruiscullo, T., Saw, S. M., Rajan, U., . . . Chew, S. J. (2003). A randomized trial of rigid gas permeable contact lenses to reduce progression of children's myopia. *American Journal of Ophthalmology*, 136(1), 82-90.
- Kawabata, H., & Adachi-Usami, E. (1997). Multifocal electroretinogram in myopia. *Investigative Ophthalmology and Visual Science*, 38(13), 2844-2851.
- Kee, C. S., Marzani, D., & Wallman, J. (2001). Differences in time course and visual requirements of ocular responses to lenses and diffusers. *Investigative Ophthalmology and Visual Science*, 42(3), 575-583.
- Knill, D. C., Field, D., & Kersten, D. (1990). Human discrimination of fractal images. *Journal of the Optical Society of America A*, 7(6), 1113-1123.
- Kruger, P. B., Mathews, S., Aggarwala, K. R., & Sanchez, N. (1993). Chromatic aberration and ocular focus: Fincham revisited. *Vision Res*, 33(10), 1397-1411.
- Kuo, A., Sinatra, R. B., & Donahue, S. P. (2003). Distribution of refractive error in healthy infants. *Journal of American Association for Pediatric Ophthalmology and Strabismus*, 7(3), 174-177. doi:10.1016/mpa.2003.S109185310300017X
- Lam, C. S., Goldschmidt, E., & Edwards, M. H. (2004). Prevalence of myopia in local and international schools in Hong Kong. *Optometry and Vision Science*, 81(5), 317-322.
- Lam, C. S. Y., Tang, W. C., Tse, D. Y. Y., Tang, Y. Y., & To, C. H. (2013). Defocus Incorporated Soft Contact (DISC) lens slows myopia progression in Hong Kong Chinese schoolchildren: a 2-year randomised clinical trial. *British Journal of Ophthalmology*, bjophthalmol-2013-303914.
- Laughlin, S. (1983). Matching coding to scenes to enhance efficiency. In

- Physical and Biological Processing of Images* (pp. 42-52): Springer.
- Leung, J. T., & Brown, B. (1999). Progression of myopia in Hong Kong Chinese schoolchildren is slowed by wearing progressive lenses. *Optometry and Vision Science, 76*(6), 346-354.
- Lin, L. L., Shih, Y. F., Hsiao, C. K., & Chen, C. J. (2004). Prevalence of myopia in Taiwanese schoolchildren: 1983 to 2000. *Annals of the Academy of Medicine, Singapore, 33*(1), 27-33.
- Lin, L. L., Shih, Y. F., Lee, Y. C., Hung, P. T., & Hou, P. K. (1996). Changes in ocular refraction and its components among medical students--a 5-year longitudinal study. *Optometry and Vision Science, 73*(7), 495-498.
- Lin, Z., Vasudevan, B., Jhanji, V., Mao, G. Y., Gao, T. Y., Wang, F. H., . . . Liang, Y. B. (2014). Near work, outdoor activity, and their association with refractive error. *Optometry and Vision Science, 91*(4), 376-382. doi:10.1097/OPX.0000000000000219
- Liu, Y., & Wildsoet, C. (2012). The Effective Add Inherent in 2-Zone Negative Lenses Inhibits Eye Growth in Myopic Young Chicks-2-Zone Lenses Inhibit Growth in Myopic Young Chicks. *Investigative Ophthalmology and Visual Science, 53*(8), 5085-5093.
- Logan, N. S., Shah, P., Rudnicka, A. R., Gilmartin, B., & Owen, C. G. (2011). Childhood ethnic differences in ametropia and ocular biometry: the Aston Eye Study. *Ophthalmic and Physiological Optics, 31*(5), 550-558. doi:10.1111/j.1475-1313.2011.00862.x
- Long, Q., Chen, D., & Chu, R. (2009). Illumination with monochromatic long-wavelength light promotes myopic shift and ocular elongation in newborn pigmented guinea pigs. *Cutan Ocul Toxicol, 28*(4), 176-180. doi:10.3109/15569520903178364
- Lu, B., Congdon, N., Liu, X., Choi, K., Lam, D. S., Zhang, M., . . . Song, Y. (2009). Associations between near work, outdoor activity, and myopia among adolescent students in rural China: the Xichang Pediatric Refractive Error Study report no. 2. *Archives of Ophthalmology, 127*(6), 769-775. doi:10.1001/archophthalmol.2009.105
- Luft, W. A., Ming, Y., & Stell, W. K. (2003). Variable effects of previously untested muscarinic receptor antagonists on experimental myopia. *Investigative Ophthalmology and Visual Science, 44*(3), 1330-1338.
- Lung, J. C., & Chan, H. H. (2010). Effects of luminance combinations on the characteristics of the global flash multifocal electroretinogram

- (mfERG). *Graefe's Archive for Clinical and Experimental Ophthalmology*, 248(8), 1117-1125. doi:10.1007/s00417-010-1346-5
- Luu, C. D., Lau, A. M., & Lee, S. Y. (2006). Multifocal electroretinogram in adults and children with myopia. *Archives of Ophthalmology*, 124(3), 328-334. doi:10.1001/archophth.124.3.328
- Marsh-Tootle, W. L., & Norton, T. T. (1989). Refractive and structural measures of lid-suture myopia in tree shrew. *Investigative Ophthalmology and Visual Science*, 30(10), 2245-2257.
- Masland, R. H. (2012). The tasks of amacrine cells. *Visual neuroscience*, 29(01), 3-9.
- Mathews, S., & Kruger, P. B. (1994). Spatiotemporal transfer function of human accommodation. *Vision Res*, 34(15), 1965-1980.
- McBrien, N. A., Lawlor, P., & Gentle, A. (2000). Scleral remodeling during the development of and recovery from axial myopia in the tree shrew. *Investigative Ophthalmology and Visual Science*, 41(12), 3713-3719.
- McBrien, N. A., Moghaddam, H. O., Cottrill, C. L., Leech, E. M., & Cornell, L. M. (1995). The effects of blockade of retinal cell action potentials on ocular growth, emmetropization and form deprivation myopia in young chicks. *Vision Res*, 35(9), 1141-1152.
- McBrien, N. A., Moghaddam, H. O., & Reeder, A. P. (1993). Atropine reduces experimental myopia and eye enlargement via a nonaccommodative mechanism. *Investigative Ophthalmology and Visual Science*, 34(1), 205-215.
- McFadden, S. A., Howlett, M. H., & Mertz, J. R. (2004). Retinoic acid signals the direction of ocular elongation in the guinea pig eye. *Vision Res*, 44(7), 643-653.
- McFadden, S. A., Tse, D. Y., Bowrey, H. E., Leotta, A. J., Lam, C. S., Wildsoet, C. F., & To, C. H. (2014). Integration of defocus by dual power Fresnel lenses inhibits myopia in the mammalian eye. *Investigative Ophthalmology and Visual Science*, 55(2), 908-917. doi:10.1167/iovs.13-11724
- McFadden, S. A., & Wildsoet, C. F. (2009). Mammalian eyes need an intact optic nerve to detect the sign of defocus during emmetropisation. *Investigative Ophthalmology and Visual Science*, 50(ARVO E-Abstract), 1620.
- McGonigle, C., van der Linde, I., Pardhan, S., Engel, S. A., Mallen, E. A., & Allen, P. M. (2016). Myopes experience greater contrast adaptation

- during reading. *Vision Res*, 121, 1-9.  
doi:10.1016/j.visres.2016.01.001
- Meng, W., Butterworth, J., Malecaze, F., & Calvas, P. (2011). Axial length of myopia: a review of current research. *Ophthalmologica*, 225(3), 127-134. doi:10.1159/000317072
- Mertz, J. R., & Wallman, J. (2000). Choroidal retinoic acid synthesis: a possible mediator between refractive error and compensatory eye growth. *Experimental eye research*, 70(4), 519-527.
- Meyer, C., Mueller, M. F., Duncker, G. I. W., & Meyer, H. J. (1999). Experimental Animal Myopia Models Are Applicable to Human Juvenile-Onset Myopia. *Survey of Ophthalmology*, 44, Supplement 1, S93-S102. doi:[http://dx.doi.org/10.1016/S0039-6257\(99\)00091-0](http://dx.doi.org/10.1016/S0039-6257(99)00091-0)
- Miles, F. A., & Wallman, J. (1990). Local ocular compensation for imposed local refractive error. *Vision Res*, 30(3), 339-349.
- Millane, R. P., Alzaidi, S., & Hsiao, W. H. (2003). *Scaling and power spectra of natural images*. Paper presented at the Proceedings of the Image and Vision Computing New Zealand.
- Millodot, M. (1981). Effect of ametropia on peripheral refraction. *Optometry and Vision Science*, 58(9), 691-695.
- Miyake, Y., Shiroyama, N., Horiguchi, M., & Ota, I. (1989). Asymmetry of focal ERG in human macular region. *Investigative Ophthalmology and Visual Science*, 30(8), 1743-1749.
- Mohan, M., Pakrasi, S., & Garg, S. P. (1988). The role of environmental factors and hereditary predisposition in the causation of low myopia. *Acta ophthalmologica*, 185(S185), 54-57.
- Mok, A. K. H., & Chung, C. S. T. (2011). Seven-year retrospective analysis of the myopic control effect of orthokeratology in children: A pilot study. *Journal of Clinical Optometry*, 3, 1-4.
- Mon-Williams, M., Tresilian, J. R., Strang, N. C., Kochhar, P., & Wann, J. P. (1998). Improving vision: neural compensation for optical defocus. *Proceedings of the Royal Society of London B: Biological Sciences*, 265(1390), 71-77.
- Morgan, I. G., Ashby, R. S., & Nickla, D. L. (2013). Form deprivation and lens-induced myopia: are they different? *Ophthalmic and Physiological Optics*, 33(3), 355-361.
- Mrsic-Flogel, T. D., Hofer, S. B., Ohki, K., Reid, R. C., Bonhoeffer, T., & Hubener, M. (2007). Homeostatic regulation of eye-specific responses in visual cortex during ocular dominance plasticity.

- Neuron*, 54(6), 961-972. doi:10.1016/j.neuron.2007.05.028
- Mutti, D. O., Mitchell, G. L., Hayes, J. R., Jones, L. A., Moeschberger, M. L., Cotter, S. A., . . . Group, C. S. (2006). Accommodative lag before and after the onset of myopia. *Investigative Ophthalmology and Visual Science*, 47(3), 837-846. doi:10.1167/iovs.05-0888
- Mutti, D. O., Mitchell, G. L., Jones, L. A., Friedman, N. E., Frane, S. L., Lin, W. K., . . . Zadnik, K. (2005). Axial growth and changes in lenticular and corneal power during emmetropization in infants. *Investigative Ophthalmology and Visual Science*, 46(9), 3074-3080.
- Mutti, D. O., Mitchell, G. L., Moeschberger, M. L., Jones, L. A., & Zadnik, K. (2002). Parental myopia, near work, school achievement, and children's refractive error. *Investigative Ophthalmology and Visual Science*, 43(12), 3633-3640.
- Nau, A. C., Wildoet, C. F., & Troilo, D. (1999). *Hyperopic defocus from spectacle lenses alters the pattern of accommodative behavior in chicks*. Paper presented at the Investigative Ophthalmology and Visual Science.
- Neelam, K., Cheung, C. M., Ohno-Matsui, K., Lai, T. Y., & Wong, T. Y. (2012). Choroidal neovascularization in pathological myopia. *Progress in retinal and eye research*, 31(5), 495-525. doi:10.1016/j.preteyeres.2012.04.001
- Nevin, S. T., Schmid, K. L., & Wildsoet, C. F. (1998). Sharp vision: a prerequisite for compensation to myopic defocus in the chick? *Current eye research*, 17(3), 322-331.
- Ng, Y. F., Chan, H. H., Chu, P. H., Siu, A. W., To, C. H., Beale, B. A., . . . Wong, F. (2008a). Pharmacologically defined components of the normal porcine multifocal ERG. *Documenta ophthalmologica*, 116(3), 165-176. doi:10.1007/s10633-007-9076-7
- Ng, Y. F., Chan, H. H., To, C. H., & Yap, M. K. (2008b). The characteristics of multifocal electroretinogram in isolated perfused porcine eye. *Documenta ophthalmologica*, 117(3), 205-214.
- Norn, M., & Jensen, O. A. (2004). Marius Tscherning (1854-1939): his life and work in optical physiology. *Acta Ophthalmologica Scandinavica Foundation*, 82(5), 501-508. doi:10.1111/j.1600-0420.2004.00340.x
- Norton, T. T., Essinger, J. A., & McBrien, N. A. (1994). Lid-suture myopia in tree shrews with retinal ganglion cell blockade. *Visual neuroscience*, 11(1), 143-153.
- Norton, T. T., & McBrien, N. A. (1992). Normal development of refractive

- state and ocular component dimensions in the tree shrew (*Tupaia belangeri*). *Vision Res*, 32(5), 833-842.
- Norton, T. T., & Siegwart, J. T. (1991). *Local myopia produced by partial visual-field deprivation in tree shrew*. Paper presented at the Society for Neuroscience Abstracts.
- Norton, T. T., & Siegwart, J. T. (2013). Light levels, refractive development, and myopia—a speculative review. *Experimental eye research*, 114, 48-57.
- Norton, T. T., Siegwart, J. T., & Amedo, A. O. (2006). Effectiveness of hyperopic defocus, minimal defocus, or myopic defocus in competition with a myopiagenic stimulus in tree shrew eyes. *Investigative Ophthalmology and Visual Science*, 47(11), 4687-4699.
- Norton, T. T., & Siegwart, J. T., Jr. (1995). Animal models of emmetropization: matching axial length to the focal plane. *Journal of the American optometric association*, 66(7), 405-414.
- Ohlendorf, A., & Schaeffel, F. (2009). Contrast adaptation induced by defocus—A possible error signal for emmetropization? *Vision Res*, 49(2), 249-256.
- Ohno-Matsui, K., Kawasaki, R., Jonas, J. B., Cheung, C. M., Saw, S. M., Verhoeven, V. J., . . . Group, M.-a. f. P. M. S. (2015). International photographic classification and grading system for myopic maculopathy. *American Journal of Ophthalmology*, 159(5), 877-883 e877. doi:10.1016/j.ajo.2015.01.022
- Over, R., & Moore, D. (1981). Spatial acuity of the chicken. *Brain research*, 211(2), 424-426.
- Owens, D. A., & Wolfe, J. M. (1985). Accommodation for flickering stimuli. *Ophthalmic and Physiological Optics*, 5(3), 291-296.
- Pan, C. W., Chen, Q., Sheng, X., Li, J., Niu, Z., Zhou, H., . . . Zhong, H. (2015a). Ethnic variations in myopia and ocular biometry among adults in a rural community in China: the Yunnan minority eye studies. *Investigative Ophthalmology and Visual Science*, 56(5), 3235-3241. doi:10.1167/iovs.14-16357
- Pan, C. W., Dirani, M., Cheng, C. Y., Wong, T. Y., & Saw, S. M. (2015b). The age-specific prevalence of myopia in Asia: a meta-analysis. *Optometry and Vision Science*, 92(3), 258-266. doi:10.1097/OPX.0000000000000516
- Pan, C. W., Ramamurthy, D., & Saw, S. M. (2012). Worldwide prevalence and risk factors for myopia. *Ophthalmic and Physiological Optics*,

32(1), 3-16. doi:10.1111/j.1475-1313.2011.00884.x

- Pang, J. J., Gao, F., & Wu, S. M. (2002). Segregation and integration of visual channels: layer-by-layer computation of ON–OFF signals by amacrine cell dendrites. *The Journal of neuroscience*, 22(11), 4693-4701.
- Park, D. J., & Congdon, N. G. (2004). Evidence for an "epidemic" of myopia. *Annals of the Academy of Medicine, Singapore*, 33(1), 21-26.
- Park, T. W., Winawer, J., & Wallman, J. (2003). Further evidence that chick eyes use the sign of blur in spectacle lens compensation. *Vision Res*, 43(14), 1519-1531.
- Parraga, C. A., Troscianko, T., & Tolhurst, D. J. (2000). The human visual system is optimised for processing the spatial information in natural visual images. *Current Biology*, 10(1), 35-38.
- Pascolini, D., & Mariotti, S. P. (2012). Global estimates of visual impairment: 2010. *British Journal of Ophthalmology*, 96(5), 614-618. doi:10.1136/bjophthalmol-2011-300539
- Perlman, I., Meyer, E., Haim, T., & Zonis, S. (1984). Retinal function in high refractive error assessed electroretinographically. *British Journal of Ophthalmology*, 68(2), 79-84.
- Pesudovs, K., & Brennan, N. A. (1993). Decreased uncorrected vision after a period of distance fixation with spectacle wear. *Optometry and Vision Science*, 70(7), 528-531.
- Petry, H. M., Fox, R., & Casagrande, V. A. (1984). Spatial contrast sensitivity of the tree shrew. *Vision Res*, 24(9), 1037-1042.
- Prashar, A., Hocking, P. M., Erichsen, J. T., Fan, Q., Saw, S. M., & Guggenheim, J. A. (2009). Common determinants of body size and eye size in chickens from an advanced intercross line. *Experimental eye research*, 89(1), 42-48.
- Rada, J. A., Shelton, S., & Norton, T. T. (2006). The sclera and myopia. *Experimental eye research*, 82(2), 185-200.
- Ramessur, R., Williams, K. M., & Hammond, C. J. (2015). Risk factors for myopia in a discordant monozygotic twin study. *Ophthalmic and Physiological Optics*, 35(6), 643-651. doi:10.1111/opo.12246
- Raviola, E., & Wiesel, T. N. (1978). Effect of dark-rearing on experimental myopia in monkeys. *Investigative Ophthalmology and Visual Science*, 17(6), 485-488.
- Read, S. A., Collins, M. J., & Sander, B. P. (2010). Human optical axial

- length and defocus. *Investigative Ophthalmology and Visual Science*, 51(12), 6262-6269. doi:10.1167/iovs.10-5457 [doi]
- Rose, K. A., Morgan, I. G., Ip, J., Kifley, A., Huynh, S., Smith, W., & Mitchell, P. (2008). Outdoor activity reduces the prevalence of myopia in children. *Ophthalmology*, 115(8), 1279-1285. doi:10.1016/j.ophtha.2007.12.019
- Rovamo, J., Virsu, V., Laurinen, P., & Hyvärinen, L. (1982). Resolution of gratings oriented along and across meridians in peripheral vision. *Investigative Ophthalmology and Visual Science*, 23(5), 666-670.
- Rucker, F. J., & Kruger, P. B. (2004). The role of short-wavelength sensitive cones and chromatic aberration in the response to stationary and step accommodation stimuli. *Vision Res*, 44(2), 197-208.
- Rucker, F. J., & Wallman, J. (2009). Chick eyes compensate for chromatic simulations of hyperopic and myopic defocus: evidence that the eye uses longitudinal chromatic aberration to guide eye-growth. *Vision Res*, 49(14), 1775-1783.
- Ruderman, D. L. (1994). The statistics of natural images. *Network: computation in neural systems*, 5(4), 517-548.
- Ruderman, D. L., & Bialek, W. (1994). Statistics of natural images: Scaling in the woods. *Phys Rev Lett*, 73(6), 814-817. doi:10.1103/PhysRevLett.73.814
- Sachs, M. B., Nachmias, J., & Robson, J. G. (1971). Spatial-frequency channels in human vision. *The Journal of the Optical Society of America*, 61(9), 1176-1186.
- Sankaridurg, P., Holden, B. A., Smith, E. L., 3rd, Naduvilath, T. J., Chen, X., de la Jara, P. L., . . . Frick, K. (2011). Decrease in rate of myopia progression with a contact lens designed to reduce relative peripheral hyperopia: one-year results. *Investigative Ophthalmology and Visual Science*, 52(13), 9362-9367.
- Sato, T. (1980). *Criticism of various accommodogeous theories on school myopia*. Paper presented at the Third International Conference on Myopia Copenhagen, August 24–27, 1980.
- Saunders, K. J., Woodhouse, J. M., & Westall, C. A. (1995). Emmetropisation in human infancy: rate of change is related to initial refractive error. *Vision Res*, 35(9), 1325-1328.
- Saw, S. M., Gazzard, G., Shih-Yen, E. C., & Chua, W. H. (2005). Myopia and associated pathological complications. *Ophthalmic and Physiological Optics*, 25(5), 381-391. doi:10.1111/j.1475-

1313.2005.00298.x

- Saw, S. M., Shih-Yen, E. C., Koh, A., & Tan, D. (2002). Interventions to retard myopia progression in children: an evidence-based update. *Ophthalmology*, *109*(3), 415-421; discussion 422-424; quiz 425-426, 443.
- Schaeffel, F. (2006). Myopia: the importance of seeing fine detail. *Current Biology*, *16*(7), R257-R259.
- Schaeffel, F., Bartmann, M., Hagel, G., & Zrenner, E. (1995). Studies on the role of the retinal dopamine/melatonin system in experimental refractive errors in chickens. *Vision Res*, *35*(9), 1247-1264.
- Schaeffel, F., Burkhardt, E., Howland, H. C., & Williams, R. W. (2004). Measurement of refractive state and deprivation myopia in two strains of mice. *Optometry and Vision Science*, *81*(2), 99-110.
- Schaeffel, F., & Diether, S. (1999). The growing eye: an autofocus system that works on very poor images. *Vision Res*, *39*(9), 1585-1589.
- Schaeffel, F., Glasser, A., & Howland, H. C. (1988). Accommodation, refractive error and eye growth in chickens. *Vision Res*, *28*(5), 639-657.
- Schaeffel, F., Howland, H. C., & Farkas, L. (1986). Natural accommodation in the growing chicken. *Vision Res*, *26*(12), 1977-1993.
- Schaeffel, F., Troilo, D., Wallman, J., & Howland, H. C. (1990). Developing eyes that lack accommodation grow to compensate for imposed defocus. *Visual neuroscience*, *4*(02), 177-183.
- Schaeffel, F., & Wildsoet, C. F. (2013). Can the retina alone detect the sign of defocus? *Ophthalmic and Physiological Optics*, *33*(3), 362-367.
- Schmid, K. L., Brinkworth, D. R., Wallace, K. M., & Hess, R. (2006). The effect of manipulations to target contrast on emmetropization in chick. *Vision Res*, *46*(6-7), 1099-1107.  
doi:10.1016/j.visres.2005.08.017
- Schmid, K. L., Rayner, C. L., & Brown, B. (2013). Hemi-field and full-field form-deprivation induce timing changes in multifocal ERG responses in chick. *Ophthalmic and Physiological Optics*, *33*(3), 257-266.
- Schmid, K. L., Strang, N. C., & Wildsoet, C. F. (1999). Imposed Retinal Image Size Changes-Do They Provide a Cue to the Sign of Lens-Induced Defocus in Chick? *Optometry and Vision Science*, *76*(5), 320-325.
- Schmid, K. L., & Wildsoet, C. F. (1996). Effects on the compensatory

- responses to positive and negative lenses of intermittent lens wear and ciliary nerve section in chicks. *Vision Res*, 36(7), 1023-1036.
- Schmid, K. L., & Wildsoet, C. F. (1997). Contrast and spatial-frequency requirements for emmetropization in chicks. *Vision Res*, 37(15), 2011-2021.
- Schmid, K. L., & Wildsoet, C. F. (1998). Assessment of visual acuity and contrast sensitivity in the chick using an optokinetic nystagmus paradigm. *Vision Res*, 38(17), 2629-2634.
- Schwahn, H. N., & Schaeffel, F. (1994). Chick eyes under cycloplegia compensate for spectacle lenses despite six-hydroxy dopamine treatment. *Investigative Ophthalmology and Visual Science*, 35(9), 3516-3524.
- Seidemann, A., & Schaeffel, F. (2002). Effects of longitudinal chromatic aberration on accommodation and emmetropization. *Vision Res*, 42(21), 2409-2417.
- Seiple, W. H., Siegel, I. M., Carr, R. E., & Mayron, C. (1986). Evaluating macular function using the focal ERG. *Investigative Ophthalmology and Visual Science*, 27(7), 1123-1130.
- Seiple, W. H., Vajaranant, T. S., Pepperberg, D. R., & Szlyk, J. P. (2001). Lateral spread of adaptation as measured with the multifocal electroretinogram. *Visual neuroscience*, 18(5), 687-694.
- Sekuler, R., Wilson, H. R., & Owsley, C. (1984). Structural modeling of spatial vision. *Vision Res*, 24(7), 689-700.
- Shaikh, A. W., Siegwart, J. T., Jr., & Norton, T. T. (1999). Effect of interrupted lens wear on compensation for a minus lens in tree shrews. *Optometry and Vision Science*, 76(5), 308-315.
- Shapley, R., & Lennie, P. (1985). Spatial frequency analysis in the visual system. *Annual review of neuroscience*, 8(1), 547-581.
- Shen, W., Vijayan, M., & Sivak, J. G. (2005). Inducing form-deprivation myopia in fish. *Investigative Ophthalmology and Visual Science*, 46(5), 1797-1803.
- Sherman, S. M., Norton, T. T., & Casagrande, V. A. (1977). Myopia in the lid-sutured tree shrew (*Tupaia glis*). *Brain research*, 124(1), 154-157.
- Sherwin, J. C., Hewitt, A. W., Coroneo, M. T., Kearns, L. S., Griffiths, L. R., & Mackey, D. A. (2012a). The association between time spent outdoors and myopia using a novel biomarker of outdoor light exposure. *Investigative Ophthalmology and Visual Science*, 53(8),

4363-4370.

- Sherwin, J. C., Reacher, M. H., Keogh, R. H., Khawaja, A. P., Mackey, D. A., & Foster, P. J. (2012b). The association between time spent outdoors and myopia in children and adolescents: a systematic review and meta-analysis. *Ophthalmology*, *119*(10), 2141-2151. doi:10.1016/j.ophtha.2012.04.020
- Shih, Y. F., Chiang, T. H., Hsiao, C. K., Chen, C. J., Hung, P. T., & Lin, L. (2010). Comparing myopic progression of urban and rural Taiwanese schoolchildren. *The Japanese Journal of Ophthalmology*, *54*(5), 446-451. doi:10.1007/s10384-010-0860-7
- Shih, Y. F., Fitzgerald, M. E., & Reiner, A. (1994). The effects of choroidal or ciliary nerve transection on myopic eye growth induced by goggles. *Investigative Ophthalmology and Visual Science*, *35*(10), 3691-3701.
- Shimada, Y., Bearse, M. A., Jr., & Sutter, E. E. (2005). Multifocal electroretinograms combined with periodic flashes: direct responses and induced components. *Graefes Archive for Clinical and Experimental Ophthalmology*, *243*(2), 132-141. doi:10.1007/s00417-004-1072-y
- Shimada, Y., Li, Y., Bearse, M. A., Jr., Sutter, E. E., & Fung, W. (2001). Assessment of early retinal changes in diabetes using a new multifocal ERG protocol. *Br J Ophthalmol*, *85*(4), 414-419.
- Sieglwart, J. T., Jr., & Norton, T. T. (1999). Regulation of the mechanical properties of tree shrew sclera by the visual environment. *Vision Res*, *39*(2), 387-407.
- Sieglwart, J. T., Jr., & Norton, T. T. (2005). Selective regulation of MMP and TIMP mRNA levels in tree shrew sclera during minus lens compensation and recovery. *Investigative Ophthalmology and Visual Science*, *46*(10), 3484-3492. doi:10.1167/iovs.05-0194
- Sieglwart, J. T., Jr., & Norton, T. T. (2011). Perspective: how might emmetropization and genetic factors produce myopia in normal eyes? *Optometry and Vision Science*, *88*(3), E365-372.
- Sieglwart, J. T., Jr., Ward, A. H., & Norton, T. T. (2012). Moderately elevated fluorescent light levels slow form deprivation and minus lens-induced myopia development in tree shrews. *Investigative Ophthalmology and Visual Science*, *53*(14), 3457-3457.
- Sinclair, J. R., Jacobs, A. L., & Nirenberg, S. (2004). Selective ablation of a class of amacrine cells alters spatial processing in the retina. *The*

*Journal of neuroscience*, 24(6), 1459-1467.

- Smith, E. L., 3rd, Bradley, D. V., Fernandes, A., & Boothe, R. G. (1999). Form deprivation myopia in adolescent monkeys. *Optometry and Vision Science*, 76(6), 428-432.
- Smith, E. L., 3rd, & Hung, L. F. (1999). The role of optical defocus in regulating refractive development in infant monkeys. *Vision Res*, 39(8), 1415-1435.
- Smith, E. L., 3rd, & Hung, L. F. (2000). Form-deprivation myopia in monkeys is a graded phenomenon. *Vision Res*, 40(4), 371-381.
- Smith, E. L., 3rd, Hung, L. F., Arumugam, B., Holden, B. A., Neitz, M., & Neitz, J. (2015). Effects of Long-Wavelength Lighting on Refractive Development in Infant Rhesus Monkeys. Red Lens-Induced Hyperopia. *Investigative Ophthalmology and Visual Science*, 56(11), 6490-6500.
- Smith, E. L., 3rd, Hung, L. F., & Huang, J. (2009). Relative peripheral hyperopic defocus alters central refractive development in infant monkeys. *Vision Res*, 49(19), 2386-2392.  
doi:10.1016/j.visres.2009.07.011
- Smith, E. L., 3rd, Hung, L. F., & Huang, J. (2012). Protective effects of high ambient lighting on the development of form-deprivation myopia in rhesus monkeys. *Investigative Ophthalmology and Visual Science*, 53(1), 421-428. doi:10.1167/iovs.11-8652
- Smith, E. L., 3rd, Hung, L. F., Huang, J., Blasdel, T. L., Humbird, T. L., & Bockhorst, K. H. (2010). Effects of optical defocus on refractive development in monkeys: evidence for local, regionally selective mechanisms. *Investigative Ophthalmology and Visual Science*, 51(8), 3864-3873. doi:10.1167/iovs.09-4969
- Smith, E. L., 3rd, Hung, L. F., Kee, C. S., & Qiao, Y. (2002). Effects of brief periods of unrestricted vision on the development of form-deprivation myopia in monkeys. *Investigative Ophthalmology and Visual Science*, 43(2), 291-299.
- Smith, E. L., 3rd, Kee, C. S., Ramamirtham, R., Qiao-Grider, Y., & Hung, L. F. (2005). Peripheral vision can influence eye growth and refractive development in infant monkeys. *Investigative Ophthalmology and Visual Science*, 46(11), 3965-3972.
- Smith, E. L., 3rd, Ramamirtham, R., Qiao-Grider, Y., Hung, L. F., Huang, J., Kee, C. S., . . . Paysse, E. (2007). Effects of foveal ablation on emmetropization and form-deprivation myopia. *Investigative*

- Ophthalmology and Visual Science*, 48(9), 3914-3922.  
doi:10.1167/iovs.06-1264
- Stiles, W. S., & Crawford, B. H. (1933). The luminous efficiency of rays entering the eye pupil at different points. *Proceedings of the Royal Society B: Biological Sciences*, 112(778), 428-450.
- Sutter, E. E. (2000). The interpretation of multifocal binary kernels. *Documenta ophthalmologica*, 100(2-3), 49-75.
- Sutter, E. E. (2001). Imaging visual function with the multifocal m-sequence technique. *Vision Res*, 41(10), 1241-1255.
- Sutter, E. E., Shimada, Y., Li, Y., & Bearse, M. A. Mapping inner retinal function through enhancement of adaptive components in the M-ERG. *Vision science and its applications. Technical digest series. Optical Society of America*, 52-55.
- Sutter, E. E., Shimada, Y., Li, Y., & Bearse, M. A. (1999). Mapping inner retinal function through enhancement of adaptive components in the M-ERG. *Vision Science and its Applications. Technical digest series. Optical Society of America, Washington, DC, 1*, 52-55.
- Sutter, E. E., & Tran, D. (1992). The field topography of ERG components in man; XI. The photopic luminance response. *Vision Res*, 32(3), 433-446.
- Tarczy-Hornoch, K. (2012). Accommodative lag and refractive error in infants and toddlers. *Journal of American Association for Pediatric Ophthalmology and Strabismus*, 16(2), 112-117.  
doi:10.1016/j.jaapos.2011.10.015
- Tejedor, J., & de la Villa, P. (2003). Refractive changes induced by form deprivation in the mouse eye. *Investigative Ophthalmology and Visual Science*, 44(1), 32-36.
- Thibos, L. N., & Werblin, F. S. (1978). The response properties of the steady antagonistic surround in the mudpuppy retina. *The Journal of physiology*, 278, 79-99.
- Tran, N., Chiu, S., Tian, Y., & Wildsoet, C. F. (2008). The significance of retinal image contrast and spatial frequency composition for eye growth modulation in young chicks. *Vision Res*, 48(15), 1655-1662.  
doi:10.1016/j.visres.2008.03.022
- Troilo, D., Gottlieb, M. D., & Wallman, J. (1987). Visual deprivation causes myopia in chicks with optic nerve section. *Current eye research*, 6(8), 993-999.
- Troilo, D., & Judge, S. J. (1993). Ocular development and visual deprivation

- myopia in the common marmoset (*Callithrix jacchus*). *Vision Res*, 33(10), 1311-1324.
- Troilo, D., Nickla, D. L., Mertz, J. R., & Summers Rada, J. A. (2006). Change in the synthesis rates of ocular retinoic acid and scleral glycosaminoglycan during experimentally altered eye growth in marmosets. *Investigative Ophthalmology and Visual Science*, 47(5), 1768-1777. doi:10.1167/iovs.05-0298
- Troilo, D., Nickla, D. L., & Wildsoet, C. F. (2000). Form deprivation myopia in mature common marmosets (*Callithrix jacchus*). *Investigative Ophthalmology and Visual Science*, 41(8), 2043-2049.
- Troilo, D., & Wallman, J. (1987). Changes in corneal curvature during accommodation in chicks. *Vision Res*, 27(2), 241-247.
- Tscherning, M. (1882). Studies on myopia etiology. In: Kobenhavn.
- Tse, D. Y., Lam, C. S., Guggenheim, J. A., Lam, C., Li, K. K., Liu, Q., & To, C. H. (2007). Simultaneous defocus integration during refractive development. *Investigative Ophthalmology and Visual Science*, 48(12), 5352-5359. doi:10.1167/iovs.07-0383
- Tse, D. Y., & To, C. H. (2011). Graded competing regional myopic and hyperopic defocus produce summated emmetropization set points in chick. *Investigative Ophthalmology and Visual Science*, 52(11), 8056-8062. doi:10.1167/iovs.10-5207
- von Noorden, G. K., & Lewis, R. A. (1987). Ocular axial length in unilateral congenital cataracts and blepharoptosis. *Investigative Ophthalmology and Visual Science*, 28(4), 750-752.
- Walline, J. J., Greiner, K. L., McVey, M. E., & Jones-Jordan, L. A. (2013). Multifocal contact lens myopia control. *Optometry and Vision Science*, 90(11), 1207-1214.
- Wallman, J., Adams, J. I., & Trachtman, J. N. (1981). The eyes of young chickens grow toward emmetropia. *Investigative Ophthalmology and Visual Science*, 20(4), 557-561.
- Wallman, J., Gottlieb, M. D., Rajaram, V., & Fugate-Wentzek, L. A. (1987). Local retinal regions control local eye growth and myopia. *Science*, 237(4810), 73-77.
- Wallman, J., Turkel, J., & Trachtman, J. (1978). Extreme myopia produced by modest change in early visual experience. *Science*, 201(4362), 1249-1251.
- Wallman, J., & Winawer, J. (2004). Homeostasis of eye growth and the question of myopia. *Neuron*, 43(4), 447-468.

- Wang, Y. Z., Thibos, L. N., & Bradley, A. (1997). Effects of refractive error on detection acuity and resolution acuity in peripheral vision. *Investigative Ophthalmology and Visual Science*, 38(10), 2134-2143.
- Watson, A. B. (2014). A formula for human retinal ganglion cell receptive field density as a function of visual field. *Journal of vision*, 14(7), 15.
- Webster, M. A., Georgeson, M. A., & Webster, S. M. (2002). Neural adjustments to image blur. *Nature neuroscience*, 5(9), 839-840.
- Webster, M. A., & Miyahara, E. (1997). Contrast adaptation and the spatial structure of natural images. *The Journal of the Optical Society of America A*, 14(9), 2355-2366.
- Werblin, F. S. (1972). Lateral interactions at inner plexiform layer of vertebrate retina: antagonistic responses to change. *Science*, 175(4025), 1008-1010.
- Werblin, F. S. (1974). Control of retinal sensitivity II. Lateral interactions at the outer plexiform layer. *The Journal of general physiology*, 63(1), 62-87.
- Werblin, F. S., & Dowling, J. E. (1969). Organization of the retina of the mudpuppy, *Necturus maculosus*. II. Intracellular recording. *Journal of neurophysiology*, 32(3), 339-355.
- Westheimer, G. (1964). Pupil size and visual resolution. *Vision Res*, 4(1), 39-45.
- Whatham, A. R., & Judge, S. J. (2001). Compensatory changes in eye growth and refraction induced by daily wear of soft contact lenses in young marmosets. *Vision Res*, 41(3), 267-273.
- Wiesel, T. N., & Raviola, E. (1977). Myopia and eye enlargement after neonatal lid fusion in monkeys. *Nature*, 266(5597), 66-68.
- Wiesel, T. N., & Raviola, E. (1979). Increase in axial length of the macaque monkey eye after corneal opacification. *Investigative Ophthalmology and Visual Science*, 18(12), 1232-1236.
- Wildsoet, C. F. (2003). Neural pathways subserving negative lens-induced emmetropization in chicks—insights from selective lesions of the optic nerve and ciliary nerve. *Current eye research*, 27(6), 371-385.
- Wildsoet, C. F., & Collins, M. J. (2000). Competing defocus stimuli of opposite sign produce opposite effects in eyes with intact and sectioned optic nerves in the chick. *Investigative Ophthalmology and Visual Science*, 41, S738.
- Wildsoet, C. F., Howland, H. C., Falconer, S., & Dick, K. (1993). Chromatic

- aberration and accommodation: their role in emmetropization in the chick. *Vision Res*, 33(12), 1593-1603.
- Wildsoet, C. F., & McFadden, S. A. (2010). Optic nerve section does not prevent form deprivation-induced myopia or recovery from it in the mammalian eye. *Investigative Ophthalmology and Visual Science*, 51(5), S1737.
- Wildsoet, C. F., & Schmid, K. L. (2001). Emmetropization in chicks uses optical vergence and relative distance cues to decode defocus. *Vision Res*, 41(24), 3197-3204.
- Wildsoet, C. F., & Wallman, J. (1995). Choroidal and scleral mechanisms of compensation for spectacle lenses in chicks. *Vision Res*, 35(9), 1175-1194.
- Wilkinson, M. O., Anderson, R. S., Bradley, A., & Thibos, L. N. (2016). Neural bandwidth of veridical perception across the visual field. *Journal of vision*, 16(2), 1-1.
- Williams, D. R. (1985). Aliasing in human foveal vision. *Vision Res*, 25(2), 195-205.
- Williams, K. M., Bentham, G. C. G., Young, I. S., McGinty, A., McKay, G. J., Hogg, R., . . . Seland, J. (2017). Association between myopia, ultraviolet B radiation exposure, serum vitamin D concentrations, and genetic polymorphisms in vitamin D metabolic pathways in a Multicountry European Study. *Jama ophthalmology*, 135(1), 47-53.
- Winawer, J., & Wallman, J. (2002). Temporal constraints on lens compensation in chicks. *Vision Res*, 42(24), 2651-2668.
- Winawer, J., Zhu, X., Choi, J., & Wallman, J. (2005). Ocular compensation for alternating myopic and hyperopic defocus. *Vision Res*, 45(13), 1667-1677. doi:10.1016/j.visres.2004.12.013
- Wojciechowski, R. (2011). Nature and nurture: the complex genetics of myopia and refractive error. *Clinical Genetics*, 79(4), 301-320. doi:10.1111/j.1399-0004.2010.01592.x
- Wojciechowski, R., Congdon, N., Bowie, H., Munoz, B., Gilbert, D., & West, S. K. (2005). Heritability of refractive error and familial aggregation of myopia in an elderly American population. *Investigative Ophthalmology and Visual Science*, 46(5), 1588-1592. doi:10.1167/iovs.04-0740
- Wong, T. Y., Ferreira, A., Hughes, R., Carter, G., & Mitchell, P. (2014). Epidemiology and disease burden of pathologic myopia and myopic choroidal neovascularization: an evidence-based systematic review.

- American Journal of Ophthalmology*, 157(1), 9-25 e12.  
doi:10.1016/j.ajo.2013.08.010
- Wu, P. C., Tsai, C. L., Wu, H. L., Yang, Y. H., & Kuo, H. K. (2013). Outdoor activity during class recess reduces myopia onset and progression in school children. *Ophthalmology*, 120(5), 1080-1085.  
doi:10.1016/j.ophtha.2012.11.009; 10.1016/j.ophtha.2012.11.009
- Wu, S., & Sutter, E. E. (1995). A topographic study of oscillatory potentials in man. *Visual neuroscience*, 12(6), 1013-1025.
- Yamada, K., Matsumoto, C. S., & Nakatsuka, K. (2006). Effect of spatial frequency of stimulus on focal macular ERGs in monkeys : fmacERG dependence on the spatial-frequency. *Documenta ophthalmologica*, 113(2), 83-91. doi:10.1007/s10633-006-9017-x
- Yeo, A. C., Atchison, D. A., Lai, N. S., & Schmid, K. L. (2012). Near Work–Induced Contrast Adaptation in Emmetropic and Myopic Children Near Work–Induced Contrast Adaptation. *Investigative Ophthalmology and Visual Science*, 53(7), 3441-3448.
- Yinon, U., Koslowe, K. C., Lobel, D., Landshman, N., & Barishak, Y. R. (1982). Lid suture myopia in developing chicks: optical and structural considerations. *Current eye research*, 2(12), 877-882.
- Yoshii, M., Yanashima, K., Wada, H., Sakemi, F., Enoki, T., & Okisaka, S. (2001). Analysis of second-order kernel response components of multifocal electroretinograms elicited from normal subjects. *Japanese journal of ophthalmology*, 45(3), 247-251.
- You, Q. S., Wu, L. J., Duan, J. L., Luo, Y. X., Liu, L. J., Li, X., . . . Guo, X. H. (2014). Prevalence of myopia in school children in greater Beijing: the Beijing Childhood Eye Study. *Acta ophthalmologica*, 92(5), e398-406.
- Young, F. A. (1965). The Effect of Atropine on the Development of Myopia in Monkeys. *American journal of optometry and archives of American Academy of Optometry*, 42(8), 439-449.
- Young, F. A. (1977). The nature and control of myopia. *Journal of the American optometric association*, 48(4), 451-457.
- Zhang, Z., & Li, S. (1996). The visual deprivation and increase in axial length in patients with cataracts. *Yan Ke Xue Bao*, 12(3), 135-137.
- Zhi, Z., Pan, M., Xie, R., Xiong, S., Zhou, X., & Qu, J. (2013). The effect of temporal and spatial stimuli on the refractive status of guinea pigs following natural emmetropization. *Investigative Ophthalmology and Visual Science*, 54(1), 890-897. doi:10.1167/iovs.11-8064;

10.1167/iovs.11-8064

- Zhong, X., Ge, J., Smith, E. L., 3rd, & Stell, W. K. (2004). Image defocus modulates activity of bipolar and amacrine cells in macaque retina. *Investigative Ophthalmology and Visual Science*, *45*(7), 2065-2074.
- Zhou, X., Qu, J., Xie, R., Wang, R., Jiang, L., Zhao, H., . . . Lu, F. (2006). Normal development of refractive state and ocular dimensions in guinea pigs. *Vision Res*, *46*(18), 2815-2823.
- Zhu, X., Winawer, J. A., & Wallman, J. (2003). Potency of myopic defocus in spectacle lens compensation. *Investigative Ophthalmology and Visual Science*, *44*(7), 2818-2827.